MONTHLY NOTICES

OF THE

ROYAL ASTRONOMICAL SOCIETY

Vol. III No. 3 1951

Published and Sold by the

ROYAL ASTRONOMICAL SOCIETY
BURLINGTON HOUSE
LONDON, W. 1

Price Nine Shillings

NOTICE TO AUTHORS

1. *Communications.*—Papers must be communicated to the Society by a Fellow. They should be accompanied by a summary at the *beginning* of the paper conveying briefly the content of the paper, and drawing attention to important new information and to the main conclusions. The summary should be intelligible in itself, without reference to the paper, to a reader with some knowledge of the subject; it should not normally exceed 200 words in length. **Authors are requested to submit MSS. in duplicate. These should be typed using double spacing and leaving a margin of not less than one inch on the left-hand side. Corrections to the MSS. should be made in the text and not in the margin.** Unless a paper reaches the Secretaries more than seven days before a Council meeting it will not normally be considered at that meeting. By Council decision, MSS. of of accepted papers are retained by the Society for one year after publication; unless their return is then requested by the author, they are destroyed.

2. *Presentation.*—Authors are allowed considerable latitude, but they are requested to follow the general style and arrangement of *Monthly Notices*. References to literature should be given in the standard form, including a date, for printing either as footnotes or in a numbered list at the end of the paper. Each reference should give the **name and initials** of the author cited, irrespective of the occurrence of the name in the text (some latitude being permissible, however, in the case of an author referring to his own work). The following examples indicate the style of reference appropriate for a paper and a book, respectively :—

A. Corlin, *Zeits. f. Astrophys.*, **15**, 239, 1938.
A. S. Eddington, *Internal Constitution of the Stars*, Cambridge, p. 182, Table 24, 1926.

3. *Notation.*—Authors should conform closely to the recommendations of Commission 3 of the International Astronomical Union (*Trans. I.A.U.*, Vol. VI, p. 345, 1938). Council has decided to adopt the I.A.U. 4-letter abbreviations for constellations where contraction is desirable (Vol. IV, p. 221, 1932).

4. *Diagrams.*—**These should be drawn about twice the size required in print and prepared for direct photographic reproduction except for the lettering which should be inserted in pencil. Legends should be given in the manuscript indicating where in the text the figure should appear.** Blocks are retained by the Society for 10 years; unless the author requires them before the end of this period they are then destroyed.

5. *Tables.*—**These should be arranged so that they can be printed upright on the page.**

6. *Proofs.*—Costs of alteration exceeding 5 per cent of composition must be borne by the author. Fellows are warned that such costs have risen sharply in recent years, and it is in their own and the Society's interests to seek the maximum conciseness and simplification of symbols and equations consistent with clarity.

7. *Revised Manuscripts.*—When papers are submitted in revised form it is especially requested that they be accompanied by the original MS.

Reading of Papers at Meetings

8. When submitting papers authors are requested to indicate whether they will be willing and able to read the paper at the next or some subsequent meeting, and approximately how long they would like to be allotted for speaking.

9. Postcards giving the programme of each meeting are issued some days before the meeting concerned. Fellows wishing to receive such cards whether for Ordinary Meetings or for the Geophysical Discussions or both should notify the Assistant Secretary.

MONTHLY NOTICES

OF THE

ROYAL ASTRONOMICAL SOCIETY

Vol. 111 No. 3

MEETING OF 1951 MARCH 9

Professor H. Dingle, President, in the Chair

The election by the Council of the following Fellows was duly confirmed :—

Edmond Robert Glanville Burrin, M.I.N., Merchant Service Officers' Guild of New Zealand, Wellington, New Zealand (proposed by I. L. Thomsen);

Charles Henry Cotter, 9 Atherton Road, Clayhall, Ilford, Essex (proposed by E. W. Turner);

Fahmy Ibrahim Mikhail, M.Sc., 33 Lancaster Court, London, S.E.27 (proposed by W. H. McCrea);

*Sydney Nevil Milford, B.A., Ph.D., Yerkes Observatory, Williams Bay, Wisconsin, U.S.A. (proposed by S. Chandrasekhar);

Felix Bernhard Schmeidler, The Observatories, Madingley Road, Cambridge (proposed by R. O. Redman);

Thomas Whitham, 38 Breamish Street, Newcastle-on-Tyne (proposed by F. J. Acfield); and

Ralph E. Williamson, David Dunlap Observatory, Richmond Hill, Ontario, Canada (proposed by S. Chandrasekhar).

The election by the Council of the following Junior Member was duly confirmed :—

Alan Pennell Lenham, 43 Newcastle Street, Swindon, Wiltshire (proposed by D. W. G. Arthur).

One hundred and twenty-five presents were announced as having been received since the last meeting, including :—

L. M. Milne-Thomson, *Jacobian Elliptic Function Tables* (presented by the author).

* Transferred from Junior Membership.

ON THE STRUCTURE OF COMETS AND THE FORMATION OF TAILS

R. A. Lyttleton

(Received 1950 April 11)

Summary

The self-gravitation of comets is shown to be negligibly small compared with the differential force due to the Sun, and hence the separate particles of comets move practically in independent orbits, except possibly for comets that recede to several hundred astronomical units. A comet cannot be regarded as possessing any permanent shape. The changes in dimensions perpendicular to the general orbital plane are shown to be large. Near perihelion every particle of the comet must cross through this plane. Collisions between a proportion of the particles will occur and reduce them to finer dust, thereby producing particles sufficiently small for the effect of radiation pressure to create a tail. Changes of dimensions in the orbital plane during a revolution are far smaller. Any slight differences of period must gradually result in particles of the comet being distributed right round the orbit. The possible contribution of the process to the acceleration of Encke's comet is briefly discussed.

1. *Introduction.*—In an earlier paper * the theory of the formation of comets was considered and led to the conclusion that comets consist of loose aggregations of widely separated dust particles, and that they have masses of order $10^{18\pm3}$ gm. and mean densities of order less than 10^{-12} gm. cm.$^{-3}$. The linear dimensions of comets as observed are subject to considerable uncertainty, for the measured size must necessarily refer to the visible portion, whereas it is likely that some of its particles extend at lower space density much beyond this limit. Also the observed sizes and shapes are themselves subject to curious extensive changes, not merely as the orbit is pursued, but sometimes of an irreversible nature not repeated even approximately in subsequent revolutions. An extreme instance is the actual break-up of a comet into two or more separate smaller comets. Accordingly there is difficulty in defining or attaching permanent meaning to the linear dimensions or forms of comets, since we have little or no idea just how far the particles extend at a density below that necessary for observable effects. Even so the observed values will give some general indications of the lower limit of possible sizes. The following values are quoted by Chambers † as observed examples of large comas:

TABLE I

	Radius of coma
Comet 1811 I	$9{\cdot}2\times10^{10}$ cm.
Halley (1835)	$4{\cdot}5\times10^{10}$ cm.
Encke (1828) maximum	$2{\cdot}5\times10^{10}$ cm.
minimum	$2{\cdot}4\times10^{8}$ cm.
Holmes 1892 III	$1{\cdot}2\times10^{11}$ cm.

The object of the present paper is to show how, guided by these general indications of cometary masses and dimensions, we are led to simple dynamical reasons for the observed changes of shape and the emission from the comet of

* R. A. Lyttleton, *M.N.*, **108**, 465, 1948.

† G. F. Chambers, *The Story of the Comets*, Oxford, p. 222, 1909.

material in the form of sufficiently finely divided dust for radiation pressure of sunlight to bring about the formation of tails.

2. ***Demonstration of the negligible self-gravitation of comets.***—If the main mass of a comet resides in a central nucleus, the gravitational attraction at points outside this nucleus may be calculated as if the comet were a point mass. On the other hand, if the central condensation is not appreciable the same method of calculating the force due to the comet can be used at points external to it, but with less accurate approximation at internal points. If m_c denotes the mass of the comet, the force at distance r_c from it, in gravitational units, will be m_c/r_c^2. But if R is the distance of the comet from the Sun, the differential force due to the Sun at points distant r_c apart in the radial direction (for which it is greatest) is $2Mr_c/R^3$, where M denotes the mass of the Sun. The comet's influence will therefore be stronger if

$$r_c < (m_c/2M)^{1/3}R. \qquad (1)$$

As a numerical example, if $m_c = 10^{17}$ gm. and R is measured in astronomical units (A.U.), this gives $r_c < 4{\cdot}5 \times 10^7 R$ cm. Supposing 10^{17} gm. to be an estimate of the mass of Encke's comet, whose greatest distance is 4·1 A.U., we have $r_c(\text{aphelion}) < 1{\cdot}8 \times 10^8$ cm., while at the least distance from the Sun of 0·34 A.U. we have $r_c(\text{perihelion}) < 1{\cdot}5 \times 10^7$ cm. As a second example, if $m_c = 10^{18}$ gm. is taken as an estimate for Halley's comet for which $a = 17{\cdot}95$, $e = 0{\cdot}9673$, it is found that $r_c(\text{aphelion}) < 3{\cdot}3 \times 10^9$ cm. and $r_c(\text{perihelion}) < 5{\cdot}0 \times 10^7$ cm. Since r_c involves m_c only to the one-third power, these values are not much affected by moderate uncertainty in the assumed mass. It follows that only particles at central distances within these values would be controlled chiefly by the comet's attraction and this only if the main mass lay within the same distances. But the values of Table I for the observed maximum and minimum sizes of Encke's comet, for example, are so much greater than these that the attraction of the comet itself must be utterly negligible compared with the differential field of the Sun. This means that particles at such distances, and indeed those much nearer the centre of the comet, must pursue practically independent orbits round the Sun.

This result is of such importance to the subsequent argument that it may be worth while further emphasizing its validity by calculating the actual ratio of the force of the comet on its outer particles to that of the Sun in the above cases. This ratio is of order $m_c R^3/2Mr_c^3$. If for particles at the outer edge of Encke's comet when at aphelion $r_c = 2{\cdot}5 \times 10^{10}$ cm., the ratio is about 3×10^{-7}, while for $r_c = 2{\cdot}4 \times 10^8$ cm. at perihelion it is about 2×10^{-4}. Similarly for Halley's comet, using $m_c = 10^{18}$ gm. and considering the ratio of forces at distance $r_c = 4{\cdot}5 \times 10^{10}$ cm. in both cases, then at aphelion the ratio is about 4×10^{-4} and at perihelion it is about 2×10^{-9}.

To illustrate still further the complete validity of regarding the outer particles as moving practically independently of the other parts of the comet we can consider the time that would be required for such a particle to fall to the centre of the comet if otherwise uninfluenced. Thus for Encke's comet a particle falling from rest at initial distance $2{\cdot}5 \times 10^{10}$ cm. would describe a line ellipse of semi-axis $1{\cdot}25 \times 10^{10}$ cm., and with $m_c = 10^{17}$ gm. Kepler's law gives for the time of fall about 2000 years. This makes clear that during the orbital period (about 3·3 years) the effect of the mass of the comet would be negligible.

The orbits of the comets show such variety of sizes and shapes that the circumstances of each particular one would have to be considered in applying

the above picture. The conclusion will hold at all parts of the orbit for most periodic comets, but for a long-period comet moving in a highly elongated orbit the self-attraction of the comet at comparable distances from itself will be far more effective at aphelion than at perihelion, the ratio in the two cases depending on $(1+e)^3/(1-e)^3$, which may be quite large when e is near 1.

This is perhaps a suitable point to refer to a mistaken impression that seems to be held by many writers on comets concerning the so-called "tidal influence" of the Sun. The usual condition for stability of figure against tidal disruption, which is necessarily of similar form to the criterion (1) reached above (viz. $m_c/r_c^2 \gg 2Mr_c/R^3$), is examined and found to fail by a large factor. It is thence maintained that comets must be unstable and therefore disrupted at perihelion unless there were additional internal forces to prevent it. The argument however is not a valid application of tidal theory, for the comet is not a fluid in the hydrodynamic sense; collisions between its particles are very infrequent and certainly not elastic. The idea of pressure implied in the condition for the free surface to be an equipotential does not apply for a cloud of particles moving independently of each other. This criticism does not mean that disruption or similar effects cannot occur, indeed it will be shown that they may, but that the question is not one to which tidal ideas can be directly applied.

Accounts of early theories of the changes of form of comets and the formation of tails are given in detail by Tisserand.* These theories were based on the assumption that a comet consists of a tenuous gaseous atmosphere of negligible mass controlled by the field of a heavy central nucleus but also influenced by the Sun and in some theories by rotation of the comet as a whole. The forms of cometary figures were then investigated by means of equilibrium tidal theory, but agreement with observation appears to have been considered by the authors to have been far from satisfactory. For instance, as a result of his researches on these lines Bessel regarded the existence of an additional repulsive force as essential, while Schiaparelli maintained that comets must consist of "special material" on which the Sun exerted less attraction than on ordinary matter. These studies were made at a time when little or no evidence was available for the masses of comets or of their structure. It now seems clear that, in contrast, the masses are negligible as far as action on the comet is concerned, and that it is not permissible to treat the material as a gas.

3. *Behaviour of particles of the comet near perihelion.*—The equation of the path of a particle situated at the centre of the comet (supposing this to be a definite point) may be written in polar form

$$a(1-e^2) = r(1+e\cos\theta), \qquad (e<1) \tag{2}$$

and this will be referred to as the standard orbit, and its plane as the standard plane. Assuming the other particles of the comet to have the same period (this is discussed later), each orbit will have the same value of a and the same point as focus. A possible adjacent orbit for any other particle can be obtained, without change in e, by slightly rotating the major axis ASA′ in the standard plane. A possible orbit can also be obtained by a slight rotation of the standard orbit about AA′ or LL′ (Fig. 1). It is also possible to obtain a near orbit by slightly changing e. Lastly, it would be possible for another particle to move in precisely the standard orbit but differ slightly in time of perihelion passage. These cases, and any

* F. F. Tisserand, *Mécanique Céleste*, IV, Ch. XV and XVI, 1896.

combinations of them, are of course representable by slight changes in the appropriate elements.

These adjacent orbits can be regarded as obtained in two ways. First, by changes entirely within the standard plane. Second, by a small rotation of any one of these first orbits about any line such as NSN′ (Fig. 1) in the standard plane. Part of any orbit obtained in this way will evidently lie above the standard plane and part below it. Accordingly, a particle describing such an orbit must cross through the standard plane twice during each revolution, namely at N and N′. Moreover since NN′ necessarily passes through S, it follows that every particle of the comet crosses through the standard plane during the time the comet is traversing the perihelion side LAL′ between the ends of the latus rectum.

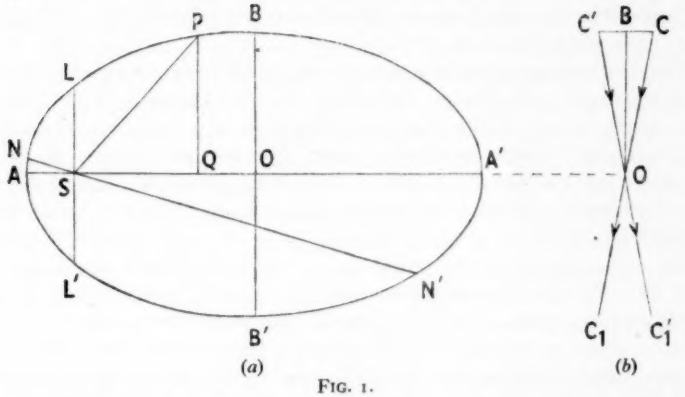

(*a*) (*b*)

FIG. 1.

For a comet of period P and eccentricity e close to unity, it is easily shown from Kepler's equation that the time spent on the arc LAL′ is approximately $\frac{3}{5}(1-e)^{3/2}P$, and is therefore small compared with P. For example, for Halley's comet this is about $0{\cdot}0034P$, which is about three months. For some long-period comets this part of the orbit may be described in a few days, though the whole period may be several centuries. In a time of this order, at most, the whole comet must therefore "turn itself inside out", as it were; particles above the plane on the aphelion side of the orbit crossing below, and vice versa.

There is however an additional feature of nearly parabolic motion tending to shorten still further the time during which this occurs for most of the particles of the comet. For if, as might reasonably be expected, the nodes N′ on the aphelion side, are distributed more or less uniformly round the orbit, then the nodes N on the perihelion portion LAL′ will tend to be strongly concentrated near A. This will happen simply because in a highly elongated orbit by far the greater part of it lies on the aphelion side. In the same way, if the nodes N′ were distributed round the orbit more or less at equal time intervals apart, a similar result will hold and a strong concentration of the N-nodes occur near A, because the comet moves so much more slowly on the aphelion side. The nature of the distribution can easily be calculated.

If n denotes the mean motion, the angular distribution of the points N can be found by expressing $(1/2\pi)n\,dt$ as a distribution function in terms of θ. This leads without difficulty to

$$\frac{n\,dt}{2\pi} = f(\theta)\frac{d\theta}{\pi} = \frac{(1-e^2)^{3/2}(1+e^2)}{(1-e^2\cos^2\theta)^2}\frac{d\theta}{\pi}, \qquad -\frac{\pi}{2} < \theta < \frac{\pi}{2}. \tag{3}$$

From this result the following values have been calculated for Encke's and Halley's comets of the proportion between $-\theta$ and θ of the total integrated value between $-\pi/2$ and $\pi/2$.

TABLE II

Encke $e=0{\cdot}846$		Halley $e=0{\cdot}967$	
θ	proportion within $\pm\theta$	θ	proportion within $\pm\theta$
10°	0·31	10°	0·65
20°	0·55	20°	0·88
30°	0·70	30°	0·95
40°	0·80	40°	0·98
60°	0·90	60°	0·99

In both cases the figures show the strong concentration towards perihelion, and comparison of the two sets of values shows how rapidly the degree of concentration increases as e approaches unity.

4. *The release of material in form suitable for production of tails.*—We come now to a consequence of the theory that seems to throw considerable light on the question of the source of the material going to form the tails of comets. The difficulty has been to understand why certain comets should more or less suddenly begin to emit material for tail formation and how they are able to repeat the process almost indefinitely. The present theory appears to go a long way towards solving these problems.

As already mentioned, the actual extents of comets may much exceed the observed extents, and the fact that meteor streams of great width surround a large part of the orbits of some comets also suggests that comets have greater extents than those observed. Meteor showers lasting more than a week are on record, and numerous instances of ones lasting for a period of the order of a day. This affords an estimate of the widths of streams and thence roughly the overall dimensions of comets transverse to their orbits. In a week the Earth describes about 2×10^{12} cm. along its orbit and in a day nearly 3×10^{11} cm. Because of the high eccentricity of cometary orbits, in most cases the Earth would cross the width of the stream more or less directly, though not necessarily through its central regions. It is seen that these figures exceed the maximum observed diameters of Table I by factors ranging from 2 to about 20. The transverse dimensions $2\delta H$ of comets may accordingly exceed the observed sizes by a factor of at least 2.

Referring now to Fig. 1 (*b*), let us consider two of the particles of the comet initially at points C and C′ on opposite sides of the standard plane when the comet is at the end of the minor axis of its orbit and approaching perihelion. The figure can also be interpreted as a vector diagram of the velocities of C and C′ and of the centre of the comet B when at perihelion. Hence the relative velocity of C and C′ will be, with sufficient accuracy, denoting COC′ by $2i$,

$$2i\times\text{velocity of comet at perihelion},$$

since $2i$ turns out in all cases to be small and of order 10^{-2} radian. Since the velocities of comets at perihelion are of order at least 50 km. sec.$^{-1}$ it follows that the relative speed of two such particles at, or near, perihelion is about $\frac{1}{2}$ km. sec.$^{-1}$. The following are estimates for a number of comets:

TABLE III

Comet	Estimated radius δH	Angular size $2i$	Perihelion vel. (cm. sec.$^{-1}$)	Relative velocity
Encke	5×10^{10}	6×10^{-3}	7×10^{6}	4×10^{4}
Halley	10^{11}	3×10^{-3}	6×10^{6}	2×10^{4}
Holmes	$2{\cdot}5\times10^{11}$	8×10^{-3}	$2{\cdot}5\times10^{6}$	2×10^{4}

In this table the radius δH has been estimated by taking, in round figures, twice the observed greatest radius quoted in Table I. In some cases higher velocity may occur if this underestimates the radius, but for inner particles the speed would be less, and also for particles arrested at the standard plane by material already at rest there.

This brings us to the important feature that the attempted crossing of particles through the standard plane in a part of the orbit concentrated near perihelion may be prevented by collisions, at speeds of the above order, with other particles crossing towards them from the opposite side. A first estimate of the probability of a particle undergoing a collision in this way is provided by the brightnesses of comets when at great distances from the Sun, at which stage presumably a comet shines mainly by reflected light and is in a fairly quiescent state. According to Russell, for Halley's comet only $\frac{1}{300,000}$ of the whole *area* within its apparent boundary is actually occupied by material, the comet being regarded as a two-dimensional object projected on the background. If only this proportion of the total mass, say 10^{18} gm., were involved in collisions through the present cause it would nevertheless mean about 3×10^{12} gm. On the other hand, once such collisions start, some of the material will tend to remain near the standard plane and increase the likelihood of further collisions, and also some contraction, on the whole, of the comet is to be expected near perihelion, as will be seen later. This estimate must thus be regarded as a lower limit to the proportion of mass concerned in collisions in the neighbourhood of perihelion.

Now a speed of 2×10^4 cm. sec.$^{-1}$ represents a high velocity judged by ordinary standards—it would require free fall in the Earth's field from a height of about 2 km. to produce it—and there is no doubt that the resulting impulses on particles called into play by such collisions would produce stresses far exceeding the strengths of ordinary materials. Thus one of the main results of the process would be to pulverize the particles of the comet into much smaller particles. The proportions of different sizes so produced would probably be roughly in accordance with a Poisson distribution, though the parameter would be difficult if not impossible to settle theoretically, and there is little doubt that a practically continuous distribution of sizes would occur. Now it has long been agreed that the tails of comets could be produced by the pressure of sunlight on dust particles with dimensions of the same order as the wave-length of the light. It has been shown by Schwarzschild *, Nicholson †, Proudman ‡, and others that for a range of sizes of the order of the wave-length the outward repulsive force attains to about twenty times the gravitational attraction of the Sun. Thus as a comet approaches perihelion it will produce, through these simple dynamical causes, particles of dust of all sizes smaller than its original constituent particles, and as soon as this happens those in a critical range of size will be violently "blown away" by radiation pressure to form the tail.

In comets that show little or no tail it must be the case that the mechanism no longer functions to any appreciable degree. This might result from a general reduction in the extent of the comet perpendicular to the standard plane and a consequent lowering of the speeds of collision, which would tend to come about from the loss of transverse motion in inelastic collisions, and it might also result from diminution in the number of particles of sizes exceeding the critical size.

* K. Schwarzschild, *Sitz. d. Math. Phys.*, Munich, **31**, 293, 1901–2.
† J. W. Nicholson, *M.N.*, **70**, 544, 1910.
‡ J. Proudman, *M.N.*, **73**, 535, 1913.

For if the comet consisted chiefly of particles already smaller than the critical size their further break-up would not produce particles within the critical range, and no material suitable for tail formation would be produced.

A further point worth mentioning is the alleged observation of envelopes of material emitted with almost explosive violence, often illustrated by drawings of Donati's comet. It seems more likely, on the present theory, that what is actually seen is the apparent transmission of an effect through the comet. Collisions will not necessarily occur simultaneously at all points of the area of the standard plane occupied by the comet, and the envelopes emerging might well be the advancing front in the standard plane of the colliding material coming from above and below the plane as it becomes observable through being transformed to finer dust.

It is also possible that the collisions would produce considerable heating effects. At speed 2×10^4 cm. sec.$^{-1}$ a particle possesses kinetic energy 2×10^8 ergs per gm. which converted to thermal energy distributed through the whole material would raise its temperature by the order of 100 deg. only. But the impacts would involve relatively small areas of contact, and energy lost through collisions might initially be communicated to only a small part of the mass involved. An action similar to that when flints are rubbed together to produce visible flashes must accompany the collisions, but with far higher speeds for the particles. In such a way much greater heating than 100 deg. might result for a small proportion of the material.

5. *Changes in dimensions of comets*

(i) *Perpendicular to the orbital plane.*—The line of nodes NSN′ for most particles of a comet with e near to unity will lie near the standard major axis ASA′. This means that a high proportion of particles tends to pass through the standard plane somewhere near A. Those particles that do not do so but have their nodes near L or L′ will be so much less in number that they will be too sparsely distributed (away from the standard plane) to give any observable coma, and the observable extent of the comet will depend on the distribution of particles close to the standard plane. Thus a general idea of the changes in size measured perpendicular to the plane may be obtained by supposing all the nodes to lie precisely at A. In that case the width of the comet $2\delta H$, say, at right angles to the plane at a general point P(θ) will be related to the width $2\delta H_B$ at the end of the minor axis by the equation

$$\frac{\delta H}{\delta H_B} = \frac{PQ}{BO} = \frac{(1-e^2)^{1/2}\sin\theta}{1+e\cos\theta}. \tag{4}$$

For long-period comets with e very near unity, observations as far from perihelion as B are not possible, but if the thickness at the end of the latus rectum, $2\delta H_L$ say, is taken as unit, the corresponding formula reduces to

$$\frac{\delta H}{\delta H_L} = \tan\tfrac{1}{2}\theta. \tag{5}$$

Since $\theta = 0$ corresponds to A, these formulae give theoretically a contraction right down to zero at perihelion, but this obviously arises from the approximation involved in taking all the nodes at A, so that the results will not be expected to hold very near to A. Even so it may be mentioned that a contraction by a factor of 100, as between a point near B and perihelion, has been observed for Encke's comet.

Systematic measures of the sizes of comets do not figure prominently in available data, but a series of values for Encke's comet are quoted by Chambers.* In the following table are given the theoretical and observed values of $-\log 100\delta H/\delta H_B$.

TABLE IV

	(*a*) Theoretical			(*b*) Observed	
$\theta°$	r (A.U.)	$-\log 100\delta H/\delta H_B$	Radius (10^3 miles)	r	$-\log 100\delta H/\delta H_B$
150	2·36	2·00	158·6	2·36	2·00
130	1·39	1·95	142·8	1·42	1·95
110	0·89	1·85	61·2	1·19	1·59
90	0·63	1·73	40·2	1·00	1·40
70	0·49	1·59	37·6	0·88	1·37
60	0·44	1·51	32·0	0·83	1·31
50	0·41	1·42	28·2	0·76	1·25
40	0·38	1·32	19·6	0·71	1·09
30	0·37	1·19	15·2	0·69	0·98
20	0·35	1·01	3·4	0·39	0·32
10	0·34	0·71	2·8	0·36	0·24
5	0·34	0·40	2·2	0·35	0·13
0	0·34	$-\infty$	1·5	0·34	− 0·02

The general run of agreement between the two sets of values is as satisfactory as could be expected in view of the likely sources of uncertainty. It is not stated by Chambers which dimension of the comet was observed nor its relation to the orbit, though it may probably have been the greatest. (Many drawings of Encke's comet show it as fan-shaped.) There might be some reduction from the possible maximum size owing to the greatest extent not lying perpendicular to the line of sight. Also the *observed* size would depend on the mode of observation and on the distribution of particles within the comet at each stage. The space density of particles probably decreases outwards and there is no reason to suppose that the observed limit of the coma closely corresponds to the actual limit of the comet beyond which no particles ever pass, if indeed any such limit exists. As the comet changes shape, and with this the space distribution of particles within it, the observable limit will not necessarily move with the particles. In view of these various considerations, comparison of the observed and calculated changes of size can only be regarded as of a general nature.

(ii) *Changes in the orbital plane.*—Still assuming that a comet consists of particles moving with identical periods, it is plain that, as the orbital velocity changes, the spacing of particles must change in proportion. If we consider two particles X and Y on the orbit of the centre of the comet at a distance δD apart, the time taken for X to move into the position formerly occupied by Y is $\delta D/v$, where v is the velocity at this part of the orbit. If after a finite interval a pair of independently moving particles initially at X and Y have reached points X' and Y' distance $\delta D'$ apart and have orbital velocity v', then clearly $\delta D/v = \delta D'/v'$. If δD_p is the distance between the particles when in the immediate neighbourhood of perihelion, it is readily found that at a general point of the orbit

$$\delta D = \frac{\sqrt{(1+2e\cos\theta+e^2)}}{1+e}\delta D_p. \qquad (6)$$

By means of this relation the following values for $\delta D/\delta D_p$ at various points of the orbit have been computed for Encke's comet and Halley's comet, and also the limiting values for a strictly parabolic orbit.

* G. F. Chambers, *The Story of the Comets*, Oxford, p. 223, 1909.

TABLE V

Lengthwise expansion of comet : $\delta D/\delta D_p$

θ	Encke	Halley	Parabola
180	0·083	0·017	0
120	0·505	0·500	1/2
90	0·710	0·707	$1/\sqrt{2}$
0	1·0	1·0	1

This change of dimension is obviously a purely periodic one involving no tendency for the leading and following particles to be lost from the comet nor any tendency to produce collisions.

It may be mentioned in regard to these results that few comets are observable at positions much beyond the ends of the minor axis, if that, and hence a change by a factor of two in its longitudinal extent is the most that is likely to arise observationally from this cause. It is also to be remembered that a change in the actual overall dimensions of a distribution of particles will not necessarily produce a corresponding change in its observable extent. Indeed the two effects might even go in opposite ways, for obviously if a distribution of cometary particles were dispersed to occupy an infinite volume it would become entirely unobservable.

6. *The assumption of equality of periods of the particles.*—Where long-period comets are concerned, as the mechanism of their formation shows, these can hold together by self-gravitation when near aphelion, and the common periods of their particles may thereby be brought about. But in any event only a single sweep round the Sun of a long-period comet is observable, and there seems to be no particular feature likely to develop, during the short portion of its arc for which observation is possible, from any slight departure from the standard period of a proportion of its particles.

For short-period comets, however, self-gravitation must be always negligible. It has long been agreed that these comets have come about through deflections by Jupiter of long-period comets. In any such deflection, because of the finite size of a comet, a distribution of slightly different periods would be produced among its particles. Now the effect of a slightly different period for any particle will obviously be to cause it to move gradually out of the comet and either go on ahead if the period is less or fall back relative to the comet as a whole if the period is greater. In the same way collisions within a comet of its particles may cause slight changes in period and again lead to a gradual dispersal along the orbit of such particles. It is of course well known that meteor streams occupying the whole or a large part of the orbits are associated with certain comets. On this picture a comet is therefore to be regarded as a distribution of particles extending, in the orbital direction, far beyond its observable limits. The observable portion probably corresponds to the small densest region (per unit area) of this distribution. Short-period comets are faint objects and probably represent only small proportions of the original long-period comets from which they have survived, the remaining part having gradually become dispersed along the orbit.

7. *The acceleration of Encke's comet.*—The collision of particles coming from opposite sides of the standard plane must result in slight changes in the orbital elements for the motion of the statistical centre of the mass as a whole. If we consider two equal symmetrically placed particles, such as C and C′ of Fig. 1 (*b*), their angular momentum vectors before collision are inclined at angles i and $-i$ to the normal to the standard plane, but after an ideal inelastic collision both

would be perpendicular to it. Supposing for simplicity that collisions occur at perihelion, the changes will be such that $a(1-e)$ remains unaltered but the velocity there and angular momentum are reduced by a factor $\cos i$. Actually for the comet only a proportion of its mass would be involved in such collisions, but the general effect of the process on the orbital elements must nevertheless be that of a decrease in h without change in $a(1-e)$. From the usual formulae for elliptic motion it is readily found in the present case that

$$\left.\begin{aligned} \frac{\delta n}{n} &= -\frac{3}{2}\frac{\delta a}{a} = -\frac{3(1+e)}{1-e}\frac{\delta h}{h}, \\ \frac{\delta e}{e} &= \frac{2}{e}(1+e)\frac{\delta h}{h}, \qquad \frac{\delta l}{l} = 2\frac{\delta h}{h}. \end{aligned}\right\} \tag{7}$$

For Encke's comet $e=0{\cdot}8458$, and the changes are in the following ratios:

$$\frac{\delta l/l}{2} = \frac{\delta e/e}{4{\cdot}36} = \frac{\delta a/a}{23{\cdot}9} = \frac{\delta n/n}{-35{\cdot}9} = \frac{\delta h}{h}. \tag{8}$$

These values are substantially different from the corresponding changes due to the Poynting-Robertson effect *, for which the values are

$$\frac{\delta l/l}{2} = \frac{\delta e/e}{2{\cdot}5} = \frac{\delta a/a}{14{\cdot}6} = \frac{\delta n/n}{-21{\cdot}9} \tag{9}$$

when adjusted to agree for $\delta l/l$. Robertson himself concludes from his study of the effect of radiation pressure that the drag produced leads to values that cannot be reconciled simultaneously between the several elements. But the present process provides a further mechanism that alters the elements in a different way. It seems probable that a suitable combination of the two effects could lead to a resolution or improvement of the difficulty referred to by Robertson, but its discussion would go beyond the object of the present paper.

St. John's College,
Cambridge:
1950 *April* 10.

* H. P. Robertson, *M.N.*, **97**, 436, 1937.

ROTATIONAL CURRENTS

E. J. Öpik

(Received 1950 September 28)*

Summary

An analysis of rotational currents is made for the case of small oblateness and constant angular velocity, $\omega = \text{const}$. Contrary to von Zeipel's paradox, the average energy generation over a level surface of the rotating star is subject to no restrictions; the balancing convective circulation is derived by developing Eddington's method in more detail; a complete system of circulation is calculated for a particular model. As compared with the speed of nuclear reactions, the mixing efficiency of the rotational currents for $\omega = 10^{-4}$ (or 30 times the solar rotation) is almost negligible, being of the same order as gas diffusion and being capable of mixing efficiently not more than the innermost 20 per cent of the stellar mass; for the solar angular velocity the effect is 1000 times smaller, thus practically nil. Eddington's suggestion that rotational currents are capable of maintaining uniform chemical composition in the radiative equilibrium layers of a star must be definitely rejected except for configurations on the verge of disruption by rotation.

1. From a paradoxical theorem of von Zeipel (**1**), Eddington (**2**) and Vogt (**3**) concluded that in the radiative equilibrium layers of a rotating star, convection currents must necessarily arise; these are forced large-scale currents working their way against the stable temperature gradient. Since then the question has been treated by different authors on several occasions (**4, 5, 6, 12**). Eddington (**7**) gave a formula to estimate the average velocity of the currents; however, for the Sun's angular velocity of rotation the velocity is far too slow to produce appreciable mixing of the material (**8**).

In view of the fundamental importance of this question from the standpoint of stellar evolution, let us reconsider the von Zeipel problem of constant angular velocity of rotation for the case of ω small (small oblateness). We start from Eddington's equation (2) (**7**):

$$f(\Phi)(4\pi G\rho - 2\omega^2) - f'(\Phi)(d\Phi/dn)^2 = \rho(\epsilon_1 + \epsilon_2), \tag{1}$$

where Φ is the potential (from combined gravitation and rotation), $g = -d\Phi/dn$ is the surface gravity and

$$f(\Phi) = -\frac{Q}{d\Phi/dn} = \frac{Q}{g} \tag{2}$$

is a pure function of Φ (**9**) with Q denoting the outward flux of radiation in the direction of the normal per unit of time and area of the level surface; ρ is the density, $\epsilon_1 + \epsilon_2$ is the energy generated per unit of mass and time. Evidently $f'(\Phi) = df/d\Phi$ is also a pure function of Φ, thus remaining constant over the level surface.

Von Zeipel's paradox follows, when we assume that $\epsilon_1 + \epsilon_2$ is constant over the level surface; as $(d\Phi/dn)^2$ is not constant, its coefficient in (1) $f'(\Phi)$ must be zero, $f(\Phi) = \text{const.}$ and from (1)

$$\epsilon_1 + \epsilon_2 \sim \left(1 - \frac{\omega^2}{2\pi G\rho}\right). \tag{3}$$

* Received in original form 1949 December 1.

This conclusion has been criticized ordinarily from the standpoint of physical soundness; the intrinsic energy sources will never follow a law like that, and convectional transfer of heat has been advocated to obtain the peculiar prescribed form (3) of the energy generation. In this case, of course, convection is treated as a supplementary source of energy. However, the only conclusion so far is that $\epsilon_1+\epsilon_2$ cannot be constant over a level surface of a rotating star.

Let ϵ_1 be constant over a level surface, $\epsilon_1=\epsilon_1(\Phi)$ being a pure function of the potential, and ϵ_2 be the variable component of energy generation, its zero point being chosen in such a manner that the mean value of ϵ_2 over the level surface is zero. Thus, over a level surface $\overline{\epsilon_1+\epsilon_2}=\epsilon_1$. Consider the case of small oblateness, when

$$\alpha=\frac{\omega^2 r_0}{g_0} \tag{4}$$

is small (r_0 and g_0 being certain average values of radius and gravity for the level surface), so that squares and higher powers of α can be neglected. In such a case $g=-d\Phi/dn$ involves a second zonal spherical harmonic of the astrocentric co-latitude $\pi/2-\phi$,

$$-\frac{d\Phi}{dn}=g=g_0[1+A\alpha(\sin^2\phi-\tfrac{1}{3})], \tag{5}$$

where A is a factor between 2 and 1·5, g_0 the acceleration of gravity at $r=r_0$, and $\sin^2\phi_0=\frac{1}{3}$, $\phi_0=35^\circ\,15'$; the average over the level surface is evidently

$$\bar{g}=\left(\int_0^{\pi/2} g\sin\phi\,d\phi\right)\Big/\left(\int_0^{\pi/2}\sin\phi\,d\phi\right)=g_0.$$

According to (1) and (2), with (5) as the only zonal variable, both ϵ_2 and Q involve second zonal spherical harmonics similar to (5) but with different amplitude factors; their mean values over a level surface coincide therefore with their true values at $r=r_0$, $\phi=\phi_0$.

When α is small, the angle (n,r) between the normal and the radius is of the order of α, thus $\cos(n,r)$ differs from 1 by a small quantity of second order. Thus

$$\frac{d\Phi}{dn}=\frac{\partial\Phi}{\partial r}\Big/\cos(n,r)=\frac{\partial\Phi}{\partial r}$$

may be assumed.

In (1), $(d\Phi/dn)^2=g_0^2+(g^2-g_0^2)$ consists of a constant part g_0^2 and a variable $g^2-g_0^2$, the average of which is zero, according to (5) when α^2 is neglected. Separating the terms which are constant from those which are variable over a level surface in (1), we obtain two conditions:

$$f(\Phi)(4\pi G\rho-2\omega^2)-f'(\Phi)\,.\,g_0^2=\rho\epsilon_1 \tag{6}$$

and

$$-f'(\Phi)(g^2-g_0^2)=-f'(\Phi)\,.\,g_0^2\left(\frac{g^2}{g_0^2}-1\right)=\rho\epsilon_2. \tag{7}$$

Along the radius at $\phi=\phi_0$, the gravitational force is equal to the attraction of a spherical body with $r=r_0$ and the same mass and radial density distribution; thus the potential is

$$\Phi=G\int_{r_0}^{\infty}\frac{M}{r_0^2}\,dr_0+\tfrac{1}{2}\omega^2 r_0^2\cos^2\phi_0, \tag{8}$$

M denoting the mass inside the level surface of r_0, and

$$r_0 = r_e(1 - k\sin^2\phi_0) = r_e(1 - \tfrac{1}{3}k), \tag{9}$$

where r_e is the equatorial radius, k the oblateness $(a-b)/a$.

From (8), with $\cos^2\phi_0 = \frac{2}{3}$,

$$-\frac{d\Phi}{dr_0} = g_0 = \frac{GM}{r_0^2} - \tfrac{2}{3}\omega^2 r_0. \tag{10}$$

With $Q_0 = L/4\pi r_0^2$, L denoting the total radiation flux through the level surface, (10) inserted into (2) yields

$$f(\Phi) = \frac{L}{4\pi r_0^2 g_0} = \frac{L}{4\pi(GM - \frac{2}{3}\omega^2 r_0^3)}. \tag{11}$$

Further,

$$f'(\Phi) = \frac{df(\Phi)}{dr_0} \Big/ \frac{d\Phi}{dr_0} = -\frac{1}{g_0}\frac{df(\Phi)}{dr_0},$$

or from (11) and (10), with $dL = 4\pi r_0^2 \rho\epsilon_1\, dr_0$ and $dM = 4\pi r_0^2 \rho dr_0$,

$$f'(\Phi)g_0^2 = -\rho\epsilon_1 + \frac{G\rho L}{r_0^2 g_0} - \frac{\omega^2 L}{2\pi r_0^2 g_0}. \tag{12}$$

Substituting (12) and (11) into (6) we find that everything cancels, and that (6) is satisfied by arbitrary ϵ_1. No condition upon ϵ_1, the principal component of energy generation, is imposed by equation (1). The average energy generation is not affected by rotation.

Substituting now (12) into (7), a formula for the convective energy generation is obtained, with the aid of (10):

$$\epsilon_2 = \left(\frac{g_e^2}{\bar{g}_0^2} - 1\right)\left[\epsilon_1 - \bar{\epsilon}_1 \frac{\left(1 - \dfrac{\omega^2}{2\pi G\rho}\right)}{\left(1 - \dfrac{\omega^2}{2\pi G\bar{\rho}}\right)}\right]; \tag{13}$$

here $\bar{\epsilon}_1 = L/M$ and $\bar{\rho} = M/(4\pi r_0^3/3)$ are the average interior energy generation and density. Formula (13) is essentially Eddington's (**7**) formula (8) but with a little more detail. In the equatorial plane $g_e < g_0$, and as $\epsilon_1 \ll \bar{\epsilon}_1$ according to our present ideas of stellar energy generation, ϵ_2 is positive; energy must be released along the equatorial plane which, in a stable stratification such as a radiative equilibrium layer normally is, requires a downward motion along the equatorial radii and an upward polar current, with a dead line at 35° latitude.

No condition regarding molecular weight has been imposed; therefore the conclusions are valid also in the case of a radial stratification by molecular weight. The rotational currents indicated by (13) will work toward equalization of the chemical composition even when there is stable stratification by molecular weight. However, in an exhausted central portion of an advanced stellar model, the hydrogen abundance may increase outwards so fast that ϵ_1 may increase, in spite of the decreasing temperature and pressure; in such a case $\epsilon_1 > \bar{\epsilon}_1$ and by (13) the direction of the current will be reversed—up at the equator, down from the poles.

Following Eddington we may evaluate the vertical velocity of the current; as there is no actual excess of temperature, and as the convection is required to balance the prescribed amount transported by radiation, no allowance for a lateral loss of heat is to be made, as should have been done in the case of thermal

convection (**13**). Let unit mass be moving so as to change its state according to a polytropic index n; n is prescribed by the conditions of radiative equilibrium. For an infinitesimal change of state dP, dV ($V=1/\rho$), dT, the external work is equal to the sum of dq, the energy released (transported away by radiation), and the kinetic energy of the molecules stored inside,

$$-PdV=dq+c_v dT. \tag{14}$$

Together with the gas equation $PV=(\gamma-1)c_v T$, where $\gamma=c_p/c_v$, and with the polytropic equation $P\propto T^{n+1}$, this yields

$$dq=c_v dT[n(\gamma-1)-1]=c_v dT\left(\frac{n}{n_a}-1\right), \tag{15}$$

where $n_a=1/(\gamma-1)$ is the "adiabatic" value of the polytropic index. Following Eddington (**7**), call δT the potential change of temperature under adiabatic conditions. According to (**13**), equation (30),

$$\frac{\delta T}{dT}=\frac{n+1}{n_a+1}, \quad \text{whence} \quad dT=\frac{\left(1+\frac{1}{n_a}\right)}{\left(\frac{n}{n_a}-1\right)}(\delta T-dT);$$

substituting this into (15), and with $1+1/n_a=\gamma$, $\gamma c_v=c_p$, we obtain

$$dq=c_p(\delta T-dT). \tag{16}$$

Eddington (**7**) uses here c_v for c_p, which needs to be corrected.

Let the vertical velocity of the current be $v_r=dr/dt$. Evidently

$$\epsilon_2=dq/dt=c_v(dT/dr)\,.\,v_r[n(\gamma-1)-1],$$

by (15). With the aid of (**13**), equation (24), we obtain

$$\frac{dr}{dt}=v_r=\frac{\epsilon_2}{\xi c_v[n(\gamma-1)-1]}=-\frac{\epsilon_2(n+1)}{g(n-n_a)}, \tag{17}$$

where $\xi=dT/dr$. Eddington (**7**) obtains v_r too large by a factor of γ, as the consequence of the above-mentioned inaccuracy.

The effective acceleration of gravity varies over a level surface according to (5), with g_0 given by (10). For a complete concentration of mass in the centre the theorem of Clairaut yields, for an oblateness $k=\frac{1}{2}\alpha$, $A=2$; for the Earth, the observed values are $k=0{\cdot}980\alpha$ and $A=1{\cdot}539$. $A=\frac{5}{2}-k/\alpha$ is a relatively slow function of the density concentration; with Chandrasekhar's (**10**) calculations for polytropes the run of the oblateness ratio k/α is as follows:

Polytrope index n	...	4	3	2	1·5	1·0	(Earth)
ρ_c/ρ_m	∞	622	54·2	11·40	5·99	3·29	(1·8)
k/α	0·5	0·502	0·515	0·575	0·639	0·760	0·980
Interpolation	0·5	0·501	0·516	0·575	0·643	0·760	0·975

The last line gives an empirical interpolation according to $k/\alpha=0{\cdot}5+0{\cdot}856\rho_m/\rho_c$; the agreement is excellent, even in the case of the non-polytropic Earth. We may therefore assume, for a level ellipsoidal surface with $\bar{\rho}$ as the mean density inside the surface,

$$A=2-\frac{0{\cdot}856\bar{\rho}}{\rho_c}. \tag{18}$$

Although (18) is not meant to apply to an interior level surface, we may safely use it also in that case, the approximation being better than, e. g., the assumption $A = \text{const.}$

For a nearly spherical star, α being small and $g = GM_r/r^2$ practically, the expression for the vertical component velocity of the rotational heat exchange circulation becomes finally (from (17), (13), (5) and (18))

$$v_r = \frac{\left(4 - \frac{1{\cdot}7128\bar{\rho}}{\rho_c}\right)\alpha}{g} \cdot \frac{(n+1)}{(n-n_a)} \left\{ \frac{L_r}{M_r} \left[1 - \tfrac{2}{3}\alpha \left(\frac{\bar{\rho}}{\rho} - 1 \right) \right] - \epsilon_1 \right\} (\sin^2\phi - \tfrac{1}{3}), \quad (19)$$

the factors containing $\frac{2}{3}\alpha$ being retained, in order that the formula be valid also for the lowest values of the density.

For an interior point of the Sun when $\omega = 3 \times 10^{-6} = \text{const.}$, $M_r = 0{\cdot}3 M_\odot$, $r = 0{\cdot}2 R_\odot$, $g = 2 \times 10^5$, $\bar{\epsilon} = 6{\cdot}7$ erg/gm.sec., $\epsilon_1 = 0$, $n = 2{\cdot}5$, $n_a = 1{\cdot}5$, $\alpha = 6{\cdot}3 \times 10^{-7}$, $\bar{\rho}/\rho_c = \frac{1}{2}$, we get $v_r = 2 \times 10^{-10} (\sin^2\phi - \frac{1}{3})$ cm./sec. This current velocity is negligible; the maximum value in the direction of the pole, $\phi = 90°$, would correspond to a displacement of only 100 kilometres in 3000 million years. Even with a tenfold value of ω the mixing effect would still be negligible, giving a displacement of $\frac{1}{70}$ of the solar radius in 3×10^9 years. It should be safe to conclude, in the case of the Sun at least, that the mixing efficiency of the rotational currents in the interior is practically nil.

For an external subphotospheric region ((**14**), B_0'), $\omega = 3 \times 10^{-6}$, $r = 0{\cdot}95 R_\odot$, $M_r = M_\odot$, $g = 3 \times 10^4$, $\bar{\epsilon} = 2$, $\epsilon_1 = 0$, $n = 2{\cdot}0$, $\rho_c/\bar{\rho} = 63$, $\alpha = 2 \times 10^{-5}$, we obtain $v_r = 3{\cdot}2 \times 10^{-8} (\sin^2\phi - \frac{1}{3})$*, thus a value 160 times the value for the interior. In 3×10^9 years the maximum vertical displacement is 2×10^9 cm., a value which is small but not inconsiderable, amounting to two-thirds of the depth of the layer below the photosphere; thus, in the peripheral zone of the Sun rotational currents may play a noticeable role.

In fast-rotating stars conditions may be different. Our formulae may be used for order-of-magnitude estimates even with large values of α. Take for the same interior point as before $\omega = 1{\cdot}5 \times 10^{-3}$ (period of revolution 1·2 hours), $\alpha = 0{\cdot}25$, $k \simeq 0{\cdot}25$ (oblateness), thus a marginal case near instability; this gives $v_r = 6 \times 10^{-5} (\sin^2\phi - \frac{1}{3})$, covering one-fifth of the Sun's radius within ten to twenty million years. The mixing efficiency would appear quite considerable but for the inevitable stratification which would limit the circulation to separate zones, without much exchange of matter between the zones (*cf.* (**9**), p. 286, and following pages of the present paper).

2. The Coriolis deflection of thermal convection in a rotating medium breaks up the circulation into small-scale vortices (cellular or irregular) (**13**). It is otherwise with the rotational currents in a thermally stable medium, considered in the preceding section. The vertical motion is the same over a whole zone of latitude; the medium as a whole is lifted or lowered, supported by the radial force of pressure versus gravitation; it is a case of motion under a purely central force, in which case the law of conservation of angular momentum

$$\omega s^2 = \text{const.} \quad (20)$$

applies, where $s = r\cos\phi$ is the distance from the axis of rotation. This applies equally to the radial and to the meridional displacements which are the necessary

* Valid only when $\bar{\rho}/\rho < 10^5 \sim \alpha^{-1}$. If this is not the case, the sign of v_r will be reversed.

consequences of the radial movements. No vortices will be created except by friction which, however, in the absence of turbulence, is small at stellar dimensions. Differences in the angular velocity of rotation will be created which change the basic picture of von Zeipel's problem and ultimately influence the result; at the start, however, the conclusions of Section 1 should be valid and, as the Sun cannot have proceeded far from the start with respect to rotational currents, in that particular case we are entitled to apply the theory with some confidence. Considering that peripheral turbulence makes the photospheric rotation follow the rotation of the underlying radiative equilibrium layer (*cf.* also (**12**)), and assuming for the latter a radial outward displacement in the polar region of 2×10^9 cm. or $\frac{1}{35}$ part of the radius as estimated above, we should expect in 3×10^9 years a polar slowing down of rotation by $\frac{1}{18}$ and an equatorial acceleration by $\frac{1}{35}$ of the average, at photospheric level; this would give a difference in the period of rotation of 2·2 days, about 25 per cent of the observed difference. The agreement can be improved by setting the top of the radiative zone somewhat nearer to the surface than assumed in the present sample computation.

Here only radial displacements are considered; this is correct for the pole and the equator but not for intermediate latitudes. However, for an incomplete circuit as in the present case, meridional displacements directed from the pole toward the equator will always lead to an equatorial acceleration and will not change the picture. This apparent paradox may be easily understood if we consider that, although the meridional displacement away from the pole leads to a decrease in the angular velocity of rotation, the decrease is insignificant at the equator and is largest near the pole; thus the resulting angular velocity will be largest at the equator. With $s=r\cos\phi$ and $r=\text{const.}$ (20) yields $d\omega=2\omega\tan\phi\,d\phi$. If the original angular velocity, ω_0, is assumed to be uniform, the resulting angular velocity after a frictionless displacement $\Delta\phi$ is $\omega=\omega_0+2\omega_0\tan\phi\,\Delta\phi$. For $\Delta\phi<0$, or a displacement toward the equator, the angular velocity will steadily decrease from equator to pole, for any reasonable law of variation of $\Delta\phi$ with latitude.

3. The structure and stratification of the rotational circulation at an initial stage can be easily derived from the condition of continuity of flow, for the case of small oblateness as before. The radial velocity of the forced flow as given by (19) may be written as

$$v_r=v_0(\sin^2\phi-\tfrac{1}{3}), \tag{21}$$

where v_0 contains all except the zonal harmonic factor of (19) and is constant over a level surface, depending solely upon the average radius r of that surface. The radial flow of mass through a zone between $\phi_1=0$ and $\phi_2=\phi$ is

$$F_r=\int_{\phi_1}^{\phi_2}\rho v_r\,.\,2\pi r\cos\phi\,.\,r\,d\phi=-\tfrac{2}{3}\pi\rho r^2v_0\sin\phi\cos^2\phi. \tag{22}$$

The total inward flow through the equatorial zone between $\phi_1=0$ and $\phi_2=\phi_0=35^\circ15'$ is

$$F_0=-\frac{4\pi}{9\sqrt{3}}\rho r^2v_0, \tag{23}$$

being equal and opposite in sign to the total outward flow toward the polar cap (between $\phi_1=\phi_0$ and $\phi_2=90^\circ$). The flow is of the same sign as v_r, i.e. to be reckoned positive outwards.

Let v_t denote the tangential meridional component of velocity, positive when ϕ increases (motion from equator to pole). The condition of continuity requires the excess of the radial flow to be removed by the meridional displacement, $dF_r = -2\pi r \cos\phi \,.\, dr \,.\, \rho v_t$, or with (22) at $\phi = \text{const.}$ (conical lateral surface)

$$v_t = +\frac{\sin\phi\cos\phi}{3\rho r}\frac{d}{dr}(\rho r^2 v_0). \tag{24}$$

The meridional or lateral velocity through the conical surface $\phi = \phi_0$ ($\sin^2\phi_0 = \frac{1}{3}$) is

$$v_m = \frac{\sqrt{2}}{9\rho r}\frac{d}{dr}(\rho r^2 v_0); \tag{25}$$

at this surface $v_r = 0$, thus the flow is purely lateral.

The third rotational component at right angles to v_r and v_t does not influence these results as long as formulae (21) or (19) remain valid.

With (25), (24) may be written in the form

$$v_t = \frac{3v_m}{\sqrt{2}}\sin\phi\cos\phi, \tag{26}$$

v_m being a constant for a given level surface.

The equation of a stream-line (projected rotationally on a meridian plane) follows then from $dr/dt = v_r$, $r\,d\phi/dt = v_t$, (21) and (26) as

$$\theta(r) - \theta(r_0) = A(\phi), \tag{27}$$

where

$$\theta(r) = \int \frac{v_m dr}{v_0 r}, \tag{28}$$

with

$$A = -0{\cdot}3618[0{\cdot}4147 + \log(\sin\phi\cos^2\phi)],$$

$r = r_0$, $\phi = \phi_0$ being the starting coordinates for the integration; r_0 is a maximum or a minimum radius of the stream-line.

For a certain composite model "B_0'" of uniform composition (**14**) the stream-lines and the time intervals (t_0) covered by the circuit are calculated. Table I contains the basic functions (the complete description of the model is given in another paper (**14**)), Table II the characteristics of the stream-lines, all calculated with $\omega = 10^{-4}$, corresponding to a period of rotation of 17·4 hours or an equatorial velocity of rotation of 63 km./sec. and an oblateness of 0·00912 (at photospheric level). The boundary condition chosen is $\log p_p = \bar{8}{\cdot}572$, at $T_e = 6406°$, being close enough to the photospheric conditions of a model solar atmosphere in which absorption by the negative ion of hydrogen is taken into account (**11**).*

The resulting system of rotational circulation is represented graphically in Fig. 1.

There are two major circulations; one, linked with the core, limited by $r = 49{\cdot}32 \times 10^9$ cm., which contains 99 per cent of the mass, its stream-lines emanating from the pole of the core and returning to its equator; an isolated circulation of not much importance is included, around a dead point at $\phi = 35°{\cdot}2$, $r = 29{\cdot}7 \times 10^9$. Another circulation, connected with the peripheral convective regions, occupies the zone outside $r = 49{\cdot}32 \times 10^9$. The stream-lines meet the equator at different angles from 0° to 90°, whereas they leave the pole tangentially. At the boundaries of the core ($r = 7{\cdot}58 \times 10^9$) and of the peripheral convective

* For 3 per cent metals Münch's data yield $\log p_p = \bar{8}{\cdot}70$ at $T_e = 5713°$.

region ($r = 6{\cdot}1 \times 10^{10}$) singularities arise, as the velocity components become infinite ($n = n_a$, *cf.* equations (19) and (24)); this means that our equations of static equilibrium become invalid near these critical surfaces, as soon as v_r or v_t cease to be small compared with ωr; this happens, however, in a layer some metres thick and is of no practical importance. Enhanced singularities appear at the pole and the equator of the core (and of the bottom of the peripheral convective zone) which, however, are equally of little consequence.

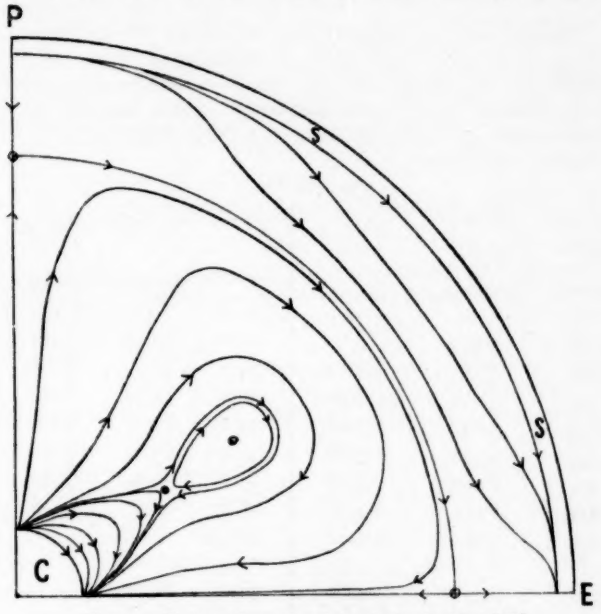

FIG. 1.—*System of rotational circulation in Model* B_0'.
The figure represents a meridional quadrant with the stream-lines projected thereon.
○: *Dead points (dead rings).*
C: Central convective region.
S: Sub-photospheric convective region.
E: Equator.
P: Pole.

More important than the spatial stratification is the "stratification in time"; the time of circulation varies from 10^7 to 10^{11} years in the interior, thus from a fraction to a large multiple of the possible life-time of the star. No complete mixing can be achieved by such a circulation. Not more than 0·2 of the inner mass can be assumed to get effectively mixed within a time interval of about 3×10^9 years, the rest being hopelessly separated; a stratification along the stream-lines themselves ensues, as the result of the changing composition and size of the core during such intervals of time (**14**). It may be inferred that in the polar direction heavier material containing less hydrogen will be sucked out from the core which gets more and more "exhausted"; a systematic increase of the mean molecular weight from the equator toward the pole over the same level surface follows. This tends to diminish the oblateness in the central region and to increase it at the periphery*; with a sufficient contrast in molecular

* This follows from $T \sim 1/\mu$ over a level surface, whereas $-dT/dn \sim \mu g$.

weight the variation of gravity over a level surface may become zero and, according to equation (13), the circulation may stop altogether at a certain distance outside the core; on the other hand, the rotational circulation will continue at an accelerated rate in the outer regions. The conclusion is that the central region around the core can never be completely mixed with the outside by rotational circulation.

TABLE I

Characteristics of Rotational Currents of Stellar Model " B_0'*"*

Uniform composition with 0·03 metal, 0·57 hydrogen, 0·40 helium content. $M=2\cdot117\times10^{33}$ gm.; $R=6\cdot308\times10^{10}$ cm. Convective core with 0·1060 of total mass, $r_1=7\cdot58\times10^{9}$ cm. $T_c=2\times10^{7}$ deg.; $\log\rho_c=2\cdot1647$; $\rho_c/\rho_m=72\cdot6$. Peripheral convective region from $r_2=6\cdot100\times10^{10}$ cm. to surface, includes $1\cdot13\times10^{-6}$ of total mass. $L_o=4\cdot825\times10^{33}$ erg/sec.

$\omega=10^{-4}$ sec.$^{-1}$

r 10^9 cm.	$\log\lvert v_0\rvert$ cm./sec.	$\log\lvert v_m\rvert$ cm./sec.	$\theta(r)$	r	$\log\lvert v_0\rvert$	$\log\lvert v_m\rvert$	$\theta(r)$
	positive	negative			positive	negative	
7·58	$+\infty$	$+\infty$	$+\infty$	31·2	$\bar{7}\cdot522$	$\bar{9}\cdot942$	−0·4780
8·0	$\bar{7}\cdot978$	$\bar{6}\cdot573$	0	32·8	$\bar{7}\cdot616$	$\bar{8}\cdot438$	−0·4801
8·8	$\bar{7}\cdot508$	$\bar{7}\cdot587$	−0·2190	34·4	$\bar{7}\cdot707$	$\bar{8}\cdot786$	−0·4844
9·6	$\bar{7}\cdot265$	$\bar{7}\cdot128$	−0·3016	36·0	$\bar{7}\cdot795$	$\bar{7}\cdot070$	−0·4913
10·4	$\bar{7}\cdot100$	$\bar{8}\cdot845$	−0·3528	39·2	$\bar{7}\cdot955$	$\bar{7}\cdot540$	−0·5146
11·2	$\bar{8}\cdot979$	$\bar{8}\cdot598$	−0·3886	42·4	$\bar{6}\cdot082$	$\bar{7}\cdot956$	−0·5573
12·0	$\bar{8}\cdot902$	$\bar{8}\cdot406$	−0·4138	45·6	$\bar{6}\cdot124$	$\bar{6}\cdot360$	−0·6419
12·8	$\bar{8}\cdot847$	$\bar{8}\cdot275$	−0·4327	48·8	$\bar{7}\cdot617$	$\bar{6}\cdot776$	−1·0448
13·6	$\bar{8}\cdot809$	$\bar{8}\cdot160$	−0·4476	49·32	$-\infty$	...	$-\infty$
					negative		
15·2	$\bar{8}\cdot776$	$\bar{9}\cdot922$	−0·4676	52·0	$\bar{6}\cdot725$	$\bar{5}\cdot239$	0
16·8	$\bar{8}\cdot789$	$\bar{9}\cdot681$	−0·4783	53·6	$\bar{5}\cdot164$	$\bar{5}\cdot499$	+0·0812
18·4	$\bar{8}\cdot829$	$\bar{9}\cdot424$	−0·4835	56·0	$\bar{5}\cdot773$	$\bar{5}\cdot960$	+0·1615
20·0	$\bar{8}\cdot889$	$\bar{10}\cdot820$	−0·4852	58·4	$\bar{4}\cdot455$	$\bar{4}\cdot575$	+0·2213
20·6	...	$-\infty$	−0·4853	59·2	$\bar{4}\cdot726$	$\bar{4}\cdot860$	+0·2395
		positive					
21·6	$\bar{8}\cdot965$	$\bar{9}\cdot044$	−0·4850	59·6	$\bar{4}\cdot876$	$\bar{3}\cdot073$	+0·2494
23·2	$\bar{7}\cdot048$	$\bar{9}\cdot468$	−0·4837	60·0	$\bar{3}\cdot043$	$\bar{3}\cdot408$	+0·2623
24·8	$\bar{7}\cdot138$	$\bar{9}\cdot661$	−0·4817	60·4	$\bar{3}\cdot244$	$\bar{2}\cdot055$	+0·2892
26·4	$\bar{7}\cdot232$	$\bar{9}\cdot745$	−0·4796	60·8	$\bar{3}\cdot617$	$\bar{1}\cdot197$	+0·4071
28·0	$\bar{7}\cdot330$	$\bar{9}\cdot669$	−0·4780	61·00	$+\infty$	$+\infty$	$+\infty$
29·6	$\bar{7}\cdot426$	$\bar{10}\cdot390$	−0·4774				
29·7	...	$-\infty$	−0·4774				

In the course of the circulation, especially at its initial stage (in which most of our chosen model remains even at the high assumed speed of rotation), the displacements are such that conservation of angular momentum leads to accelerated rotation in the equatorial plane; the amplitude in gravity is evidently increased by this effect, which thus tends to accelerate the circulation itself should the von Zeipel–Eddington theorem remain valid. However, as ω is no longer constant, equation (1) cannot be strictly applied. In the time intervals considered

here, however, the contrast in molecular weight will be the more important factor and will stop the circulation in the interior in spite of the possible contrary effect of the equatorial acceleration of rotation.

For a solar speed of rotation, $\omega = 3 \times 10^{-6}$, the time intervals given above are to be increased by a factor of about 1000; the circulation becomes so slow that its mixing effect during the life-time of a star is practically nil; the nuclear reactions in the core proceed much faster than the minute displacements produced by rotational circulation. The system of circulation differs in such a case from the preceding; no reversal of the direction of v_r occurs because $1 > \frac{2}{3}\alpha(\bar{\rho}/\rho - 1)$ remains valid in (19) all through the radiative equilibrium zone. This zone constitutes one system of circulation, the central and the peripheral convective regions being linked together; however, the time of circulation from core to periphery, 3×10^{13} years, is so large that the link has no practical significance.

TABLE II

Stream-lines of Rotational Currents in Model " B_0' " (14)

$\omega = 10^{-4}$ sec.$^{-1}$

r = radius in 10^9 cm.; ϕ = latitude; t_0 = time of complete circuit in years; m_i = fraction of total mass of the model inside the stream-line surface of revolution

t_0	m_i	ϕ				
		0°; 90°	20°	35°·2	50°	75°
		r				
$6{\cdot}3 \times 10^7$	0·12	7·581	7·928	8·00	7·941	7·685
$7{\cdot}0 \times 10^8$	0·14	7·58	8·58	8·80	8·62	7·89
$1{\cdot}7 \times 10^9$	0·16	7·58	9·17	9·60	9·26	8·04
$3{\cdot}4 \times 10^9$	0·19	7·58	9·77	10·40	9·89	8·16
$1{\cdot}8 \times 10^{10}$	0·28	7·58	11·85	13·60	12·13	8·51
$4{\cdot}5 \times 10^{10}$	0·36	7·58	13·18	16·80	13·60	8·66
$1{\cdot}1 \times 10^{11}$	...	7·58	13·58	20·00	14·11	8·72
$7{\cdot}2 \times 10^{10}$	...	...	...	21·60 34·56	...	...
$1{\cdot}1 \times 10^{11}$	...	7·58	13·69	35·00	14·23	8·73
$7{\cdot}3 \times 10^{10}$	...	7·58	16·46	39·30	34·27 23·02 18·62	8·92
$4{\cdot}4 \times 10^{10}$	...	7·58	44·32	45·60	44·63	10·58
$4{\cdot}8 \times 10^{10}$	0·986	7·58	48·66	48·80	48·68	47·35
∞	...	7·58 61·00	49·32	49·32	49·32	49·32
$8{\cdot}6 \times 10^7$	...	61·00	52·68	52·00	52·54	60·29
$1{\cdot}2 \times 10^7$	...	61·00	57·34	56·00	57·06	60·82
5×10^5	...	61·00	60·49	60·00	60·43	60·88

The internal law of rotation of the Sun is unknown; it is not impossible that ω increases inwards but, as shown by the above computations, even a much larger value of $\omega \sim 10^{-4}$ would not make much practical difference. If the suggestion, based on the evidence of lithium abundance, that the Sun to a considerable depth has gone through a phase of turbulent mixing at an early stage of its life corresponds to reality, it is very likely that uniform angular velocity

(as the result of eddy-viscosity) represents the initial state of solar rotation, except, perhaps, for a small metallic core of meteoric origin.

The author acknowledges with gratitude the assistance given by Professor T. G. Cowling in the form of critical comments and help in preparing the manuscript for press.

Armagh Observatory,
Northern Ireland:
1950 *September* 26.

References

(1) H. von Zeipel, *Festschrift f. H. von Seeliger*, 144, 1924.
(2) A. S. Eddington, *The Observatory*, **48**, 73, 1925.
(3) H. Vogt, *A.N.*, **223**, 229, 1925.
(4) H. Vogt, *Aufbau u. Entwicklung d. Sterne*, Leipzig, 1943.
(5) S. Rosseland, *Ap. J.*, **63**, 342, 1926; *Astrophys. Norvegica*, **2**, 173, 1936.
(6) G. Randers, *Astrophys. Norvegica*, **3**, 97, 1939.
(7) A. S. Eddington, *M.N.*, **90**, 54, 1929.
(8) E. Öpik, *Proc. Roy. Irish Acad.*, **53** A, 1, 1949; *Contrib. Armagh Obs.*, No. 2.
(9) A. S. Eddington, *Internal Constitution of the Stars*, Cambridge, 1926.
(10) S. Chandrasekhar, *M.N.*, **93**, 390, 449, 462 and 539, 1933.
(11) G. Münch, *Ap. J.*, **106**, 217, 1947.
(12) J. Wasiutynski, *Astrophys. Norvegica*, **4**, 1946.
(13) E. Öpik, *M.N.*, **110**, 559, 1950.
(14) E. Öpik, *Proc. Roy. Irish Acad.*, **54** A, 49, 1951; *Contrib. Armagh Obs.*, No. 3.

A DIFFRACTION THEORY OF THE SCINTILLATION OF STARS ON OPTICAL AND RADIO WAVE-LENGTHS

C. G. Little

(Communicated by A. C. B. Lovell)

(Received in revised form 1950 December 27) *

Summary

A review of current theories of the scintillation of stars on optical wave-lengths shows that the refraction theory of scintillation requires excessive atmospheric density gradients, and fails to explain the observed scintillation in colour, whilst the physiological explanations are insufficient to explain all the observed phenomena. A new theory, in which the scintillation phenomena are attributed to Fresnel diffraction at a non-homogeneous atmospheric layer, is shown to explain the observed effects, and to require considerably smaller density gradients. A similar theory, taking into account the effect of a wave-length change of $\times 10^7$, is shown to explain the observed fluctuations in intensity of radio waves from the localized extra-terrestrial sources of radio noise.

1. *Introduction.*—Neither of the two main theories of the scintillation of stars on optical wave-lengths appears to be fully satisfactory. The physiological theory, as developed by Hartridge and Weale (**1**), fails to explain all the observed phenomena. These authors have shown that under certain circumstances the human eye registers scintillations even when illuminated by a constant-intensity source, and have suggested that the scintillation of stars may be due to this property of the eye. However, photographic observations by Gaviola (**2**), and photoelectric observations by Boutet (**3**), indicate that the intensity of the light from a star received by the eye does in fact vary, and hence that physiological factors cannot provide a complete explanation of the phenomena.

The refraction theory of scintillation (**2, 4**) explains the production of light and dark striae some centimetres apart on the Earth's surface by the focusing effect of irregularities of the same order of size and situated at a temperature inversion layer at a height of some $3\frac{1}{2}$ km., but it will be shown that the theory requires excessively high density gradients.

Fluctuations in the intensity of the radio emission from the localized sources of galactic noise were first observed by Hey, Parsons and Phillips (**5**) and recent work (**6, 7**) has shown that these fluctuations are introduced by a local medium and may therefore be analogous to scintillation on optical wave-lengths.

In this paper the effect of Fresnel diffraction at a non-homogeneous transmitting layer is considered. It is shown that such a mechanism is capable of explaining the observed optical and radio phenomena by invoking known irregularities in the atmosphere and ionosphere respectively.

2. *The refraction theory of scintillation on optical wave-lengths.*—The refraction theory of the scintillation of stars on optical wave-lengths explains the production of striae on the Earth's surface by means of the focusing effect of atmospheric irregularities at a temperature inversion layer (Fig. 1).

* Originally submitted 1950 May 3.

An analysis of the theory, given below, shows that it may be criticized on three main accounts:—

(*a*) It requires excessively high atmospheric density gradients.

(*b*) The atmospheric "lenses" postulated by the theory are so small that diffraction considerations show that they would have negligible focusing effect.

(*c*) The theory fails to explain the observed scintillation in colour.

The refraction theory as developed by various workers (**2, 4, 10**) postulates the presence of atmospheric "lenses", both convergent and divergent, spaced some 5 cm. apart at a range of about $3\frac{1}{2}$ km. from the observer. These will, of course, be irregular in shape, position and size, but as a simplification they may be idealized to a series of perfectly cylindrical lenses some 5 cm. apart, of radius of curvature ~ 2 cm. and at a range of $3\frac{1}{2}$ km.

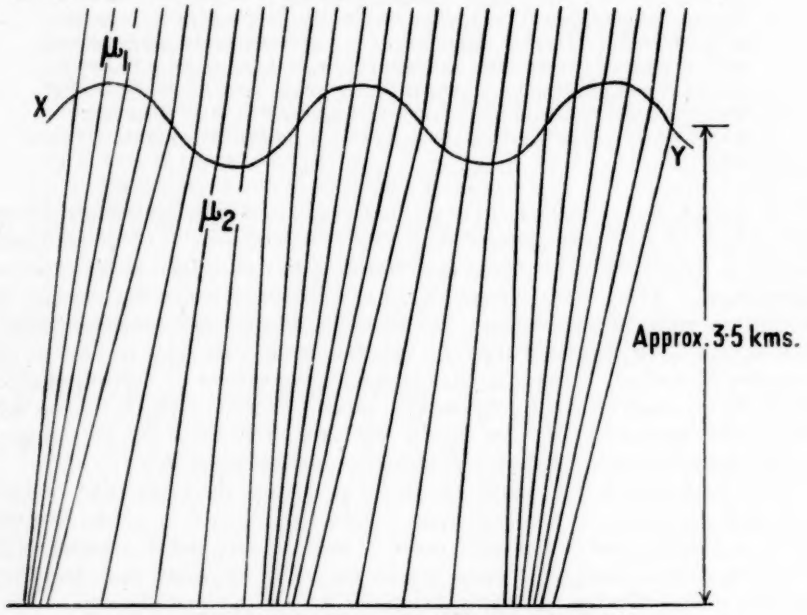

FIG. 1.—*The Refraction Theory of Scintillation (after Gaviola).*

XY represents the irregular boundary between two layers of air of different refractive indices, μ_1 and μ_2. The boundary is taken to be at a height of approximately $3\frac{1}{2}$ km. and the irregularities in its surface, some 5 cm. apart, are thought to redistribute the light from a star by refraction into striae on the Earth's surface.

For such a lens we may write:

$$\frac{1}{f} = (\mu_2 - \mu_1)\frac{2}{r},$$

where f is the focal length of the lens, r is the radius of curvature (~ 2 cm.) and μ_2 and μ_1 are the refractive indices of the lens and the surrounding air respectively.

In order that the focal length of the lens should be of the order of $3\frac{1}{2}$ km., it will be necessary that $(\mu_2 - \mu_1) = \frac{2}{r}\left(\frac{1}{3{\cdot}5 \times 10^5}\right)$ or $(\mu_2 - \mu_1) \simeq 3 \times 10^{-6}$, since $r = 2$ cm.

The refractive index of air at N.T.P. is 1·0003 and changes by $1{\cdot}0 \times 10^{-6}$ for a 0·3 per cent change in density. Hence, if $(\mu_2 - \mu_1)$ is to be 3×10^{-6}, a 1 per cent change in atmospheric density would be required in a distance of the order of 2 cm.

Such atmospheric density gradients are considerably in excess of those known to exist even under turbulent conditions at the Earth's surface (**8**) and hence could not be expected to occur at heights of the order of 4 km. It is of interest that this difficulty was first pointed out by Lord Rayleigh (**9**), whose comments, however, do not appear to have been considered in recent discussions on scintillation phenomena.

A more fundamental difficulty is that diffraction considerations show that lenses of the size and range postulated could not focus the light effectively. The resolving power of a cylindrical lens is given by λ/a, where λ is the wave-length and a is the lens aperture. Hence the image formed of a distant source will be of diameter $D = 2f\lambda/a$. Substituting the values of f, λ and a postulated by the refraction theory, we have $D \simeq 10$ cm. for $\lambda = 6000$ A., and therefore the diffraction disk is larger than the lens itself, i.e. the lens is too small to focus the light appreciably.

A third failure of the refraction theory is its inability to explain the observed scintillation in colour at high angles of elevation. This has been attributed to the chromatic aberration of the atmospheric lenses (**10**). However, since $(\mu - 1)$ differs by only 1 per cent for red and green-blue light, the various colours will be concentrated to approximately the same degree by any given atmospheric lens, and scintillation in colour would therefore not be expected on a simple refraction theory.

3. *Some general considerations of diffraction at an irregular screen.* (*a*) *Introduction.*—The discussion in the last section has shown that the atmospheric lenses postulated to explain optical scintillation phenomena are smaller than the first Fresnel zone in the disturbing region. This fact suggests that the phenomena should best be considered as due to a Fresnel diffraction mechanism in which the idea of individual atmospheric lenses is replaced by the consideration of the distortion of the Fresnel Half Period Zone pattern of a plane wave viewed through a medium of slightly non-homogeneous refractive index.

Such considerations indicate that the change in relative areas of odd and even numbered zones due to varying optical path lengths in the medium can markedly affect the observed intensity. Diffraction theory shows that the complete reversal of phase of one of the zones will increase the received intensity by 25 or 9 times, according to whether the zone is even or odd in number (Fig. 2 (*b*) and (*c*)). Such a phase change could hardly occur from a random distribution of refractive index irregularities, but a change in the relative area of the odd and even numbered zones, at any particular instant, of about 0·2 of a zone would not be unlikely. In such a case the received intensity would be increased or decreased by about three times, depending upon the area affected and the change in phase (Fig. 2 (*d*) and (*e*)).

It is not practicable to pursue these simple Fresnel zone considerations to explain the scintillation phenomena due to an irregular diffracting screen, since it would be necessary to sum the effect of each of the resultant distortions of the Fresnel zone pattern *over the whole wave-front*. In this case statistical methods must be used, such as those developed by Booker, Ratcliffe and Shinn (**11**).

These authors have shown that the effect of an irregular diffracting screen may be analysed in terms of the generalized auto-correlation function of the electromagnetic field strength across a plane immediately below the disturbing layer.

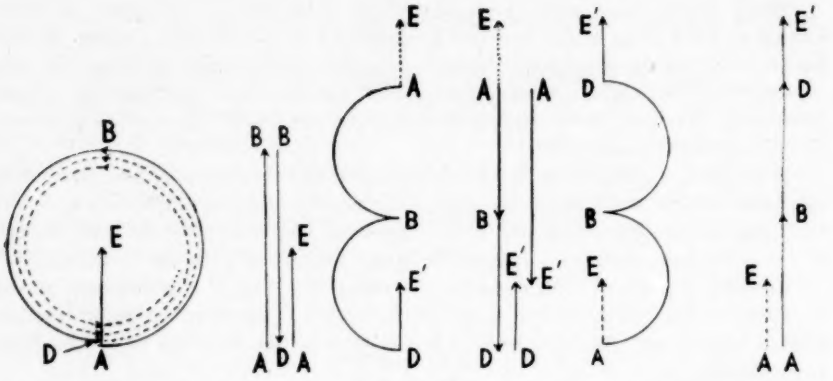

(*a*) *Phase change=0. No resultant change in amplitude.*

(*b*) *First zone changed by π. Amplitude increased three times, intensity nine times.*

(*c*) *Second zone changed by π. Amplitude increased to five times, intensity 25 times.*

(*d*) *Central portion of first zone advanced by $\phi < \pi/2$. Amplitude increased to 1·7 times, intensity to approximately three times.*

(*e*) *Central portion of first zone retarded by $\phi < \pi/2$. Amplitude decreased to 0·6 times, intensity to 0·36 times.*

FIG. 2.—*Effect of Distorting the Fresnel Zone Pattern. Amplitude–Phase Diagrams.*

AB=resultant of first zone.
BD=resultant of second zone.
DE^1=resultant of all subsequent zones (assumed undistorted).
AE=resultont of undistorted pattern.
AE^1=resultant of distorted pattern.

It has been proved (11) that the average angular power spectrum observed by a recording device receiving radiation from an irregular diffracting screen is the Fourier transform of the average auto-correlation function $\rho_E(\xi)$* of the wave-field across a plane immediately below the disturbing region. This means that an observer receiving radiation through an optical screen possessing irregular transmission properties receives radiation not only along the line of sight but from a cone whose angle is determined by the auto-correlation function $\rho_E(\xi)$, i.e. by the "average size" of the irregularities in the wave-front.

* See appendix for definition of the auto-correlation function.

For the optical and radio wave-lengths considered in the present paper, absorption or reflection in the atmosphere or ionosphere can be neglected, and the amplitude of the wave-field immediately below the disturbing layer may be taken as constant. However, due to the differing path lengths of the radiation through the disturbing regions, the emergent wave-front will be distorted and we now proceed to discuss the effects of this distortion at different distances below the disturbing layer. In this connection it will be found that the ratio of the radius of the first Fresnel zone, $\sqrt{(R\lambda)}$, to the distance ξ_0 at which $\rho_E(\xi)$ falls to zero is an important criterion determining the type of scintillation phenomena observed.

(*b*) $\sqrt{(R\lambda)}$ *large compared with* ξ_0.—It is proved in the appendix that when $\sqrt{(R\lambda)} \simeq \xi_0$, the angle subtended by one irregularity in the emergent wave-front is approximately equal in size to the received cone of radiation. By the property of Fourier transforms, if ξ_0 is now taken to be small compared with $\sqrt{(R\lambda)}$, the received cone of radiation will be large compared with the angle subtended by the first Fresnel zone. But since the irregularities in the emergent wave-front are small compared with the first Fresnel zone, this means that a large number* of irregularities are contributing to the observed intensity at any given point. These irregularities have random phase and hence the resultant intensity will have a Rayleigh distribution.

A further point of interest in this case is the effect of varying the observing wave-length slightly, on the assumption that the *phase* change introduced by an irregularity in the disturbing region is independent of wave-length. The phase of a point on the wave-front at the extreme edge of the received cone relative to the centre point is critically dependent upon the wave-length (owing to the large width of the cone relative to the first Fresnel zone) and it can be shown, on the assumption that the irregularities are large in size compared with λ, that if N is the ratio of the radius of the first Fresnel zone to the size of the irregularities, a change in the wave-length of λ/N^2 is sufficient to produce an uncorrelated scintillation record.

In the optical case, where the human observer uses a band-width of approximately one octave, this difference between the scintillations on different wave-lengths could be an important factor limiting the degree of scintillation observed. For instance, if the scintillations cease to correlate for differences in frequency of only 0·01 octaves, approximately 100 independent scintillation records would be observed simultaneously and the total resultant degree of scintillation would therefore be reduced to approximately one-tenth of that on a single wave-length.

(*c*) $\sqrt{(R\lambda)}$ *small compared with* ξ_0.—In this case the Fourier transform of $\rho_E(\xi)$ is small compared with that of the first Fresnel zone, and hence the received cone incident at a point on the Earth's surface is smaller than that subtended by the first Fresnel zone and therefore is considerably smaller than that subtended by the irregularity itself. This means that the wave-front is almost plane over the acceptance cone and hence the degree of scintillation will be very small. Also, owing to the very small variation in phase across the cone there will be a considerable degree of correlation between the scintillations on different wave-lengths, and therefore scintillation in colour would not be observed.

* Approximately N^4, where $N = \sqrt{(R\lambda)}/\xi_0$. The angular width of the received cone will be N times larger than that of the first zone and therefore covers $N^2 \times$ the area. But there are approximately N^2 irregularities per zone and hence the total number of effective irregularities is approximately N^4.

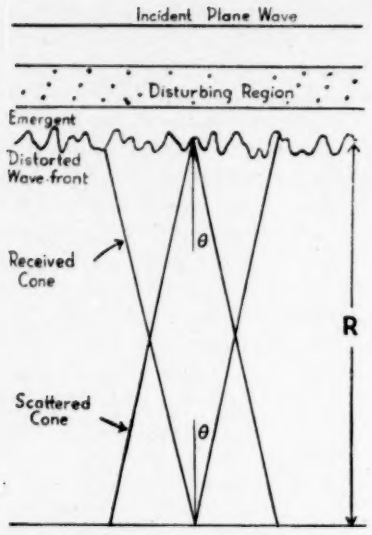

(a) *Diffraction from an irregular screen.*

The width of the scattered cone of radiation is determined by the auto-correlation function $\rho_E(\xi)$ across the emergent wave-front.

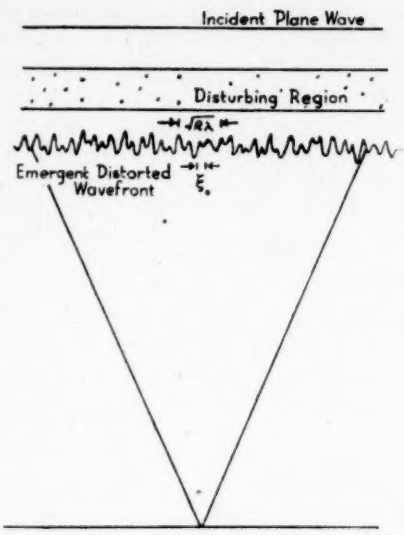

(b) $\sqrt{(R\lambda)} > \xi_0$.

The scattered cone of radiation is large compared with the angle subtended by one irregularity in the emergent wave-front.

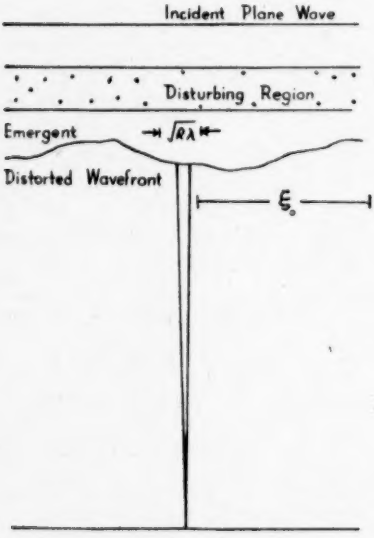

(c) $\sqrt{(R\lambda)} < \xi_0$.

The scattered cone of radiation is small compared with the angle subtended by one irregularity in the emergent wave-front.

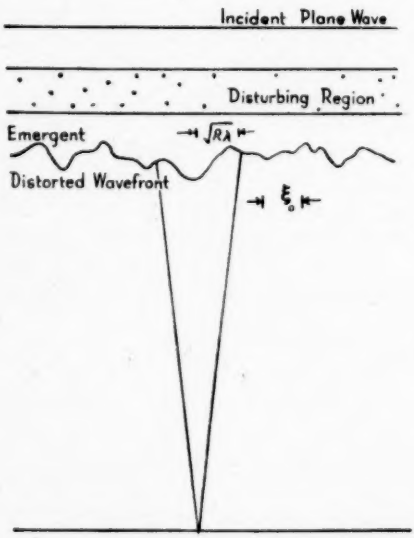

(d) $\sqrt{(R\lambda)} \simeq \xi_0$.

The scattered cone of radiation is approximately the same size as the angle subtended by one irregularity.

FIG. 3.—*Diffraction from an Irregular Screen.*

N.B.—The distortion of the emergent wave-front has been considerably exaggerated.

(*d*) $\sqrt{(R\lambda)}$ *approximately equal to* ξ_0.—In this case, as shown in the appendix, the received cone is approximately that subtended by an individual irregularity. The intensity observed will therefore depend critically upon the nature of the curvature of the wave-front inside the acceptance cone. The degree of scintillation will be considerable, but owing to the narrowness of the scattering cone, there will be a higher degree of correlation between the scintillation phenomena on different wave-lengths than in the case for $\sqrt{(R\lambda)}$ large compared with ξ_0. The limit in the optical case will be imposed by the fact that the phase change introduced by the irregularities is not constant with wave-length but is proportional to $1/\lambda$, and also that the width of the acceptance cone is proportional to λ.

(*e*) *The dimensions of the Fresnel diffraction pattern.*—It is also proved by Booker, Ratcliffe and Shinn (**11**) that the generalized auto-correlation function across the Fresnel diffraction pattern (i. e. across the scintillation pattern observed at ground level) is the same as that across the emergent wave-front itself. This result means that by observing the dimension of the diffraction pattern at ground level we are able to deduce the size of the distortions in the wave-front as it emerges from the disturbing region.

The observation that the "striations" in the scintillation patterns are some 5 cm. apart means therefore that the phase of two points more than 5 cm. apart on a plane immediately below the disturbing region is not correlated, i. e. that the distance over which the emergent wave-front is plane (to better than $\lambda/4$) is of the order of 5 cm.

4. *The application of the diffraction considerations to optical scintillation.* (*a*) *The range of the disturbing region.*—The observations of Respighi (**12**) and Ellison (**10**) on colour scintillation indicate that there is in general no close correlation between the scintillation patterns of light of wave-lengths differing by more than about 1000 A. This fact therefore suggests (by the reasoning of Section 3 (*a*), (*b*), (*c*), (*d*)) that the irregularities in the emergent wave-front are of the order of size of the first Fresnel zone $\sqrt{(R\lambda)}$. But by the theorem of Booker, Ratcliffe and Shinn quoted in Section 3(*e*), the observation that the "striations" in the scintillation pattern observed at ground level are some 5 cm. apart must mean that the irregularities in the emergent wave-front are some 5 cm. in size. Hence by writing $\sqrt{(R\lambda)} \simeq 5$ cm. we find that the disturbing region is at a distance of approximately 4 km., and that the angle subtended by these irregularities in the emergent wave-front is approximately $2\frac{1}{2}$ seconds.

(*b*) *Physical requirements of the diffraction theory.*—The total increase in optical path length introduced by the presence of the Earth's atmosphere is about $4 \times 10^6\,\lambda$ at normal incidence for $\lambda = 6000$ A. The above result therefore indicates that the path change introduced by the atmosphere varies irregularly by about one part in 10^7 for two points 5 cm. apart at the Earth's surface. These variations may have been introduced by the passage of the light through an individual, small, relatively strong irregularity, or through a number of weaker irregularities. If the irregularities are assumed to be of the order of 10 cm. in size (**8**) the density gradient required is of the order of 0·003 per cent in 5 cm. for a disturbing region 0·2 km. thick. Such gradients (approximately one-thousandth of those required for the refraction theory) are of the same order of magnitude as the mean vertical density gradient in the disturbing region, and are about one-fiftieth of those observed under turbulent conditions at ground level.

(*c*) *The duration of individual scintillations.*—As the star moves across the sky, the cone of light received at a single point on the ground moves relative to the

optical depth irregularities. The ratio of the angular subtension of the irregularities in the wave-front to the angular velocity of the star gives an estimate of the duration of the scintillations. For stars of declination 0° the rate of motion is a maximum and is about 15 seconds per second. Since the angular subtension of the irregularities is about 3 seconds (Section 4(*a*)) this suggests that the scintillation period should be of the order of 0·2 second. However, winds having a component of velocity 30 km./hr. in the plane of the emergent wave-front will reduce the scintillation period to about 0·01 second. Owing to the persistence-of-vision effect in the retina of the eye only the frequency components of the scintillations of less than approximately 30 cycles per second will be observed by the eye. This may well be the explanation of the comparative absence of scintillation on a windy night, although it should be borne in mind that a strong wind might tend to destroy the irregularities responsible for scintillations.

(*d*) *Scintillation in colour.*—The diffraction considerations described in Section 3 introduce colour effects in two ways :—

(i) The angular width of the cone of light incident at a given point on the Earth's surface is proportional to the wave-length.

(ii) The phase change introduced by a given irregularity is proportional to $1/\lambda$.

These two effects combine to cause light of different wave-lengths to be distorted in different ways, and hence to make the star scintillate in colour. This is true of all angles of elevation. In addition, however, there is a third effect, important only at low angles of elevation. For stars at elevation lower than about 15° the incident cones of radiation for red and blue light are separated by more than 2 seconds (owing to dispersion effects in the atmosphere) and hence the two cones are affected by different atmospheric irregularities. For this reason we would expect scintillation in colour to be more marked when the sources are at low angles of elevation.

(*e*) *Variation of scintillation activity with angular subtension of source.*—If the source subtends an angle very much less than that subtended by one irregularity, each point of the source will be affected similarly by the irregularity and the source will therefore be observed to scintillate as a whole. If, however, the source subtends an angle large compared with that subtended by an irregularity, then the different parts of the sources no longer scintillate in the same manner, an increase in the intensity from one point tends to be compensated by a decrease from some other point, and the source will therefore not be observed to scintillate.

This result is well borne out by the behaviour of the planets whose semi-diameters range from about 1 second to about 30 seconds. The smallest ones are not visible to the human eye and scintillation information is scanty, but those of middle angular subtensions are rarely found to scintillate and the larger ones very infrequently or never.

(*f*) *Changes in the apparent position of the source.*—Due to the phase-distorting irregularities in the disturbing region, the phase-gradient across an observing plane will not be uniform and the apparent position of the star will vary irregularly. The amplitude of these angular deviations will be given approximately by $(\lambda/2)/\xi_0$, i.e. by the ratio of the deviation of the wave-front from a plane to the linear dimensions of the irregularities. On optical wave-lengths the apparent position of the star would therefore be expected to change

irregularly, at the scintillation frequency, by ~ 1 second of arc. This is in good agreement with experimental observations (**4**).

(*g*) ***The production of striations.***—As described in Section 3 (*e*) the theoretical work of Booker, Ratcliffe and Shinn shows that the generalized auto-correlation function of the Fresnel diffraction pattern is the same as that of the emergent wave-front. If now for some reason (e. g. an atmospheric wind) the atmospheric irregularities are not isotropic, the generalized auto-correlation function of the diffraction pattern at ground level will be a function of ***direction*** across the ground. In cases where the auto-correlation function varies considerably with direction the diffraction pattern will take the form of an approximately parallel series of bands or "striae" of light and shade, instead of an irregular series of randomly shaped and orientated patches.

5. ***Comparison of the refraction and diffraction theories of the scintillation of stars on optical wave-lengths.***—The two theories may be summarized and compared by means of the two tables given below. Table I summarizes the requirements of the two theories, whilst Table II summarizes the manner in which they explain the observed phenomena.

TABLE I

Physical Requirements of the Refraction and the Diffraction Theories

Assumptions of Theory	Refraction Theory	Diffraction Theory
Range of disturbing region	Approx. 3·5 km.	Approx. 3·5 km.
Atmospheric density gradient	0·5 per cent per cm.	0·0006 per cent per cm.
Equivalent atmospheric temperature gradient	1·5 deg. C. per cm.	0·002 deg. C. per cm.
Size of irregularities	Approx. 5 cm.	Approx. 5 cm.

TABLE II

Explanation of Observed Phenomena on the Refraction and the Diffraction Theories

Observed Phenomena	Explanation on the Refraction Theory	Explanation on the Diffraction Theory
Scintillation in colour	Not explicable, except for stars very low on the horizon.	Explains scintillation in colour at all angles of elevation.
Variation of degree of scintillation with size of source	Explains these phenomena as due to refraction by atmospheric waves at the narrow boundary of two atmospheric layers of different density. Requires abnormal atmospheric density gradients.	Explains scintillation phenomena as due to diffraction by atmospheric irregularities in a relatively thick disturbing region. Requires normal atmospheric density gradients.
Duration of individual scintillation		
Changes in apparent position of the stars		

6. ***The application of the diffraction considerations to radio wave-lengths.*** (*a*) ***Introduction: the experimental observations of scintillation effects on radio wave-lengths.***—Fluctuations in the received intensity of the radio emissions of extra-terrestrial origin were first observed by Hey, Parsons and Phillips (**5**). The subsequent discovery of localized sources of radio emission (or radio stars) (**16, 17**) led to the general belief that such fluctuations were due to the variations in the emission from the sources. Recent work by Smith (**6**) and Little and Lovell (**7**)

has shown that receivers more than 20 km. apart on the Earth's surface register different scintillations and hence the fluctuations must be locally impressed. The suggestion that these fluctuations could be explained in terms of the distortion of the Fresnel zone patterns by irregularities in the ionosphere was made by Little and Lovell (**7**) and the application of the diffraction theory is here given in more detail.

(*b*) *The range of the disturbing layer.*—Experiments, to determine the correlation between radio scintillations observed at one site on different frequencies, have shown that in general there is no correlation between records taken at frequencies differing by 30 per cent (**13**). More recent work (**20**) has indicated that good correlation exists up to frequency differences of the order of 5 per cent to 10 per cent. In view of the diffraction considerations of Section 3, these results suggest that the irregularities in the emergent wave-front have dimensions of the order of the first Fresnel zone at the range of the emergent wave-front. Spaced receiver observations (**6, 7**) have shown that the correlation between fluctuation records at the same frequency remains good up to spacings of about 4 km. and, by the second theorem of Booker, Ratcliffe and Shinn (Section 3 (*e*)), this means that the irregularities in the emergent wave-front are approximately 5 km. in size. Hence, equating $\sqrt{(R\lambda)}$ to 5 km., we obtain a figure of $R \simeq 4000$ km. for $\lambda = 6$ metres. However, this relationship between $\sqrt{(R\lambda)}$ and ξ_0 is only an approximate one and, owing to the square root term, the figure for the range of the disturbing region is liable to considerable inaccuracy. In order to determine the probable location of the disturbing region more exactly, it is necessary to make use of other information, such as that obtained by correlating the occurrence of galactic noise fluctuations with anomalies in the various ionospheric layers.

(*c*) *Correlation of scintillation activity with the presence of F_2 ionospheric irregularities.*—An analysis of the occurrence of galactic noise fluctuation at the transit of the Cygnus and Cassiopeia point sources, during the period 1949 May 1 to 1950 November 30, and of the occurrence of "spread F" conditions in the F_2 layer is given elsewhere (**14**). It is sufficient to state here that a mutual coincidence of at least 75 per cent exists between the occurrence of radio scintillations (at transit) and the observation (by ionospheric workers) of "spread" or "diffuse" echoes from the F_2 layer. These echoes are thought to be due to the presence of electron clouds of varying density and height in the layer. (No similar significant correlation has been found with sporadic E phenomena.)

This high degree of correlation suggests that the galactic noise fluctuations do indeed originate in the F_2 layer. If we substitute the height of the maximum electron density in the F_2 layer (approx. 400 km.) we find, using a figure of 5 km. for ξ_0, that $\sqrt{(R\lambda)}/\xi_0$ varies between 0·3 for a source in the zenith to 0·7 for a source at low angles of elevation. The diffraction considerations of Section 3 indicate that these values for the ratio $\sqrt{(R\lambda)}/\xi_0$ are sufficiently near to unity to explain scintillation phenomena of the type observed.

(*d*) *Physical requirements of the diffraction theory to explain the observed radio scintillation phenomena.*—The spaced receiver observations already referred to suggest that the ionospheric irregularities are of the order of 5 km. in size. Since scintillation phenomena will not be observed unless the irregularities possess sufficient refractive index changes to increase or decrease the radio path length by about half a wave-length, it is possible to estimate the minimum change in electron density required to produce scintillations.

The refractive index of an ionospheric layer to a radio wave of frequency f is given by

$$\mu^2 = 1 - \frac{Ne^2}{\pi m f^2},$$

where N = number of electrons/c.c., m = mass of electron, and e = charge of electron.

If f_c is the critical frequency corresponding to an electron density N, we have

$$\mu = \left\{1 - \left(\frac{f_c}{f}\right)^2\right\}^{1/2}.$$

In the case under discussion f is large compared with f_c, and hence we may write

$$\mu = 1 - \tfrac{1}{2}(f_c/f)^2.$$

If $\Delta\mu$ is the difference in refractive index between an ionospheric irregularity and the surrounding ionosphere,

$$\Delta\mu = \frac{1}{2f^2}(f_I^2 - f_c^2),$$

where f_I is the critical frequency of the irregularity itself. The change in radio path length, introduced by an irregularity of linear dimension L and refractive index differing by $\Delta\mu$ from the surrounding medium, will be $L\Delta\mu/\lambda$ wave-lengths. If this is to equal $\frac{1}{2}\lambda$ (the requirement for the production of scintillations) we have

$$\left(\frac{L}{\lambda}\right)\frac{1}{2f^2}(f_I^2 - f_c^2) = \tfrac{1}{2}.$$

Taking $\lambda = 6$ metres, $L = 5000$ metres and $f_c = 3{\cdot}0$ Mc./s., we have

$$f_I^2 = \frac{f^2\lambda}{L} + f_c^2 = 12 \times 10^{12} \quad \text{or} \quad f_I \simeq 3{\cdot}5 \text{ Mc./s.}$$

If $\Delta\mu$ is taken as negative, we obtain $f_I \simeq 2{\cdot}5$ Mc./s. The corresponding electron densities are $7{\cdot}5 \times 10^4$ electrons/c.c. and $1{\cdot}5 \times 10^5$ electrons/c.c. These figures are based on the assumption that the disturbing region is only one irregularity thick. If there is more than one irregularity in the line of sight, smaller changes in electron density would be sufficient to produce the required distortion of the emergent wave-front. Investigations of the F region of the ionosphere indicate that under strong spread F conditions the critical frequency can extend over a range of two or more Mc./s. (**19**). Such a range would appear to be more than sufficient to produce radio scintillations.

(*e*) *The durations of individual fluctuations.*—As in the optical case, it is possible to explain the observed durations in terms of the ratio of the angular subtension of the irregularities to the angular velocity of the source; and of the ratio of the size of the irregularities to the velocity of the wind in the disturbing region. The angular subtension of one irregularity in the emergent wave-front varies between some 40 minutes (in the zenith) to about 10 minutes (at low angles of elevation). Since the angular velocity of the source is of the order of 10 minutes of arc/minute, fluctuations of period about 4 minutes would be expected at transit, in the absence of any appreciable ionospheric wind effects. However, winds of the order of 1000 km./hr. in the F_2 region of the ionosphere have been

observed (**15**) and would therefore produce fluctuations of period approximately 20 seconds. These figures agree well with the observed range in durations of from approximately 10 seconds to about 5 minutes for fluctuations at transit (**14**).

(*f*) *Variation of scintillation activity with angular subtension of source.*—Following a similar argument to that used for the optical case, sources whose angular subtensions are large compared with 40 minutes of arc will not be observed to scintillate. The radio stars have been shown by Bolton (**16**) and by Ryle and Smith (**17**) to be smaller than about 6 minutes of arc and hence all these sources would be expected to scintillate. Owing to the great difficulty of observing all but the four most intense radio stars, scintillation information on other radio stars is scanty, but there is as yet no well authenticated case of a source which does not scintillate.

(*g*) *Variation in the apparent position of the source.*—As in the optical case, the apparent position of the star will tend to fluctuate at the scintillation frequency through an angle of about one-third the width of the scattered cone. For 5 km. irregularities and a wave-length of 4 metres the scattered polar diagram will have a first minimum at an angle of approximately 3 minutes of arc from the direction of the incident radiation. In this case the random fluctuations in the apparent position of the source would be expected to have an amplitude of the order of 1 minute of arc. This figure is in good agreement with the observations of Ryle and Hewish (**18**) who have shown by using a high-resolution radio-interferometer technique that the random changes in apparent position are of the order of 1–2 minutes of arc.

(*h*) *Variation of degree of scintillation with wave-length.*—The phase change produced by a given irregularity is proportional to the wave-length and hence the degree of scintillation would be expected to decrease with decreasing wave-length. This effect has been observed (**13**), scintillations being more intense on the longer wave-lengths. It should however be pointed out that any theory seeking to explain the scintillations in terms of refractive index irregularities in the ionosphere would predict the decrease of scintillation with decreasing wave-length, since for the ionosphere $(\mu - 1)$ is proportional to λ^2.

7. *Conclusion.*—A new theory of scintillation, based on Fresnel diffraction at a non-homogeneous layer, has been shown to be capable of explaining the observed phenomena on optical and radio wave-lengths. In the optical case the theory requires considerably smaller atmospheric density gradients than are required by the simple refraction theory. The use of photoelectric cells and a photographic recording system should enable the application of the diffraction theory to optical wave-lengths to be more rigorously checked. On radio wave-lengths the study of the scintillations of the radio stars should provide a new method for studying the complexities of the F region.

8. *Acknowledgments.*—The author wishes to express his sincere thanks to Dr A. C. B. Lovell, Director of the Jodrell Bank Experimental Station, for his constant help and encouragement during the preparation of this paper; to Mr J. A. Ratcliffe of the Cavendish Laboratories, for invaluable criticisms and a most helpful discussion of the application of statistical methods to diffraction at an irregular screen; to Dr M. A. Ellison, for his helpful criticism and interest in this work; and to Mr A. Maxwell, for assistance in taking the radio observations. He is also indebted to the Department of Scientific and Industrial Research for the award of a maintenance grant.

APPENDIX

The auto-correlation function and its Fourier transform

The purpose of this appendix is:

(*a*) To define the auto-correlation function $\rho_E(\xi)$, and

(*b*) To show that the angle subtended by one irregularity in the emergent wave-front is approximately the same size as the scattered cone of radiation when $\xi_0 = \sqrt{(R\lambda)}$ (i. e. when the size of the distortions in the emergent wave-front is about that of the radius of the first Fresnel zone).

The terminology throughout is that used by Booker, Ratcliffe and Shinn (**11**).

1. *The auto-correlation function.*—Consider a plane wave incident upon an irregular diffraction screen which varies in one direction only, the X direction.

Let $E_x(x)$ be the function describing the amplitude distribution, in the direction X, of the X component of the electric field across a plane immediately below the disturbing region. Then the auto-correlation function, in the direction X, of this component of the electric field is given by

$$\rho_E(\xi) = \frac{\int_{-\infty}^{+\infty} E_x^*(x) \,.\, E_x(x+\xi) \,.\, dx}{\int_{-\infty}^{+\infty} E_x^*(x) \,.\, E_x(x) \,.\, dx}.$$

Here $E_x^*(x)$ is the complex conjugate of the amplitude of the X component of the electric field at the point x and $E_x(x+\xi)$ is the (complex) amplitude of the X component of the electric field at a point $(x+\xi)$, all distances being measured in wave-lengths. This is a symmetrical function, having a maximum value of unity for $\xi = 0$, and falling off towards zero as ξ increases. ξ_0, the distance at which the auto-correlation function has fallen to zero, is a measure of the average size of the irregularities in the emergent wave-front.

2. *The ratio of the angle subtended by one irregularity in the emergent wave-front to the semi-angle of the scattered cone of radiation.*—It is shown by Booker, Ratcliffe and Shinn (**11**) that the average angular power spectrum in the scattered cone of radiation is proportional to the Fourier transform of the auto-correlation function defined as above. If now we assume that this auto-correlation function is of the Gaussian error function type, the Fourier transform of the auto-correlation function will also be Gaussian, and we have

$$\rho_E(\xi) = e^{-\xi^2/2a^2}, \qquad |P(s)|^2 \propto e^{-2\pi^2 a^2 s^2},$$

where a is the average number of wave-lengths separating two points in a plane below the disturbing region between which the correlation is 0·61, and $1/(2\pi a)$ is the sine of the angle at which the scattered radiation has fallen to 0·61 in power.

Multiplying $1/(2\pi a)$ by the range of the disturbing region R and equating to $a\lambda$ (the condition for the average irregularity to subtend an angle equal to the scattered cone of radiation) we have

$$R/2\pi a = a\lambda \quad \text{or} \quad a = \sqrt{\left(\frac{1}{2\pi}\right)}\sqrt{\left(\frac{R}{\lambda}\right)}.$$

If we take ξ_0, the distance at which the auto-correlation function has fallen to zero, as $2a\lambda$, then

$$\xi_0 = 0{\cdot}8\sqrt{(R\lambda)}.$$

Hence we see that the scattered cone of radiation is approximately equal to the angle subtended by one irregularity in the wave-front when $\xi_0 = \sqrt{(R\lambda)}$. When ξ_0 is small compared with $\sqrt{(R\lambda)}$, the scattered cone of radiation will be large compared with the angle subtended by $\sqrt{(R\lambda)}$ and will therefore be very much larger than the angle subtended by one irregularity; on the other hand, if ξ_0 is large compared with $\sqrt{(R\lambda)}$, the scattered cone of radiation will be very small compared with the angle subtended by one irregularity.

Jodrell Bank Experimental Station,
University of Manchester :
1950 *December* 21.

References

(1) H. Hartridge and R. Weale, *Nature*, **164**, 999, 1949. H. Hartridge, *Nature*, **165**, 146, 1950; **165**, 665, 1950.
(2) E. Gaviola, *Astronomical Journal*, **54**, 155, 1949.
(3) R. Boutet, *Annales de Géophysique*, **5**, 4, 310, 1949.
(4) A. Danjon and A. Couder, *Lunettes et Téléscopes, Ed. de la Revue d'Optique*, Paris, 1935.
(5) J. S. Hey, S. J. Parsons and J. W. Phillips, *Nature*, **158**, 234, 1946.
(6) F. G. Smith, *Nature*, **165**, 422, 1950.
(7) C. G. Little and A. C. B. Lovell, *Nature*, **165**, 423, 1950.
(8) H. G. Booker and W. E. Gordon, *Proc. I.R.E.*, **38**, 401, 1950.
(9) Lord Rayleigh, *Phil. Mag.*, **36**, 129, 1893.
(10) M. A. Ellison, *Nature*, **165**, 664, 1950.
(11) H. G. Booker, J. A. Ratcliffe and D. H. Shinn, *Phil. Trans. Roy. Soc.* A, **242**, 579, 1950.
(12) L. Respighi, *Bull. Assoc. Française pour l'Avancement des Sciences*, **1**, 148, 1872.
(13) J. G. Bolton and G. J. Stanley, *Aust. J. Sc. Res.* A, **1**, 58, 1948.
(14) C. G. Little and A. Maxwell, *Phil. Mag.*, **42**, 267, 1951.
(15) J. H. Meek, *J. Geophys. Res.*, **54**, 339, 1949.
(16) J. G. Bolton, *Nature*, **162**, 141, 1948.
(17) M. Ryle and F. G. Smith, *Nature*, **162**, 462, 1948.
(18) M. Ryle and A. Hewish, *M.N.*, **110**, 381, 1950.
(19) R. Rivault, *Proc. Phys. Soc.* B, **63**, 126, 1950.
(20) C. G. Little and A. Maxwell (unpublished).

RATE OF FORMATION OF MOLECULES BY RADIATIVE ASSOCIATION

D. R. Bates

(Communicated by H. S. W. Massey)

(Received 1951 February 15)

Summary

A theoretical study is made of the rate at which free atoms form molecules by radiative association. Previous treatments of this problem are shown to be in error. A revised formula for the coefficient expressing the rate is derived. Approximate methods of evaluating this formula are discussed; and tables, designed to ease the computational labour, are presented.

The methods developed are used to obtain the rate coefficients for CH, CH^+, N_2^+ and H_2^+ formation as these are of astrophysical or geophysical importance. In the case of H_2^+ the calculations can be performed with some precision. Free-free radiative collisions between H atoms and H^+ ions are also investigated.

---

1. *Introduction.*—At low gas densities molecules are formed mainly by radiative association

$$X+Y\rightarrow XY+h\nu, \tag{1}$$

since there are too few third bodies for the reaction

$$X+Y+Z\rightarrow XY+Z \tag{2}$$

to compete. The density below which (1) is more rapid than (2) is dependent on the atoms involved, and no precise general statement regarding it can be made. But unless the transition which stabilizes the system is optically forbidden, the critical concentration of Z is unlikely to be less than 10^{12}/cm.^{3}, and is frequently several orders of magnitude greater. Consequently radiative association must be the dominant process under many naturally occurring conditions. The rate at which it proceeds can be expressed in terms of a coefficient γ, defined by the equation

$$dn(XY)/dt=\gamma n(X)n(Y), \tag{3}$$

where the n's denote the concentrations of the species indicated. In an important recent paper Kramers and ter Haar (1) studied the problem of determining the coefficient. Unfortunately an error occurs in the classical part of their treatment, as a result of which the influence that a short-range attractive interatomic field has in increasing the number of collisions was seriously overestimated; and in the quantal part the possible implications of certain correlation rules were not fully realized. Radiative association is re-investigated in the present note. A general formula for its coefficient is derived. This is then applied to compute the rates of formation of CH, CH^+, N_2^+ and H_2^+ (which are of interest to astrophysicists and geophysicists).

2. General formula

2.1. Suppose that two normal atoms, whose internuclear distance is r, approach each other. The fraction of occasions on which they move along a particular energy curve, $U_1(r)$, may generally * be taken to be g, the ratio of the statistical weight of this curve to the sum of the statistical weights of all possible curves. If the Einstein transition probability to a lower potential energy curve $U_2(r)$ is $A(r)$, then the chance of a molecule being formed is

$$g\int A(r)\,dt, \tag{4}\dagger$$

the integration being carried out for all time t for which r is such that the emission of a photon deprives the system of so much energy that the atoms cannot separate indefinitely. To obtain the rate coefficient associated with the process it is necessary to average over all values of the relative velocity v and of the impact parameter p. By the laws of motion dt and dr are connected by the relation

$$dt = dr\left\{v^2 - \frac{p^2v^2}{r^2} - \frac{2U_1(r)}{m}\right\}^{-1/2}, \tag{5}$$

where m is the reduced mass. Using this and assuming a Maxwellian distribution at temperature T, it may be shown that

$$\gamma = 8\pi^2 g\left(\frac{m}{2\pi kT}\right)^{3/2}\iiint\left[\exp\left(-\frac{mv^2}{2kT}\right)v^3A(r)p\left\{v^2 - \frac{p^2v^2}{r^2} - \frac{2U_1(r)}{m}\right\}^{-1/2}\right]dv\,dp\,dr. \tag{6}$$

k being Boltzmann's constant (1). Physically the most natural procedure is to calculate the contribution from each orbit, that is to integrate over the range of r appropriate to each p and v value. But as Kramers and ter Haar (1) have pointed out, it is mathematically easier to carry out the p integration first. Obviously the lower limit is simply zero. The upper one is p_M, the greatest value of p which is consistent with the chosen v and r. Integration yields

$$\gamma = 8\pi^2 g\left(\frac{m}{2\pi kT}\right)^{3/2}\iint A(r)r^2v\exp\left(-\frac{mv^2}{2kT}\right) \times\{(v^2 - 2U_1(r)/m)^{1/2} - (v^2 - 2U_1(r)/m - p_M^2v^2/r^2)^{1/2}\}\,dr\,dv. \tag{7}$$

At a perihelion point dr/dt vanishes. From (5), therefore, earlier workers have supposed that p_M is given by the equation

$$p_M^2 = \{r^2 - 2U_1(r)r^2/mv^2\}, \tag{8}$$

and hence that the second term in (7) is zero. This supposition is in general incorrect. Consider the graph of $\{r^2 - 2U_1(r)r^2/mv^2\}$ versus r^2. If $U_1(r)$ falls off more slowly than as r^{-2} the resulting curve increases monotonically; no complexity arises and (8) is in fact valid. But if (as is commonly the case) $U_1(r)$ falls off more quickly than as r^{-2} the situation is entirely different. The curve passes through an initial maximum, then through a minimum, and finally it too increases monotonically (*cf.* Fig. 1). In the regions $r<(\mathrm{OA})^{1/2}$ and $r>(\mathrm{OC})^{1/2}$ (8) can again be applied. However, in the important intermediate region, $(\mathrm{OA})^{1/2}<r<(\mathrm{OC})^{1/2}$, naïve use of the equation is erroneous. Thus when r is, for example, $(\mathrm{OB})^{1/2}$, it gives p_M to be $(\mathrm{BE})^{1/2}$; and if p had this value the atoms could not reach a distance $(\mathrm{OB})^{1/2}$ from one another, since dr/dt would vanish at

* See however Section 3.1.

† It is assumed here, and throughout the paper, that the radiation field is so dilute that stimulated transitions are unimportant.

a separation of $(OD)^{1/2}$. Clearly p_M is actually only $(CF)^{1/2}$, as this is the greatest value of p for which the approach is possible.

The variation of $U_1(r)$ is usually extremely rapid. Consequently, unless T is very high, it is permissible as a crude first approximation to take $(CF)^{1/2}$ to be independent of v and equal to an effective collision radius ρ, such that

$$-U_1(\rho)=\tfrac{1}{4}kT, \tag{9}$$

that is such that the potential energy at this internuclear distance is half the mean kinetic energy of approach.

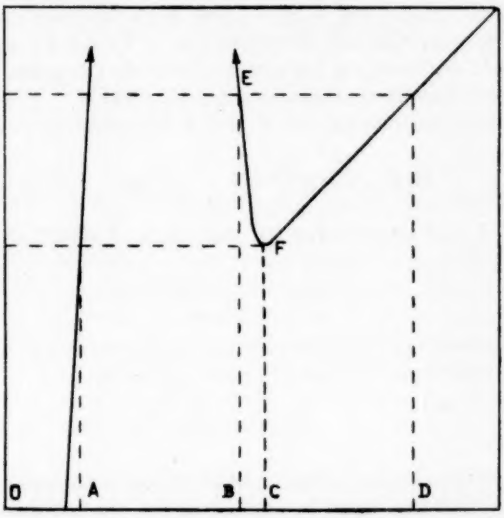

FIG. 1.—*Schematic graph of* $\{r^2-2U_1(r)r^2/mv^2\}$ *(vertical scale) versus* r^2 *(horizontal scale).*

For the integration over v the lower limit v_1 is $(2U_1(r)/m)^{1/2}$, where $U_1(r)$ is positive, and zero where $U_1(r)$ is negative*; the upper limit v_2 is $\{2(U_1(r)-U_2(r))/m\}^{1/2}$. Elementary analysis yields

$$\gamma=4\pi g(\mathscr{P}-\mathscr{Q}), \tag{10}$$

where

$$\mathscr{P}=\int_{\delta'}^{\infty}A(r)r^2\{-\mathscr{F}(x_1)+\mathscr{F}(x_2)\}\exp(x_1^2)\,dr, \tag{11}$$

$$\mathscr{Q}=\int_{\delta''}^{\rho}A(r)r^2\{\mathscr{G}(x_3)-\mathscr{G}(x_4)\}\left(\frac{\rho^2}{r^2}-1\right)^{1/2}\exp(-x_3^2)\,dr, \tag{12}$$

$$\left.\begin{aligned}\mathscr{F}(x)&=\frac{4}{\pi^{1/2}}\int_0^x x^2\exp(-x^2)\,dx,\\ \mathscr{G}(x)&=\frac{4}{\pi^{1/2}}\int_0^x x^2\exp(x^2)\,dx,\end{aligned}\right\}\quad(x\text{ real}), \tag{13, 14}$$

$$\mathscr{F}(x)=\mathscr{G}(x)=0\qquad(x\text{ imaginary}), \tag{15}$$

$$x_1^2=-U_1(r)/kT,\qquad x_2^2=-U_2(r)/kT,$$

$$x_3^2=x_1^2\Big/\left(\frac{\rho^2}{r^2}-1\right),\qquad x_4^2=x_1^2-x_2^2+x_3^2, \tag{16}$$

* It is assumed here that at small r, $U_1(r)$ is positive, and that at moderate and large r, it is negative (tending towards zero at infinity). Other cases are discussed in Section 2.4.

δ' being the value of r at which $U_2(r)$ changes sign, δ'' being that at the inner boundary of the intermediate region where (8) is inapplicable ((OA)$^{1/2}$ of Fig. 1) and ρ being the effective collision radius already defined. The r integration (with the limits as indicated) covers only half the path; to compensate for this an external multiplying factor of 2 has been introduced. Kramers and ter Haar derived the same expression for the $\mathscr{P}$ term but did not take into account the $\mathscr{Q}$ term (which may be of almost equal magnitude).

The difference between δ' and δ'' is negligible in most instances so that the distinguishing suffixes may be omitted; except at very high temperatures it is usual that $-U_1(r)$, $-U_2(r)$ and $U_1(r)-U_2(r)$, $\gg kT$ for the more important part of the region $\delta<r<\rho$; further, the condition $-U_2(r)\gg kT$ generally remains valid for that part of the region beyond in which $A(r)$ is appreciable. In these circumstances considerable simplification can be effected. Thus on making use of the asymptotic expansions for the $\mathscr{F}$ and $\mathscr{G}$ functions, (10) reduces to

$$\gamma=4\pi g\left[\rho^2\left(\frac{kT}{\pi}\right)^{1/2}\int_\delta^\rho A(r)(-U_1(r))^{-1/2}\,dr+\int_\rho^\infty A(r)r^2(1-\mathscr{F}(x_1))\exp(x_1^2)\,dr\right]. \quad (17)$$

Standard tables can be employed in the evaluation of $\mathscr{F}(x_1)$, since of course

$$\mathscr{F}(x)=\Phi(x)-\frac{2}{\pi^{1/2}}x\exp(-x^2), \quad (18)$$

where $\Phi(x)$ is the error integral. In fact, however, serious loss of accuracy is not caused by replacing the second term in the brackets by

$$\int_\rho^\infty A(r)r^2\,dr. \quad (19)$$

2.2. The development just given is useful in that it shows in a simple fashion the type of correction that must be applied to the original formula of Kramers and ter Haar. But the approximation that p_M is a constant is unsatisfactory and unnecessary. At large internuclear separation it is usually possible to express the potential by an inverse power law

$$U_1(r)=ar^{-\lambda}. \quad (20)$$

If this is permissible for *part* of the region where $-U_1(r)\gg kT$, then for all values of v of significance the minimum value of the function $r^2(1-2U_1(r)/mv^2)$ is of magnitude

$$\{\lambda/(\lambda-2)\}\{-a(\lambda-2)/mv^2\}^{2/\lambda}, \quad (21)$$

and occurs at an internuclear distance of

$$\{-a(\lambda-2)/mv^2\}^{1/\lambda}. \quad (22)$$

Thus a given r lies without the position of the minimum if

$$v^2>-ar^{-\lambda}(\lambda-2)/m, \quad (23)$$

within if

$$v^2<-ar^{-\lambda}(\lambda-2)/m, \quad (24)$$

and is less than δ'' (defined as above) if

$$r^2(1-2U_1(r)/mv^2)<\{\lambda/(\lambda-2)\}\{-a(\lambda-2)/mv^2\}^{2/\lambda}. \quad (25)$$

Consequently p_M^2 is given by (8) if (23) or (25) is satisfied, and by (21) if (24) is satisfied. Hence (7) becomes

$$\gamma = 8\pi^{1/2} g \int_{\delta'}^{\infty} \mathscr{I}(r) A(r) r^2 \, dr, \tag{26}$$

where

$$\mathscr{I}(r) = \int_{\epsilon_1}^{\epsilon_2} \{(\epsilon + H)^{1/2} - \mathcal{V}^{1/2}\} \exp(-\epsilon) \, d\epsilon, \tag{27}$$

$$\begin{cases} \mathcal{V} = 0 \text{ (for the ranges of } v \text{ given by conditions (23) or (25))} & (28) \\ \quad = \epsilon + H - \dfrac{\epsilon\lambda}{\lambda - 2} \{(\lambda - 2)K/2\epsilon\}^{2/\lambda} \text{ (otherwise),} & (29) \end{cases}$$

$$\epsilon = mv^2/2kT, \tag{30}$$

$$H = -U_1(r)/kT, \tag{31}$$

$$K = -ar^{-\lambda}/kT, \tag{32}$$

and where the limits ϵ_1 and ϵ_2 correspond to the v_1 and v_2 of the other approximation.

As mentioned before, δ' and δ'' are usually almost equal, so that the region between them is unimportant. There would of course be no difficulty in evaluating the contribution from it should the requirement arise. The integration over the remaining range is simplified by considering two extreme cases.

Case 1.—If $H \gg 1$, $\mathcal{V}$ is given by (29) except for velocities well beyond the maximum of the Maxwellian distribution. The difference between the two square roots in (27) can be obtained by the binomial expansion. The first non-vanishing term yields $\mathscr{I}(r) \simeq \mathscr{I}(r)^A$, where

$$\mathscr{I}(r)^A = \frac{1}{2H^{1/2}} \{\lambda/(\lambda - 2)\}\{K(\lambda - 2)/2\}^{2/\lambda} \int_{\epsilon_1}^{\epsilon_2} \epsilon^{(\lambda-2)/\lambda} \exp(-\epsilon) \, d\epsilon. \tag{33}$$

Since $U_1(r)$ is negative, ϵ_1 is zero. If in addition, $U_1(r) - U_2(r) \gg kT$, ϵ_2 may be taken as infinite, so that

$$\mathscr{I}(r)^A = \frac{1}{2H^{1/2}} \{K(\lambda - 2)/2\}^{2/\lambda} \Gamma((\lambda - 2)/\lambda). \tag{34}$$

The retention of the next term of the expansion gives, as an alternative approximation,

$$\mathscr{I}(r)^B = \mathscr{I}(r)^A + [\{K(\lambda - 2)/2\}^{2/\lambda}/4H^{3/2}] \times [\lambda/(\lambda - 2)\{K(\lambda - 2)/2\}^{2/\lambda} \Gamma((2\lambda - 4)/\lambda) - 2((\lambda - 1)/\lambda)\Gamma((\lambda - 2)/\lambda)]. \tag{35}$$

Attention may be drawn to the fact that if the ρ^2 factor in (17) is replaced by

$$r_0^2 = \{-a(\lambda - 2)/2kT\}^{2/\lambda} \Gamma((\lambda - 2)/\lambda), \tag{36}$$

the term involving it becomes equal to the simpler of the above approximations. The value of the ratio r_0^2/ρ^2 is 0·67 when λ is 3, 0·89 when λ is 4 and 1·07 when λ is 6.

Case 2.—If $H \ll 1$, $\mathcal{V}$ is given by (28) except for velocities well below the maximum of the Maxwellian distribution. Taking the limits as before, (27) at once yields the approximation

$$\mathscr{I}(r)^C = \frac{\pi^{1/2}}{2} (1 - \Phi(H^{1/2})) + H^{1/2}, \tag{37}$$

where $\Phi(H^{1/2})$ is again the error integral. It may be noted that the second term of (17) can be reduced to this form. A fair approximation (which will be referred to as $\mathscr{I}(r)^D$) is merely to take $\mathscr{I}(r)$ as unity.

For intermediate cases numerical methods must be used. Such cases usually occur at the large internuclear distances where H and K are identical. To facilitate the rapid computation of radiative association coefficients Tables IA, IB and IC are presented.* They relate respectively to the interaction potentials for which λ is 3, 4 and 6, and give the values of $\mathscr{I}(r)$ at sufficiently close intervals of H (or K) to permit interpolation. The ratios of $\mathscr{I}(r)^A$, $\mathscr{I}(r)^B$, $\mathscr{I}(r)^C$ and $\mathscr{I}(r)^D$ to the exact function are also displayed. As can be seen from them, the four approximations have a remarkably wide range of applicability provided high precision is not required. Indeed for many purposes it is sufficient to adopt the simple procedure of using $\mathscr{I}(r)^A$ and $\mathscr{I}(r)^D$ only, the former inside and the latter outside some suitably chosen internuclear distance.

2.3. If $D(r)$ is the dipole strength of the stabilizing transition, then

$$A(r) = \frac{64\pi^4 G_2}{3h^4c^3} D(r)\{U_1(r) - U_2(r)\}^3, \tag{38}$$

h being Planck's constant, c the velocity of light and G_2 the orbital degeneracy factor of the final state (**2**). Substitution in (26) gives

$$\gamma = \frac{512\pi^{9/2} g G_2}{3h^4c^3} \int_\delta^\infty \mathscr{I}(r) D(r)\{U_1(r) - U_2(r)\}^3 r^2\, dr, \tag{39}$$

or more conveniently

$$\gamma = \left\{1{\cdot}5_1 \times 10^{-17} g G_2 \int_\delta^\infty \mathscr{I}(r) D(r)\{U_1(r) - U_2(r)\}^3 r^2\, dr\right\} \text{cm.}^3/\text{sec.}, \tag{40}$$

where r is now in angstroms, $D(r)$ is in atomic units ($a_0^2 e^2$), $U_1(r)$ and $U_2(r)$ are in electron volts, and $\mathscr{I}(r)$ (as always) is dimensionless.

The formula based on a combination of the approximations $\mathscr{I}(r)^A$ and $\mathscr{I}(r)^D$ can similarly be reduced to

$$\gamma = \{7{\cdot}0 \times 10^{-20} g G_2 r_0^2 T^{1/2} \int_\delta^\sigma D(r)\{U_1(r) - U_2(r)\}^3 (-U_1(r))^{-1/2}\, dr$$

$$+ 1{\cdot}3_4 \times 10^{-17} g G_2 \int_\sigma^\infty D(r)\{U_1(r) - U_2(r)\}^3 r^2\, dr\} \text{cm.}^3/\text{sec.}, \tag{41}$$

with

$$r_0^2 = \{-1{\cdot}1_6 \times 10^4 a/T\}^{2/\lambda} f(\lambda) \text{ sq. angstroms}, \tag{42}$$

$$f(\lambda) = \{(\lambda-2)/2\}^{2/\lambda} \Gamma((\lambda-2)/\lambda). \tag{43}$$

Here σ is some suitable length, such that $\mathscr{I}(r)^A$ may be used for $r < \sigma$ and $\mathscr{I}(r)^D$ may be used for $r > \sigma$; a is the numerical value of the constant appearing in (20) when r and $U_1(r)$ are in the units specified in the previous paragraph; T is in deg. K. The value of $f(3)$ is 1·69, that of $f(4)$ is 1·77, and that of $f(6)$ is 1·71.

For most transitions $D(r)$ is only known in the neighbourhood of r_e, the equilibrium nuclear distance. Fortunately, owing to the $\{U_1(r) - U_2(r)\}^3$ factor, the dominant contribution usually arises from this region. Though the constant

* My thanks are due to Mrs K. Ledsham for assistance in the preparation of these tables

TABLE I

The exact function $\mathcal{J}(r)$, and the ratios to it of the approximations $\mathcal{J}(r)^A$, $\mathcal{J}(r)^B$, $\mathcal{J}(r)^C$ and $\mathcal{J}(r)^D$

IA $\lambda=3$

H (or K)	$\mathcal{J}(r)$	$\mathcal{J}(r)^A/\mathcal{J}(r)$	$\mathcal{J}(r)^B/\mathcal{J}(r)$	$\mathcal{J}(r)^C/\mathcal{J}(r)$	$\mathcal{J}(r)^D/\mathcal{J}(r)$
0·00	0·886	0·00	$-\infty$	1·00	1·13
0·25	1·028	0·65	−0·59	1·02	0·97
0·50	1·124	0·67	+0·18	1·04	0·89
0·75	1·197	0·67	0·43	1·07	0·84
1·00	1·255	0·67	0·55	1·10	0·80
1·25	1·303	0·67	0·61	1·13	0·77
1·50	1·342	0·67	0·65	1·16	0·75
1·75	1·376	0·67	0·68	1·19	0·73
2·00	1·404	0·67	0·71	1·22	0·71
3·0	1·484	0·68	0·76	1·34	0·67
4·0	1·531	0·69	0·79	1·45	0·65
5·0	1·563	0·71	0·81	1·56	0·64
7·5	1·610	0·73	0·85	1·81	0·62
10	1·641	0·75	0·87	2·02	0·61
15	1·689	0·78	0·90	2·37	0·59
20	1·728	0·80	0·92	2·65	0·58

IB $\lambda=4$

0·00	0·886	1·00	$-\infty$	1·00	1·13
0·25	1·007	0·88	−0·77	1·04	0·99
0·50	1·069	0·83	+0·25	1·10	0·94
0·75	1·105	0·80	0·52	1·16	0·91
1·00	1·126	0·79	0·64	1·22	0·89
1·25	1·137	0·78	0·70	1·29	0·88
1·50	1·143	0·78	0·74	1·36	0·87
1·75	1·145	0·77	0·77	1·43	0·87
2·00	1·144	0·77	0·79	1·50	0·87
3·0	1·128	0·79	0·84	1·76	0·89
4·0	1·108	0·80	0·88	2·01	0·90
5·0	1·091	0·81	0·90	2·24	0·92
7·5	1·058	0·84	0·93	2·75	0·94
10	1·037	0·85	0·94	3·19	0·96
15	1·011	0·88	0·96	3·95	0·99

IC $\lambda=6$

0·00	0·886	∞	$-\infty$	1·00	1·13
0·25	0·966	1·11	−0·85	1·08	1·04
0·50	0·973	0·98	+0·32	1·20	1·03
0·75	0·960	0·93	0·60	1·33	1·04
1·00	0·938	0·91	0·72	1·47	1·07
1·25	0·915	0·90	0·78	1·61	1·09
1·50	0·892	0·89	0·82	1·74	1·12
1·75	0·871	0·89	0·85	1·88	1·15
2·00	0·852	0·89	0·87	2·01	1·17
3·0	0·790	0·90	0·92	2·51	1·27
4·0	0·747	0·91	0·94	2·98	1·34
5·0	0·715	0·91	0·95	3·42	1·40
7·5	0·660	0·92	0·97	4·41	1·52
10	0·623	0·93	0·98	5·32	1·60

of proportionality in (20) is rarely well determined, this does not in general cause very serious uncertainty.

2.4. To avoid having to introduce a multiplicity of formulae it has so far been assumed that

(i) $-U_1(r) \gg kT$ for part of the region where the potential has its asymptotic form;

(ii) $U_1(r) - U_2(r) \gg kT$ throughout the region where $A(r)$ is appreciable;

(iii) $U_1(r) \leqslant 0$ (except at small r).

The treatment can readily be generalized to cover other less commonly occurring circumstances. If T is so high that (i) is invalid, then p_M^2 is not given by (21); but it may be represented by several such expressions each accurate over a limited range. Should (ii) not be satisfied, it is only necessary to take the limit ϵ_2 (in (27)) to equal $U_1(r) - U_2(r)$ instead of taking it as infinite. The most important alternative to (iii) is that $U_1(r) \geqslant 0$ everywhere; and for this case (10), with the ℓ term omitted, may be used. Awkward complications however arise when $U_1(r)$ has a positive maximum at large r but is otherwise of the form considered earlier; instead of being zero the limit ϵ_1 (in (27)) must be taken as equal to the value of $U_1(r)$ at the maximum and some suitable algebraical expression for p_M^2 must be found. The computations, though not difficult, are likely to be tedious.

3. *Applications*

3.1. Because of their possible importance in the study of interstellar clouds, calculations were carried out on the rate coefficients γ_1 and γ_2 associated with

$$C + H|(B\,^2\Sigma^-) \rightarrow CH(X\,^2\Pi) + h\nu \tag{44}$$

and

$$C^+ + H|(A\,^1\Pi) \rightarrow CH^+(X\,^1\Sigma^+) + h\nu \tag{45}$$

respectively. From the structures of the particles concerned it is apparent, *cf.* (**2**) and (**3**), that for the former,

$$g = 2/18, \qquad G_2 = 2, \qquad \lambda = 6, \tag{46}$$

and for the latter,

$$g = 2/12, \qquad G_2 = 1, \qquad \lambda = 4. \tag{47}$$

The various potentials can of course be represented by Morse curves modified to have the correct asymptotic form.* They were computed from the spectroscopic data given in Herzberg's recent book (**5**). The parameter r_0^2 (in (42)) was rather arbitrarily assigned the value $\{5 \times 10/T^{1/3}\}$ sq. angstroms for CH, and $\{4 \times 10^2/T^{1/2}\}$ sq. angstroms for CH^+. Accurate information on $D(r_e)\{B\,^2\Sigma^- - X\,^2\Pi\}$ and $D(r_e)\{A\,^1\Pi - X\,^1\Sigma^+\}$ is not available, but for reasons discussed elsewhere (**6**) it seems likely that each is about 3×10^{-2} atomic units. Unfortunately, complete confidence cannot be placed in this figure.

On evaluating (41), γ_1 was found to be some 2×10^{-18} cm.^{3}/sec. at 100 deg. K., and to vary as $T^{1/6}$ over a considerable range; and γ_2 was found to be also of this magnitude, and to be practically temperature independent.

* It may be remarked that Herzberg and Mundie (**4**) have found that the $A\,^1\Pi$ term of the molecule BH (which is isoelectronic with the ion CH^+) possesses a potential maximum. The repulsion implied by such a feature is unlikely to occur when one of the constituent atoms is charged; but if it did occur it would of course greatly reduce the radiative association coefficient at low temperatures.

It must be emphasized that the above results are not necessarily applicable under all conditions. One of the factors which makes studies of interstellar chemistry unique is that almost every atom is not merely in its lowest term, but is in the lowest level of this term. That this is the case for C and C^+ can readily be verified, noting that the Einstein transition probabilities for $C(^3P_2-{}^3P_1)$, $C(^3P_1-{}^3P_0)$ and $C^+(^2P_{3/2}-{}^2P_{1/2})$ are $2{\cdot}8\times10^{-7}$/sec., $5{\cdot}8\times10^{-8}$/sec. and $2{\cdot}4\times10^{-6}$/sec. respectively.* The fact that the carbon is mainly $C(^3P_0)$ and $C^+(^2P_{1/2})$ may profoundly influence the radiative association coefficients. Clearly the simple weighting ratio g (defined in Section 2.1) is not necessarily correct. Account must be taken of the correlations between the molecular and atomic levels. There would be no difficulty in doing this if C and C^+ had strong $\mathscr{L}$-$\mathscr{S}$ coupling; for the procedure introduced by Mulliken (**9**) could then be employed. This procedure is very simple. It depends essentially on the application of Wigner's rule that the same species of state cannot cross, and it requires only knowledge of the order in which the levels of the molecule, and of the separated atoms, lie. Provided the $\mathscr{L}$-$\mathscr{S}$ coupling is strong it generally gives the correlation uniquely. For in the circumstances the *c*-case of Hund is attained at very moderate internuclear separation and hence there is but an unimportant range where, owing to the quantum number Λ being defined, Wigner's rule is at its least powerful. In contrast, if the $\mathscr{L}$-$\mathscr{S}$ coupling is weak the range for which Λ is a good quantum number is extremely wide, and as a consequence Wigner's rule (which allows states of different Λ to cross) is insufficient to determine the correlation. The coupling in both C and C^+ is very feeble indeed, as evidenced by the fact that the extreme separation of the ground term levels is only 43 cm.$^{-1}$ for the atom and 64 cm.$^{-1}$ for the ion. Mulliken's method cannot therefore be used. A rigorous alternative method is not easy to develop, but the following is suggested as plausible.

Consider the effect of the axial electric field on a pair of atoms as they approach each other. If the $\mathscr{L}$-$\mathscr{S}$ coupling is sufficiently weak it is broken at large internuclear distances where the system can still be described by assigning quantum numbers to the individual atoms. These quantum numbers can be found from the Stark pattern (**10**); and knowing them it is possible to place restrictions on the correlations between the atomic and molecular levels. Thus in an electric field $C(^3P_0)$ probably becomes $C(^3\Sigma)$, and $C^+(^2P_{1/2})$ probably becomes $C^+(^2\Sigma)$, so that addition of $H(^2S)$ to the distorted atom can presumably only yield $CH(^2\Sigma)$ or $CH(^4\Sigma)$, and its addition to the distorted ion can presumably only yield $CH^+(^1\Sigma)$ or $CH^+(^3\Sigma)$.† Now in the formation of CH and CH^+ by radiative association the initial terms involved are $B\,^2\Sigma^-$ and $A\,^1\Pi$ respectively. Provided the movement is adiabatic it would seem that the chance that $C(^3P_0)$ and $H(^2S)$ come together along the former is $\frac{1}{3}$, and the chance that $C^+(^2P_{1/2})$ and $H(^2S)$ come together along the latter is zero. Using these values for the factor g appearing in the original formula (instead of the simple weighting ratios adopted previously) gives finally

$$\gamma_1 \simeq 6\times10^{-18}\ \text{cm.}^3/\text{sec.}, \tag{48}$$

$$\gamma_2 \simeq 0. \tag{49}$$

* The first two values are taken from the tables of Pasternack (**7**); the third value was calculated from the formula given by Shortley (**8**).

† It is satisfactory to note that similar arguments applied to CdH lead to results in agreement with the observation of Svensson (**11**) that $B^2\Sigma$ is correlated with $Cd(^3P_0)-H(^2S)$ and that $A^2\Pi_{1/2}$ is correlated with $Cd(^3P_1)-H(^2S)$. As Mulliken (**9**) has pointed out, this correlation is not given by the other scheme.

It may be remarked that if the $\mathscr{L}$-$\mathscr{S}$ coupling were strong the correlation would be such that both coefficients would be zero. As the two extremes thus agree in the case of CH^+ it seems likely that the true coefficient is indeed very small (unless the motion is not closely adiabatic). The position regarding CH is perhaps more doubtful. The coupling is certainly extremely weak, and one would therefore, for the reasons given, expect the coefficient to be comparatively large. Nevertheless it must be borne in mind that the branch of molecular theory concerned is still almost completely unexplored, and consequently the correlation scheme proposed should be treated with some reserve. In particular it is desirable to investigate the probability of non-adiabatic collisions*, and to ascertain the reason for the predicted crossing of the CH, $X\,^2\Pi_{1/2}$ and $B\,^2\Sigma^-$ potential energy curves. Mulliken (**12**) suggests that the final analysis may require detailed calculations, taking into account the interactions between the rotational, vibrational and electronic motions.

Bates and Spitzer (**6**) have studied the equilibrium in interstellar clouds, using both the sets of coefficients. They find that neither set is sufficiently large to explain the observational data if the conditions in the clouds are as generally believed (**13**). Though correlation schemes could be visualized which would lead to a decrease in the coefficients, none could lead to a significant increase. The discrepancy would thus seem real.

3.2. Knowledge of the rate coefficient, γ_3, associated with

$$N^+ + N|(B\,^2\Sigma_u^+) \rightarrow N_2^+(X\,^2\Sigma_g^+) + h\nu \tag{50}$$

is required in certain problems arising in the study of the Earth's upper atmosphere. In the case of this process

$$g = 2/36, \qquad G_2 = 1, \qquad \lambda = 4 \tag{51}$$

(*cf.* (**2**) and (**3**)). As usual r_0^2 (of (42)) is poorly determined. It was taken to be $\{5 \times 10^2/T^{1/2}\}$ sq. angstroms. For the applications envisaged the conditions are such that consideration need not be given to the detailed correlations. There is still controversy regarding the dissociation energy of N_2^+. To minimize the possible error the mean of the values advocated by Gaydon (**3**) and by Herzberg (**4**) was adopted in constructing the relevant Morse curves. According to the calculation of Shull (**14**) $D(r_e)\{B\,^2\Sigma_u^+ - X\,^2\Sigma_g^+\}$ is about 1·5 atomic units.

Taking the various quantities appearing in (41) to be as indicated above, it was found that over a wide temperature range (up to at least 2000 deg. K.)

$$\gamma_3 \simeq 3 \times 10^{-17}\ \text{cm.}^3/\text{sec.} \tag{52}$$

The suggestion has been made (**15**) that process (50) is responsible for the presence of N_2^+ ions in high-altitude sunlit aurorae. It is apparent however that the magnitude of γ_3 is much too small for this to be accepted. For even if the concentration of N atoms near the 1000 km. level were as high as $10^8/\text{cm.}^3$ the lifetime of an N^+ ion towards radiative association would be of the order of 10 years.

The extent to which the oxygen in the upper atmosphere is dissociated depends partially on the important reaction

$$O + O|(A\,^3\Sigma_u^+) \rightarrow O_2(X\,^3\Sigma_g^-) + h\nu. \tag{53}$$

* If this probability is actually large (as might be the case since the energy differences are minute) the normal weighting ratio g should be used.

Unfortunately the rate at which this proceeds cannot be determined with any precision at present as the dipole moment of the transition is not known reliably. It is interesting to observe that the photon yield P may be high. If γ_4 is the coefficient involved, $n(O)$ is the concentration of atomic oxygen in the region where it is most abundant, and H is the local scale height, then

$$P \simeq n(O)^2 H \gamma_4 / \text{cm.}^2 \text{ column/sec.} \tag{54}$$

Since $n(O)$ is about 10^{13}/cm.^{3}, and H is about 10^6 cm. (**16**), P is thus of order $10^{32}\gamma_4$/cm.^{2} column/sec., and must therefore be very considerable unless γ_4 is extremely small.* It would be of great value to measure the intensity of this continuum.

3·3. Collision processes involving hydrogen only are of special importance in astrophysics and consequently it was considered worth evaluating the rate coefficient, γ_5, associated with

$$H + H^+ | (^2\Sigma_u^+) \rightarrow H_2^+(X\,^2\Sigma_g^+) + h\nu. \tag{55}$$

Additional interest in this reaction is provided by the fact that it is an example of the class in which the approach is along a repulsive potential energy curve. A welcome feature of the calculations is that they can be carried out with some precision (for essentially the only approximation is the neglect of the wave nature of the nuclei).

TABLE II

Radiative collisions between hydrogen atoms and ions

Temperature (T) (deg. K.)	Rate coefficient for H_2^+ formation (γ_5) (cm.^{3}/sec.)	Sum of free-bound and free-free rate coefficients ($\gamma_5+\gamma_5'$) (cm.^{3}/sec.)	Mean energy of emitted photons (e.V.)
500	$1{\cdot}3\times10^{-18}$	$1{\cdot}6\times10^{-18}$	0·23
1000	$5{\cdot}2\times10^{-18}$	$6{\cdot}9\times10^{-18}$	0·41
2000	$1{\cdot}9\times10^{-17}$	$2{\cdot}7\times10^{-17}$	0·72
4000	$6{\cdot}2\times10^{-17}$	$1{\cdot}0\times10^{-16}$	1·2
8000	$1{\cdot}7\times10^{-16}$	$3{\cdot}2\times10^{-16}$	2·0
16000	$3{\cdot}5\times10^{-16}$	$9{\cdot}0\times10^{-16}$	3·2
32000	$5{\cdot}6\times10^{-16}$	$2{\cdot}2\times10^{-15}$	4·9
64000	$6{\cdot}0\times10^{-16}$	$4{\cdot}4\times10^{-15}$	7·0

In a recent quantal study of the two-centre problem Bates, Ledsham, and Stewart (**17**) have derived the potentials concerned, and Bates (**18**) has used the wave functions made available from this work to compute the Einstein coefficient at various internuclear distances. All the quantities in (11) are thus known accurately. The necessary integration was performed by numerical methods and hence from (10) (in which the weighting ratio g is here $\frac{1}{2}$) γ_5 was found. Table II shows the results. It will be noted that the coefficient increases rapidly with the temperature, as would be expected.

All radiative collisions do not of course lead to the formation of H_2^+—after some the H and H^+ particles can move apart again (with decreased kinetic energy).

* Thus P would be some 10^{12}/cm.^{2} column/sec. if, for example, γ_4 were 10^{-20} cm.^{3}/sec. As a comparison it may be noted that the number of photons emitted in the strongest line of the normal airglow is only about 10^8/cm.^{2} column/sec.

The sum of the free-bound coefficients γ_s and the free-free coefficient γ'_s can be obtained by putting $\mathcal{F}(x_2)$ in (10) equal to unity. For completeness this sum is also displayed in Table II together with the mean photon energy emitted per radiative collision.*

References

(1) H. A. Kramers and D. ter Haar, *B.A.N.*, **10**, 137, 1946.
(2) R. S. Mulliken, *J. Chem. Phys.*, **7**, 14, 1939.
(3) A. G. Gaydon, *Dissociation Energies*, London, 1947.
(4) G. Herzberg and L. G. Mundie, *J. Chem. Phys.*, **8**, 263, 1940.
(5) G. Herzberg, *Molecular Spectra and Molecular Structure—Diatomic Molecules* (Second Edition), New York, 1950.
(6) D. R. Bates and L. Spitzer, *Ap. J.*, **113**, 441, 1951.
(7) S. Pasternack, *Ap. J.*, **92**, 129, 1940.
(8) G. H. Shortley, *Phys. Rev.*, **57**, 225, 1940.
(9) R. S. Mulliken, *Phys. Rev.*, **36**, 1440, 1930.
(10) R. S. Mulliken, *Rev. Mod. Phys.*, **2**, 60, 1932.
(11) E. Svensson, *Zeits. f. Phys.*, **59**, 349, 1930.
(12) R. S. Mulliken, Private communication, 1950.
(13) B. Strömgren, *Ap. J.*, **108**, 243, 1948.
(14) H. Shull, *Ap. J.*, **112**, 352, 1950.
(15) M. Nicolet, *Conference on Ionospheric Physics*, Pennsylvania State College, 1950.
(16) R. Penndorf, *J. Geophys. Res.*, **54**, 7, 1949.
(17) D. R. Bates, K. Ledsham and A. L. Stewart (in course of preparation).
(18) D. R. Bates, *J. Chem. Phys.*, **19**, 1122, 1951.

Department of Physics†,
University College,
London:

1951 *February* 13.

* The energy distribution of the emitted photons is given by the integrand of (10) (with $\mathcal{F}(x_2)$ unity) and can be computed readily should it be required. Absorption by the inverse process is of more interest, and is being investigated.

† Now at *Department of Applied Mathematics, Queen's University, Belfast.*

THE ECLIPSING SYSTEM ZETA PHOENICIS

A. R. Hogg

(Communicated by the Commonwealth Astronomer)

(Received 1950 October 18)

Summary

Photoelectric observations of the system ζ Phoe are described. The system, which has not hitherto been recognized as light variable, undergoes total eclipses. Uniform and partially darkened solutions are given. The orbital eccentricity is determined solely from the photometric results. It is notably less than the figure derived from the spectroscopic data. Certain other discrepancies in the solution are discussed. These can be resolved by assigning to the components temperatures which are much lower than would be expected from the spectral types. Absolute dimensions are estimated.

---

1. *Introduction.*—Recently some photoelectric measures were made of certain southern stars which were known to be spectroscopic binary systems but which, as far as could be ascertained, had not been recognized as light variables. Amongst these was the system ζ Phoenicis ($\alpha = 01^h 04^m{\cdot}2$, $\delta = -55° 47'$ (1900), B8 + B8, $4^m{\cdot}13$) which had been reported as a spectroscopic binary by R. E. Wilson from Lick observations at Santiago. Later A. Colacevich* assigned a period of $1^d{\cdot}66958$ to the system and deduced a set of elements. Two spectra were reported, but the lines of the brighter were broad and those of the fainter were found on but five plates and then only with difficulty. Because of uncertainty in the measurements Colacevich regarded the elements as provisional. The photoelectric observations described here have shown the star to be a well-marked eclipsing system, one of the few to be discovered photoelectrically. The system ζ Phoe is a visual triple. SDS Rmk2 lists a pair $4^m{\cdot}2 + 8^m$ separated by 6″ and effectively stationary over the last century. Rossiter† observed a third star $7^m{\cdot}2$ separated by 0″·6 from the $4^m{\cdot}2$ component (Rst No. 1205). The present observations refer to the brighter component and any perturbations introduced by the fainter companions have been disregarded.

2. *Photometric technique.*—The star was observed with the aid of a photomultiplier tube attached to the 6-inch Farnham refractor. The photometric methods were similar to those used in the observation of S Antliae‡ in that the output meter of the amplifier was used as an indicating instrument only, the actual measurement being made by a laboratory potentiometer. A sketch of the circuit is shown in Fig 1. The 931A multiplier tube was modified so that the output, instead of being through a pin close to dynode pins at a high voltage, was led out through an earthed guard-ring in the side of the socket. The high-voltage supply was obtained from a controlled rectifier set. This offered a convenient method of adjusting the sensitivity of the photometer. The amplifier tube was run much below its rated voltages so that the grid current was negligible in comparison with the photo-current.

* A. Colacevich, *P.A.S.P.*, **47**, 84, 1935.
† R. A. Rossiter, *Mem. R.A.S.*, **65**, 40, 1933.
‡ A. R. Hogg and P. W. A. Bowe, *M.N.*, **110**, 373, 1950.

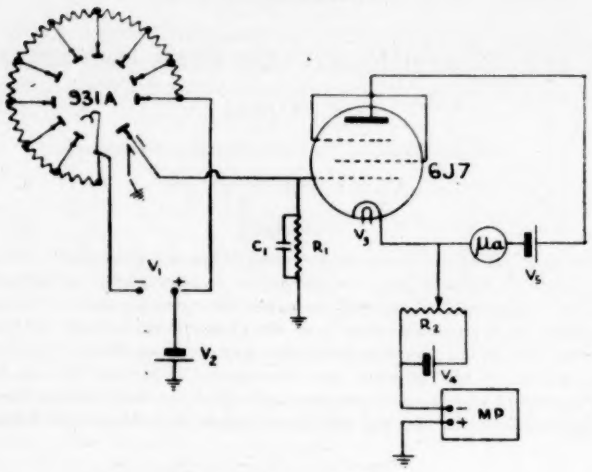

FIG. 1.—*Diagram of photo-multiplier circuit.*

V_1=600–900 v. V_2 =45 v. V_3=4·4 v. V_4=1·5 v.
V_5=22½ v. R_1 =50 megohms R_2=10,000 ohms.
C_1=0·1 μfd. *MP*=measuring potentiometer.

TABLE I

Normal Magnitude Differences α *Scul–*ζ *Phoe*

The normals are the means of ten observations arranged in increasing order of phase for a period of $1^d{\cdot}6698$ with zero phase adopted at J.D. 2432499·000

Phase	Δ*m*	Phase	Δ*m*	Phase	Δ*m*	Phase	Δ*m*
d	m	d	m	d	m	d	m
0·036	0·303	0·376	0·304	0·976	0·112	1·155	0·279
·076	·302	·416	·307	·988	·051	·165	·294
·102	·280	·434	·296	1·000	−0·029	·176	·294
·119	·226	·454	·308	·009	−0·094	·194	·300
·135	·198	·489	·312	·018	−0·154	·212	·297
·146	·153	·510	·302	·026	−0·167	·232	·299
·159	·117	·527	·313	·030	−0·177	·278	·294
·174	·077	·547	·312	·041	−0·188	·317	·299
·188	·057	·574	·310	·051	−0·170	·369	·278
·203	·056	·620	·318	·060	−0·175	·414	·295
·215	·044	·681	·300	·071	−0·139	·450	·314
·230	·064	·766	·320	·088	−0·024	·488	·317
·244	·155	·818	·299	·100	+0·055	·530	·303
·256	·151	·853	·303	·109	0·116	·550	·330
·275	·215	·867	·298	·119	·167	·567	·310
·290	·256	·882	·304	·126	·198	·579	·310
·305	·282	·900	·302	·133	·228	·591	·302
·323	·296	·929	·300	·140	·263	·606	·308
0·348	0·295	0·960	0·203	1·147	0·264	·628	·295
						1·648	0·291*

The comparison star used was α Sculptoris ($\alpha = 0^h\,53^m{\cdot}8$, $\delta = -29°\,54'$ (1900), $4^m{\cdot}39$ B5), which although rather distant from the variable was of comparable brightness and spectral type. A total of 772 comparisons on 63 nights between 1947 November and 1949 February was obtained. A comparison usually consisted of one setting on the variable, interpolated between two settings on

* Four observations only.

the comparison star. Five readings of the potentiometer were made for each setting. Because of the small size and convenience of the instrument a complete setting (finding and reading) could be done in three minutes or less. Corrections for atmospheric extinction were determined and applied as described elsewhere.* The observations were assembled on a period of $1^d.6698$, and the normals shown in Table I were derived. Each normal represents the mean of ten observations as arranged in increasing order of phase.

3. *Period.*—The period adopted in Table I ($1^d.6698$) differs slightly from the value used by Colacevich ($1^d.66958$). The adopted value was derived from the earlier portion of the photometric results and in its turn differed slightly from an improved value obtained from all the present observations. The following heliocentric times of minima were observed, viz.:—

Primary Minima	J.D. 2432772·217
	797·263
	818·978
	849·025
Secondary Minima	813·128
	889·949
	899·963

These results gave

J.D. Epoch of principal minimum = 2432667·012 + 1·66990 E.

4. *Rectified light curve.*—A plot of the normals (not shown) indicated the presence of elliptic components. Accordingly the points outside of the eclipse were formed into "super-normals" of 20 observations each and fitted by least squares to the usual expression

$$L = A_0 + A_1 \cos\theta + A_2 \cos 2\theta.$$

(L = light intensity, A_1 = reflection coefficient, A_2 = ellipticity coefficient.) The results obtained were as follows

$$A_0 = +0{\cdot}9861 \pm 0{\cdot}0009 \quad \text{(p.e.)},$$
$$A_1 = +0{\cdot}0005 \pm 0{\cdot}0014 \quad \text{(p.e.)},$$
$$A_2 = -0{\cdot}0107 \pm 0{\cdot}0016 \quad \text{(p.e.)}.$$

Thus the reflection effect (A_1) was effectively absent and the ellipticity (A_2) was small but statistically significant. The observed points were rectified for ellipticity by division by ($A_0 + A_2 \cos 2\theta$) in the usual manner. The rectified observations were then folded (*a*) about the primary minimum and (*b*) about the secondary minimum. The folded points within the eclipses were each derived from two sets of sub-normals each of five observations taken at approximately equal times before and after the minimum. The points outside the eclipses were derived in a similar manner from pairs of normals given in Table I. Thus for the folded rectified curves the final points within the eclipses each represent 10 observations (with one exception at secondary minimum) and those outside the eclipses each represent 20 observations. These folded rectified curves (Fig. 2) strongly suggested a total eclipse. The flat bottom to the secondary curve indicated an occultation eclipse, whilst the slight curvature of the bottom of the primary minimum indicated a transit eclipse (perhaps partial or perhaps total) across a darkened disk.

* A. R. Hogg, *M.N.*, **106**, 294, 1946.

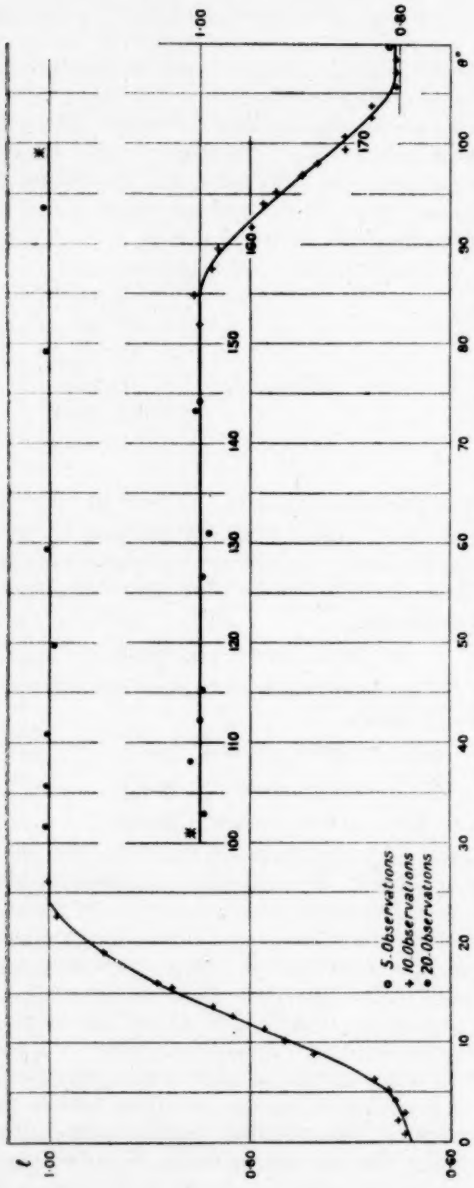

FIG. 2.—*Rectified light curves for folded primary and secondary minima. The points represent the observed normals rectified for ellipticity as described in the text. The curve is computed from the partially darkened elements.*

5. *Uniform solution.*—A solution for uniformly illuminated disks was obtained by the methods due to Russell and Shapley.* The rectified depths of the minima from a curve drawn for total eclipses were primary = 0·3525, secondary = 0·1955 (in light-intensity units). The Russell-Shapley equation (*j*), with the hypothesis that the principal minimum was an occultation, then gave, for a total eclipse, k (the ratio of the radii) = 0·550. The hypothesis that the principal minimum was a transit gave $k = 0{\cdot}662$ for a total eclipse. The light curve for primary minimum, when analysed with the aid of Russell's ψ-functions and the assumption of a total eclipse, gave $k = 0{\cdot}647$. Rather more weight was given to this latter value as the individual values of k from the ψ-functions agreed quite well, and the value of $k = 0{\cdot}65$ was adopted.

The light curve showed unequal spacing of the minima, thus indicating the existence of an eccentric orbit. The average time of occurrence of each minimum was derived from a curve drawn through the normals of both minima. Eight equidistant light levels were marked on the curve by a series of parallel lines, each one cutting the ascending and descending branches of a minimum. The mid-point of each parallel between these points of intersection gave a value for the time of minimum based on a symmetrical curve. The means of these points gave

$$\text{Phase of primary minimum} = 0^{d}{\cdot}000 \pm 0^{d}{\cdot}004 = t_1,$$

$$\text{,, secondary ,,} = 0^{d}{\cdot}8257 \pm 0^{d}{\cdot}009 = t_2.$$

As $h = e\cos\omega = (t_2 - t_1 - P/2)/P(1 + \operatorname{cosec}^2 i) = -0{\cdot}0027 \pm 0{\cdot}0003$ (p.e.), some eccentricity was indicated. ($\operatorname{Cosec}^2 i$ was taken as 1·0, an assumption justified by later results.) This result of a finite value for h indicated that the value of ω would differ from the spectroscopically determined value of $\omega = 90°$. Accordingly an attempt was made to derive the value of $g = e\sin\omega$ from the light curve by the separate analysis of the primary and secondary minima using a common value of k as described by Russell and Shapley.† Kopal‡ has shown that if $\sin^2\theta$ is plotted against $[1 + kp(k, \alpha)]^2$ a straight line will result, from the slope and intercept of which values of r_1 and i may be obtained. This method is applicable directly to normals. It has been applied to the present observations with the necessary modification to take account of the ellipticity of the components, i. e. the division of $\sin^2\theta$ by $1 - z\cos^2\theta$, where the photometric ellipticity constant was taken as $z = 4A_2$. Fig. 3 shows the graphs for primary and secondary minima. The points graphed are the actual normals, not smoothed values. The lines shown are the regression lines of the term in p on the term in θ. The results were as follows:—

	Primary Minimum	Secondary Minimum
Semi-major axis, larger star	$a' = 0{\cdot}250$	$a'' = 0{\cdot}261$
Orbital inclination i	$\cot i' = 0{\cdot}0508$	$\cot i'' = 0{\cdot}0566$
$\eta = \frac{1}{3}(2 + \cos\zeta)$§	$(g\eta)' = 0{\cdot}0218$	$(g\eta)'' = 0{\cdot}0284$

Using Russell's equations, $a_1'' = a_1'(1 + 2g\eta)$ and $\cot i'' = \cot i'(1 + 4g\eta)$, it was found that the mean value of $g\eta$ (see above) = 0·025, from which $g = e\sin\omega = 0{\cdot}026$. Combination of this with h gave, for the uniform solution,

$$e = 0{\cdot}026 \qquad \omega = 96°{\cdot}0.$$

---

* H. N. Russell and H. Shapley, *Ap. J.*, **36**, 404, 1912.

† *Loc. cit.*, p. 54.

‡ Z. Kopal, *Ap. J.*, **94**, 149, 1941.

§ $\zeta = \frac{1}{2}(\theta' + \theta'')$, where θ' and θ'' are values of θ at beginning or end of the eclipse.

For small values of $g\eta$ the true values of a_1 and $\cot i$ approach the means of the values derived from the minima separately, which are shown in Table II, along with other quantities derived by the usual methods.

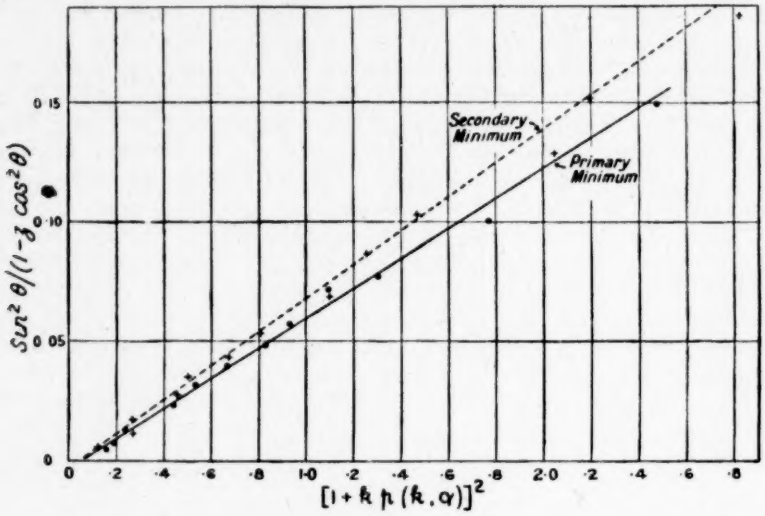

FIG. 3.—*Characteristic diagrams for primary and secondary minima. Uniform solution. Kopal's method.*

TABLE II

Solution for Ellipsoidal Stars in Eccentric Orbit

Period = 1^d·66990

Darkening Coefficient		x=0·0	x=0·2
Semi-major axis, relative orbit	a	1·00	1·00
Semi-major axis (equatorial), larger star	a_1	0·256	0·267
Semi-minor axis (equatorial), larger star	b_1	0·251	0·262
Semi-axis (polar), larger star	c_1	0·248	0·259
Semi-major axis (equatorial), smaller star	a_2	0·167	0·167
Semi-minor axis (equatorial), smaller star	b_2	0·164	0·163
Semi-axis (polar), smaller star	c_2	0·161	0·160
Axial ratio ($a_2/a_1 = b_2/b_1 = c_2/c_1$)	k	0·65	0·625
Light of larger star	L_1	0·805	0·805
Light of smaller star	L_2	0·195	0·195
Equatorial ellipticity coefficient = $\epsilon^2 \sin^2 i$	z	0·040	0·038
Inclination of orbit (corrected for polar flattening)	i	87°·0	84°·7
Eccentricity of orbit	e	0·026	0·028
Longitude of periastron	ω	96°·0	95°·6
Fractional light loss	α_0	1·00	1·004
Ratio of surface brightness	J_1/J_2	1·80	1·84

6. *Darkened solutions.*—Trials were made to obtain completely darkened circular solutions for the two minima separately on the basis of the secondary minimum being an occultation. It was found that satisfactory solutions with a common value of k as required by the eccentric orbit theory could not be obtained. Using Merrill's tables* other values of the darkening coefficient x

* J. E. Merrill, *Princeton Contr.*, No. 23, 52, 1950. I am much indebted to Dr J. E. Merrill for promptly despatching a copy of these most valuable tables, which greatly helped in the darkened solution.

were tried. The most suitable was $x = 0{\cdot}2$ and although this was rather smaller than the value normally adopted for the spectral type of the components it was used for further work. The value of the ellipticity constant z appropriate to this value of x was derived from the constant of the $(\cos 2\theta)$ term in the analysis of the inter-eclipse points, using the expression due to Russell*,

$$z = \frac{4\epsilon}{C}(A_2 - 0{\cdot}003),$$

where the value ϵ/C, representing the ratio of the geometric to the photometric ellipticities, was taken as 2·7 from Russell's data. This method gave ${}^2z = 0{\cdot}038$ which was used for the phase rectification in the usual manner.† Assuming a total occultation at secondary minimum and using Merrill's tables of ${}^2\psi^{0c}$ in conjunction with Russell's equations‡ gave a value of $k = 0{\cdot}625$ from the light curve on the basis of rectified circular elements. Circular elements were next derived for the primary eclipse with the same value of $k = 0{\cdot}625$, using Merrill's tables of ${}^2\chi^{tr}$ and eight points on the light curve. This gave $\alpha_0{}^{tr} = 1{\cdot}004$ with a value of $p = -1{\cdot}057$. The elements, determined in the same manner as for the uniform solution, together with the values of g, were as follows:—

	Primary Minimum	Secondary Minimum
Semi-major axis of larger star	$a' = 0{\cdot}262$	$a'' = 0{\cdot}272$
Inclination i	$\cot i' = 0{\cdot}0878$	$\cot i'' = 0{\cdot}1005$
$g\eta$	$(g\eta)' = 0{\cdot}019$	$(g\eta)'' = 0{\cdot}028$

Again using a mean value of $g\eta$ and combining the value of g with the value of h from the spacing of the minima gave $e = 0{\cdot}028$ and $\omega = 95°{\cdot}6$. As in the uniform solution, the actual values of a_1 and $\cot i$ for this darkened eccentric solution were obtained as the mean of the circular elements for the two separate minima, viz. $a_1 = 0{\cdot}267$ and $i = 84°{\cdot}7$. (Table II.)

A characteristic diagram, using the observed normals for the partially darkened solution, similar to that for the uniform solution, is shown in Fig. 4. For the partially darkened solution the more convenient functions from Merrill's tables have been used instead of the p-functions. At the time the uniform solution was made Merrill's tables were not available. Fig. 4 also displays the differences between primary and secondary minima indicative of an eccentric orbit.

Both the uniform and the partially darkened solutions gave satisfactory fits to the primary and secondary minima, but the bottom of the primary minimum was better represented by the partially darkened solution. The line in Fig. 2 represents the solution for the darkening coefficient $x = 0{\cdot}2$. For the paired sub-normals in the primary eclipse the s.d. of a single point was 0·003 light units; for the secondary eclipse the s.d. was 0·004 light units. The "super normals" between eclipses gave a s.d. = 0·005 units. No deviation exceeded 0·010 light units.

7. *Ellipticity of components.*—The foregoing solutions are based on the components being similar and similarly situated ellipsoids with their longest axes coinciding with the line joining their centres. This physically unlikely model may be brought nearer reality by assuming a degree of polar flattening. The polar flattening cannot be derived from the photometric results but has been introduced into the solution by Russell‡ who gives $\epsilon^2 = z\,\mathrm{cosec}^2 i$, where ϵ is the

* H. N. Russell, *Ap. J.*, **102**, 1, 1945.
† H. N. Russell and H. Shapley, *Ap. J.*, **36**, 407, 1912, equations c' and f'
‡ H. N. Russell, *Ap. J.*, **36**, 62, 1912.

eccentricity of the meridian section such that $b = a(1-\epsilon^2)^{1/2}$ and from the dynamical theory for small amounts of ϵ, $c = b - \frac{1}{2}(a-b)$. Here a, b and c are the axes of the ellipsoid in descending order of magnitude. The assumption of polar flattening requires that the value of i should be altered so that $\cot i_f = (c/b)\cot i_e$, where the subscripts e and f refer to the elliptical and the flattened conditions respectively. Values derived on this basis for both uniform and partly darkened solutions are shown in Table II.

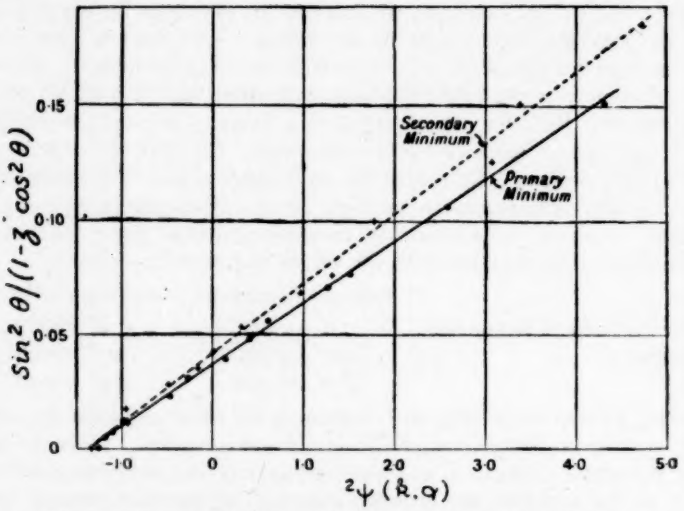

FIG. 4.—*Characteristic diagrams for primary and secondary mimima. Partially darkened solution* ($x = 0{\cdot}2$).

Certain relations should exist between the term A_2 in the inter-eclipse light curve and the elements. Results based on dynamical theory, combined with a gravity- and limb-darkening expression, led Russell* to the conclusion that the ellipticity coefficient should be given by

$$A_2 = \left[0{\cdot}073\left\{\left(\frac{E_2L_1}{E_1}r_2^2 + \frac{E_1L_2}{E_2}r_1^2\right) - \tfrac{1}{2}(C_1L_1 - C_2L_2)\right\}\right]\sin^2 i,$$

where, in addition to the usual symbols, E_1 and E_2 are the luminous efficiencies at the wave-length measured for large and small stars respectively, r_1 and r_2 the mean radii $-(abc)^{1/3}$ and C_1 and C_2 the computed photometric ellipticities. Using the derived values of r, L and i, together with results tabulated by Russell, and taking $E_1 = E_2$ as the components are of the same spectral type, the computed value of A_2 is found to be $= -0{\cdot}0099$. This is in agreement with the observed value of $-0{\cdot}0107 \pm 0{\cdot}0016$. Thus the computed values of L, r and i are consistent with the observed values of the ellipticity coefficient.

8. *Absolute dimensions, luminosity, density, etc.*—The combination of the photometric results with the spectroscopic figures of Colacevich (*l.c.*) gave the quantities shown in Table III, which refers to the $x = 0{\cdot}2$ solution. The stars appear to be main-sequence types. Colacevich, using the mass-luminosity relation, derived absolute visual magnitudes of 1·6 and 3·0 for the larger and

* H. N. Russell, *Ap. J.*, **104**, 153, 1946.

smaller components respectively. This difference of $1^m.4$ between the components is in good agreement with the present work, which gives (from the ratio L_1/L_2) a difference of $1^m.5$. Other comparisons with the spectroscopic results disclose certain difficulties. These are as follows:—

(1) The value of J_1/J_2 (and T_{e1}/T_{e2}) differs from that expected.
(2) Computed masses differ from the spectroscopic figures.
(3) The density of the faint component is several times greater than would be expected from its spectral type.
(4) The absolute magnitude differs from that to be expected from spectroscopic parallax results.

TABLE III

Absolute Values from Spectroscopic Orbit, Darkened Solution and Spectroscopic Parallax ($0''.014$)

		Star 1	Star 2
Semi-major axis, relative orbit	km. $\times 10^6$	2·47	4·07
Semi-major axis of star	km. $\times 10^6$	1·74	1·09
Mean radius, $(abc)^{1/3}$	Solar units	2·5	1·5
Mass	Solar units	2·8	2·0
Density	Solar units	0·18	0·54
Absolute magnitude		0·2	1·7

The ratio of the surface brightness of the components, J_1/J_2, was derived from a comparison of the depths of the rectified minima as 1·8; but as the two components have the same spectral type a value near unity might be expected. This discrepancy was also demonstrated by making use of an expression for computing the photographic absolute magnitude from the radius and effective temperature of a black-body star.* The effective wave-length of the photographic system is taken by these authors as 4250 A. and is probably near the effective wave-length of the photomultiplier system. From the above-mentioned expression it is easy to show that

$$\frac{1}{T_{e2}} - \frac{1}{T_{e1}} = 6{\cdot}82 \times 10^{-5} \log \frac{k^2 L_1}{L_2}.$$

Adopting a value of $T_{e1} = 12{,}500$ deg. as appropriate to a B8 star gave $T_{e2} = 10{,}700$ deg. The effective temperature of the smaller star would thus be equal to that assigned to an A1 type.

For computing masses, Gaposchkin† gives an equation combining Kepler's third law, the Stefan-Boltzmann expression and the mass-luminosity relation. Using this equation it was found, if values of $T_e = 12{,}500$ deg. and $m_1/m_2 = 0{\cdot}71$ (spectroscopic value) were adopted, that $m_1 = 5{\cdot}3$ and $m_2 = 3{\cdot}8$ in solar units. These values are about double those obtained spectroscopically.

The third discrepancy between the photometric and spectroscopic observations lies in the derived densities. Thus ρ_1 determined from the spectroscopic value of the masses and orbital dimensions combined with the photometric values for the radii and i, is 0·18 solar units, i. e. about equal to the density to be expected in a main-sequence star of the spectral type B8. On the other hand, a similar estimate of ρ_2 gave 0·54 which might be attributed to a spectral type A2 or later. This does not agree with the spectral observation of the two components being both of the same type, viz. B8. Also the values of the density derived from Russell's‡ equation 52, which depends on Kepler's third law and involves luminosity only as a correcting term, were $\rho_1 = 0{\cdot}18$ and $\rho_2 = 0{\cdot}43$.

* H. N. Russell, R. S. Dugan and J. Q. Stewart, *Astronomy*, II, p. 732, 1927.
† S. Gaposchkin, *Proc. Amer. Phil. Soc.*, **79**, 329, 1938.
‡ H. N. Russell, *Ap. J.*, **36**, 74, 1912.

The fourth discrepancy arises when the absolute magnitude, as determined by the classification of objective prism spectrograms, is used with Kuiper's* bolometric corrections and empirical mass-luminosity relation and the present photometric value of L_1/L_2, to obtain separate masses for the components. Unpublished results by Miss Woods resulting from a re-classification of spectrograms taken by Rimmer† were used. These results gave an absolute magnitude of 0·0 (pv) for the complete system, which with the photometric ratio L_1/L_2 gave figures of 0·2 and 1·7 for the large and small components respectively. These, with Kuiper's results, gave $m_1 = 4{\cdot}1$ and $m_2 = 2{\cdot}8$, in not over-good agreement with the results from the orbit. These discrepancies are all associated with the various assumptions made about the effective temperature. If temperatures of 8250 and 7450 deg. could be assumed then, approximately,

(1) The equation derived from Russell, Dugan and Stewart would be satisfied.

(2) Gaposchkin's equation would give masses in agreement with the spectroscopically observed figures.

(3) The observed densities would be more in keeping with those to be expected from the spectral classes associated with the assumed temperatures.

(4) A different bolometric correction is applicable and accordingly the values of the mass from the objective prism results become $m_1 = 3{\cdot}2$ and $m_2 = 2{\cdot}1$ solar units in quite satisfactory agreement with the orbital results.

Such an assumption however would be quite out of keeping with the assigned spectral types and their corresponding temperatures. From Colacevich's remarks there might be some doubt about the spectral type of the fainter component. Granting that the larger star was of the type given by Colacevich (B8) and assuming that the fainter star was about half a class later would overcome the J_1/J_2 difficulty but would not account for the masses and densities.‡

Conclusion.—The system of ζ Phoe is of considerable interest and worthy of further study, not only to improve the existing results but also to ascertain whether, with the passage of time, any perturbations due to the visual components might be detected. Both the direct spectroscopic parallax (0″·014) and the parallax derived from the orbit masses with the usual temperatures (0″·033) are large enough to suggest that a fair trigonometric parallax might be obtained.

Acknowledgments.—Grateful acknowledgment is made to Mr Gottlieb and Dr Simonow, who carried out the major part of the observations, as well as to Mrs Hall and Miss Beech, who reduced the observations up to the stage of the normal curve. The assistance of Mr D. G. Thomas, who was responsible for the design and construction of the regulated voltage supply, was also appreciated.

Commonwealth Observatory,
Mount Stromlo,
Canberra, Australia :
1950 *October* 11.

* G. Kuiper, *Ap. J.*, **88**, 446 and 489, 1938.

† W. B. Rimmer, *Mem. Comm. Obs.*, **2**, 1, 1930.

‡ Subsequent to writing this section the author has had a conversation with Dr Kron who states that he and Dr Herbig are of the opinion that the Lick plates show the brighter spectrum to be B7 and that the fainter spectrum, whilst not of high quality, is definitely later. The ratio L_1/L_2 could be 4.

NARROW-BAND PHOTOELECTRIC PHOTOMETRY OF BRIGHT SOUTHERN STARS

A. R. Hogg and Beryl Hall

(Communicated by the Commonwealth Astronomer)

(Received 1950 November 20)

Summary

The magnitudes of bright stars have been determined, using the band 4500–4600 A. Dispersion was effected with an objective prism spectrograph and the light intensities were measured with an electron multiplier in a null circuit.

Seven of the stars, forming a ring around the sky between $\delta = -20°$ and $-70°$, were treated as primary stars and each one was compared with the six other stars in the group. The standard deviation of a magnitude in this group was estimated as $\pm 0^{m}{\cdot}002$ (internal error of the system). The magnitudes for other stars were determined by comparison with stars of the primary group, using either two stars from this group (secondary) or a single star (tertiary). Comparisons have been made with other scales.

---

1. *Introduction.*—In defining a scale of stellar brightness there is a choice of a range of alternatives. At one extreme the scale may aim to express the ratio, from star to star, of the emission in the continuous spectrum at a particular wave-length. At the other extreme it may be based on the response of a particular receptor (e.g. an eye) to a relatively wide spectral region with consequent peculiarities due to well-known instrumental, atmospheric and physiological effects. There are practical advantages in using monochromatic light as the basis of any system. Thus (*a*) the effective wave-length of any measurement is independent of the colours of the sources involved, (*b*) greater precision is introduced into the necessary determination of atmospheric absorption coefficients which are then independent of colour of the source and zenith distance of the measured object, (*c*) any corrections for drifts in the colour response of the apparatus, e.g. change in colour of mirror, are unnecessary, (*d*) there is greater certainty in converting accurately to another magnitude system of defined wave-length, and (*e*) with a monochromatic system it is possible to specify, quite rationally, an absolute energy flux value (e.g. a specified number of watts/cm.^{2}) as the zero of the magnitude scale. There are however practical disadvantages also, including the risk, as the band width is greatly decreased, of encountering appreciable absorption (or emission) lines varying from spectral type to spectral type. This could render the results useless, from a continuous spectrum viewpoint, without the prohibitive labour of measuring the absorption in large numbers of stars.

As a compromise between these factors the scale may be based on a narrow but not infinitesimal band of wave-length located in a region of the spectrum relatively free from heavy stellar absorption lines. This compromise has been effected in the present work where the chosen band, between λ 4500 and λ 4600 A.,

is free from any very pronounced lines, does not have an excessively great atmospheric extinction and is in a region covered by the more sensitive of the present-day photoelectric equipment.

The results from such a process could differ from theoretical monochromatic magnitudes of the continuous spectrum based on some black-body concept in two ways, viz.

(i) purely on account of finite band width,

(ii) on account of stellar absorption lines.

Effect (i) was investigated theoretically for black bodies. It was found that the magnitude difference between two stars of spectral types A and K would vary by less than $0^{m}\cdot001$ when measured with band widths of 1 A. and 100 A. centred at 4550 A. Effect (ii) has recently been discussed by N. Milford (1), who estimates that it may be very considerable, especially in later spectral types. Thus in comparing α Boot (K2 pec) with β Orio (B8) the correction would exceed $0^{m}\cdot3$ for the band used in the present work.

From a practical point of view the use of a very narrow band width (say 1 A.), especially with stars having many absorption lines, could give results which would be quite sensitive to minor variations of the band width used. The use of a medium band width (say 100 A.) could be expected to give more reproducible results, because of an averaging effect between any absorption lines at the longer and shorter wave-length limits of the band. It is of course highly desirable that the cut-offs of the band should be square, otherwise the effective wave-length could alter with the colour of the source.

The figures presented here refer to the emission (uncorrected for stellar absorption) averaged over a much narrower band than is commonly employed in magnitude measurements. They may, particularly in the case of later types, deviate very considerably from monochromatic magnitudes referred to some theoretical continuous spectrum. The bulk of the present work deals however with B types where such correction appears to be small.

2. *Equipment.*—The present measures were made by an electron multiplier photo-tube attached to an objective prism spectrograph on the Reynolds reflector (30-inch). *The objective prism spectrograph* has been described by Gascoigne (2) and is shown in Fig. 1. A defining slit in the focal plane of this instrument was so placed as to pass radiation between λ4500 and λ4600 when the line $H\beta$ was centred on a locating cross-wire mounted in an adjoining slit. So as to render $H\beta$ more easily visible the locating wire was viewed through a special eyepiece containing a cylindrical lens. The light passing through the defining slit was collected by a lens (Fabry system) and fell on to the cathode of the photo-tube.

In setting up the apparatus particular attention was paid to ensuring that the expected amount of light entered the equipment. Thus with photo-cell removed, the eye was placed near the focal plane of the spectrograph when directed to a star and images of the telescope mirrors were examined to determine that all were centred and full of light. Further, to minimize the possible effect of any flexure in the telescope a circular diaphragm of diameter about $\frac{1}{4}$ inch less than the aperture of the collimated beam was placed in front of the spectrograph prism. Slight flexure was present but tests indicated that its effects were negligible. The reflector and spectrograph having been aligned on a star showing $H\beta$ prominently, the locating slit was adjusted by a screw until $H\beta$ appeared in the eyepiece as being

on the cross-wire. The defining slit then passed the required band of radiation. The guiding telescope (Fig. 1) was then moved bodily until the star image was seen on its cross-wires. These cross-wires then provided a fiducial mark when measuring stars in which $H\beta$ could not be discerned.

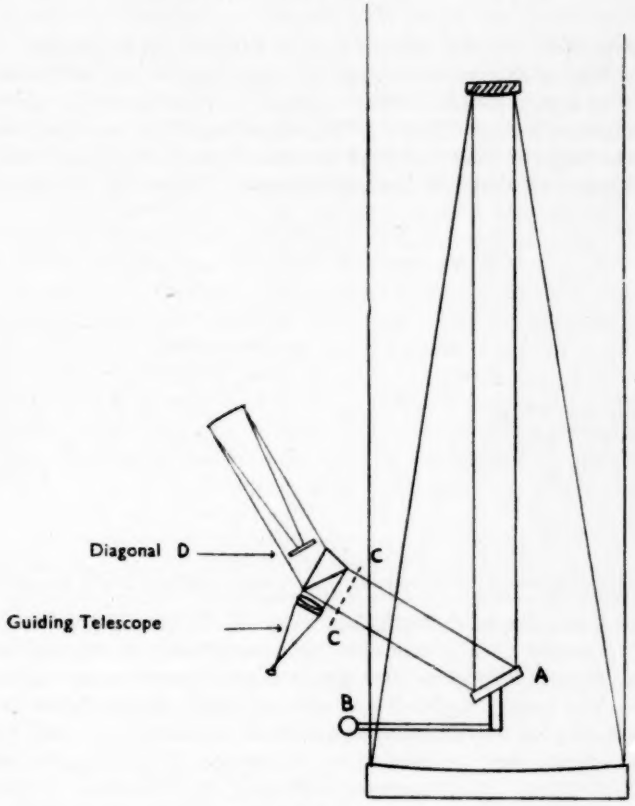

FIG. 1.—*The optical train.*

For certain comparisons a *diaphragm or a filter* was employed. The diaphragm of the Maltese-cross type was inserted at CC (Fig. 1). The two filters used were of glass coated by evaporation with a *Ni–Cr* alloy (3). The filters were spectrally neutral to a high degree but did not prove sufficiently stable for our purpose despite having been baked to 200 deg. C. in manufacture. One filter (2^m) was used in the parallel beam at position CC; the other ($0^m{\cdot}5$) was placed in the photometer mounting. Filter transmissions were determined at the telescope, using stars near the zenith on good nights. The Maltese-cross diaphragm was not suitable for the greatest precision because of possible local changes in the reflectivity of various parts of the mirror surface. Also alterations in its transmission could be expected with changes in the spectrograph setting when the instrument was replaced on the telescope after making way for other programmes. The evaporated film filters were better in this respect, but

because of their instability, the later stages of the work were arranged so that a knowledge of filter transmission was not required, i. e. full reliance was placed on the response of the cell being linear. Filters or diaphragms were then used only to bring the light intensity of the brighter star of a comparison to a convenient value and were retained in position for the measurement of the other star.

The ***photometer*** proper consisted of a selected 931A electron multiplier. The anode lead of the multiplier was detached from its pin and brought out at the side of the base through an amber insulator surrounded by an earthed guard-ring to minimize leakage effects. The output from the multiplier was passed through a 10 megohm resistor and the voltage drop over this resistor was measured by a single-valve amplifier using a null method. The circuit is shown in Fig. 2.

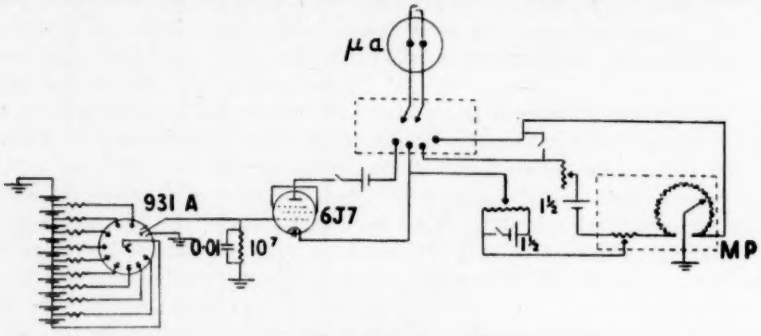

FIG. 2.—*Photometer circuit.*
The multiplier tube 931A was operated at 90 v./stage. MP=measuring potentiometer.

When no current flowed through the photo-cell, the grid of the valve was at or near earth potential and the anode current was adjusted by altering the potential of the cathode with respect to earth until the microammeter read 25 microamps. (The valve was greatly under-run to ensure a grid current below 10^{-10} amp.) When the multiplier was illuminated the anode current of the valve was thereby decreased. It was then restored to 25 microamps. by altering the potential of the cathode, using a potentiometer calibrated in millivolts. Thus the light intensities were referred to the scale of the potentiometer. By suitable switching, the microammeter was used to check the current flowing in the potentiometer circuit. This current, of 50 microamps., was found to change by less than 1 in 500 during a night's observations. As will be seen later, the method of observation served to eliminate the effect of any small uniform changes in this current except in so far as they might influence the extinction curve. Changes of 1 in 500 would be quite inappreciable here. The voltage supply for the multiplier (90 volts/stage) came from a miniature dry-battery pack which proved more suitable than a voltage-controlled rectifier supply used for earlier work. The batteries were satisfactory even after nearly two years of use.

The linearity of response of the cell was tested in several fashions, viz.

(i) by means of diaphragms of known transmission placed over the objective of a 6-inch refractor and using an actual star,

(ii) by an inverse square method,

(iii) by a summation method.

After a few preliminary trials method (i) was rejected partly because of atmospheric fluctuations and partly because of the difficulty of measuring the areas of the diaphragms to the degree of accuracy desired. Methods (ii) and (iii) necessitated the use of an artificial star. This consisted of an automobile lamp, mounted cap downwards and directed towards an inclined diffusing surface of white card from which light was scattered to a ground-glass screen and thence to a pin-hole. The "star" was mounted on an improvised optical bench and the pin-hole was focused by means of a small lens on to a diffusing glass screen mounted in contact with the cell of the multiplier. For the method (ii) the "star" was moved to definite distances (1 to 4 metres) from the focusing lens. The illumination of the lens and hence of the cell was then taken as being inversely proportional to the square of the distance. Various trials gave discrepancies of the order of $0^m{\cdot}01$ which was regarded as unsatisfactory. It was determined that these discrepancies arose in part from the alteration in size and position of the image of the star on the diffusing screen at the multiplier when the "star" was moved into different positions. For the summation method (iii), the "star" was focused on the diffusing screen of the multiplier by a thin lens 10·5 cm. diameter and 80 cm. focal length. A blue filter was used here to avoid trouble from lack of achromatism of this lens. The lens could be covered by an opaque diaphragm in which had been drilled twelve holes each of diameter 14 mm. These holes could be closed with light-proof stoppers when desired. The test consisted in measuring the light admitted through the twelve holes simultaneously, then in two groups each of six different holes, in four groups each of three different holes, and finally through each of the twelve holes singly. If the cell was linear in response then the reading for all twelve holes simultaneously (W) was expected to equal the sum of the readings (G_1, G_2 and G_3) of each of the other arrangements. The following results were obtained as the means of several sets of readings when the illumination through twelve holes gave a multiplier current of $1{\cdot}4 \times 10^{-7}$ amp. Two complete runs *a* and *b* were made for groups G_2 and G_3. Thus any systematic deviation of linearity over a range of nearly three magnitudes would be less than 1 millimagnitude.

TABLE I

Group	*m*	W−G		Mean
		(*a*)	(*b*)	(*a* and *b*)
G_1 (6 hole)	$0^m{\cdot}75$	$+0^m{\cdot}0005$	...	$+0^m{\cdot}0005$
G_2 (3 hole)	$1^m{\cdot}6$	$+0^m{\cdot}0016$	$-0{\cdot}0020$	$-0^m{\cdot}0002$
G_3 (1 hole)	$2^m{\cdot}7$	$-0^m{\cdot}0007$	$+0{\cdot}0012$	$+0^m{\cdot}0032$

(Column " m " gives the ratio G/W expressed in magnitudes.)

These results were not obtained without various precautions. Particular care was taken in the optical arrangements to ensure that the images through the various holes fell on the same part of the diffuser. The lamp voltage was checked frequently, using a potentiometer reading to 0·0002 volts. The lamp was run at 5·8 volts, approximately one-third of this voltage being shunted to the potentiometer for measuring. The accumulator supplying the lamp was charged continuously from a rectifier connected to the mains through a stabilizing transformer so that the difference between the input and output currents did not exceed a few milliamps. This was necessary as the nature of the test demanded steady illumination over several hours. Further, to take account of any steady drift in the lamp output or the multiplier response, comparison observations were

suitably intercalated and a standard routine was adopted in exposing the cell and measuring the current.

Throughout the programme the dark current was usually quite stable. After an exposure the meter needle would return to the zero position in the course of a minute or so and remain steady there. Occasionally, however, sudden bursts of dark current appeared and the cell then became unusable. This condition was associated with warmer weather and the cell was restored to its usual behaviour by keeping it for a few hours in a domestic refrigerator.

3. *The programme.*—The programme aimed initially at measuring southern stars down to $2^{m}\cdot5$ as well as a few northern stars. Actually some fainter southern stars were included. Known variable stars were omitted, as also were most double stars, unless the components differed widely in magnitude. Double stars could give superposed spectra and render the wave-length limits meaningless. The star comparisons were divided into three groups termed primary, secondary and tertiary.

The primary comparisons were measures made on seven stars forming a ring around the sky between $-20°$ and $-70°$ declination. They were restricted to stars showing the line $H\beta$ sufficiently well for setting. No double stars or stars reported as having variable radial velocity were included. Each primary star was compared with every other star in the primary group, so that 21 sets of comparisons were involved in this ring. These seven stars were used as standards for the rest of the programme.

The secondary group was composed of 24 stars in which the line $H\beta$ could usually be seen. Double stars for which the difference in brightness of the components exceeded 7^{m} were included, as errors due to the spectral uncertainty here would be small. Each of the secondary stars was measured against two primary stars, thus involving 48 sets of comparisons.

The tertiary group included 32 stars in which $H\beta$ could not usually be seen and which therefore required setting by the fiducial mark. Also some double stars differing by less than 7^{m} in brightness were included here. Thirty-two sets of comparisons were used for this group.

4. *Methods of observation.*—A single measurement of a star resulted from the mean of ten individual readings of the photometer made according to a regular plan over a period of 90 secs. These individual readings showed some variation but this usually was less than ± 2 per cent on the class of night used. A complete measurement of a single star, including setting of the telescope, required 4 minutes with two observers: one guiding, the other reading the photometer. Each pair of stars was compared in the order *a*, *b*, *a* to minimize the effect of any drift in the response of the apparatus or the transparency of the atmosphere. Comparisons were made at such times that the stars involved differed by less than 0·1 in $\sec z$ (z = zenith distance). This meant that corrections for atmospheric absorption generally were less than $0^{m}\cdot03$ (see below). The order of each night's observation was planned with the aid of a graph showing, for all programme stars, the variation of $\sec z$ with sidereal time. Each primary comparison was observed at least 10 and usually 14 times spread over a minimum of 4 nights. Secondary and tertiary pairs were observed at least 6 times, and on at least 3 nights. Observations were made on 83 nights between 1948 September and 1950 April.* To obtain extinction coefficients, nightly programmes were planned to include at least two

* The telescope was available for this programme on half the nights between the dates mentioned.

stars, each of which could be measured at several different altitudes. The linearity and smoothness of the curves obtained by plotting log readings against sec z were criteria by which the night's work was accepted or rejected.

5. *Filter and diaphragm calibrations.*—Although in the later part of the programme the observations were arranged so that a knowledge of the optical densities of the filters and diaphragm was not needed, it was necessary to determine these quantities for some of the earlier work. Densities were involved in only 18 comparisons (out of a total of 101). Even in these comparisons 39 per cent of the observations were reduced without the need of optical densities.

Measurements of the filter density showed that from 1948 September to late in 1949 April the $0^m{\cdot}5$ filter maintained a constant density ($0^m{\cdot}587 \pm 0{\cdot}001$ s.d., 10 observations). Between 1949 April 23 and 1949 April 26 it decreased suddenly in density and then remained effectively constant again (at $0^m{\cdot}556 \pm 0{\cdot}004$ s.d., 8 observations) till the completion of the observations. The determinations of

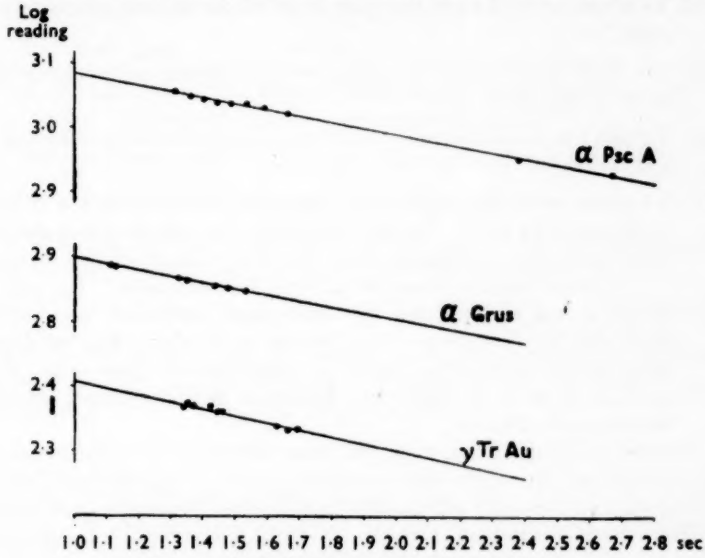

FIG. 3.—*Absorption Curves for a Typical Night.*

the optical density of the 2^m filter exhibited rather irregular scatter and a mean value (of $1^m{\cdot}979 \pm 0{\cdot}009$ s.d., 12 observations) was adopted throughout. As has been described above, the transmission factor of the Maltese-cross diaphragm could be expected to change for different series of observations. Accordingly individual values were adopted for the density of this diaphragm for the various series. These values ranged from $0^m{\cdot}898$ to $0^m{\cdot}926$. Only eight comparisons involved the Maltese-cross diaphragm.

6. *Atmospheric extinction.*—Absorption curves were obtained on 67 nights out of the 76 used in the final reduction. On most nights two or more curves were available. Curves for a typical night are shown in Fig. 3. The mean extinction as determined with rising stars differed slightly from that with setting stars. The means for 26 nights (i.e. all nights for which eastern and western curves were both available) gave the apparent rising extinction as 0·254 and setting

extinction as 0·281 (unit = magnitude/sec z). The difference, 0·027 ± 0·009 (s.d.) was statistically significant.

Several reasons might be advanced for the existence of this difference, viz.

(i) a true difference in absorption in eastern and western skies,

(ii) a fatigue effect in the cell response or some other instrumental drift,

(iii) an apparent difference due to one or both of the absorptions increasing with time,

(iv) an absorption varying with zenith distance differently in east and west.

There are no obviously important sources of local pollution to account for (i) nor is it thought that fatigue effects are significant with the low light-levels and short exposures used. In examining the results it was not practicable to separate these effects. Four methods of examination however presented themselves, viz.

(A) To adopt for each night the mean of all the coefficients measured on that night.

(B) To adopt for all nights the grand mean of all the coefficients measured in the programme.

(C) To adopt separate means derived from rising and setting stars (e. g. 0·254 and 0·281).

(D) To adopt coefficients adjusted to take account of variations of absorption coefficient with sec z. For this purpose it was assumed that the smaller mean extinction coefficient measured with rising stars (k_r) represented a value which was constant for all stars before transit. For stars after transit it was assumed that the absorption coefficient for a particular sec z was $k_s = k_r + b(\sec z - 1)$. Values of k_r and b derived from the observations were 0·254 and 0·014 respectively. This value of b was insufficient to bring about any detectable departure from linearity in the absorption curve.

Some of these methods, because of the distribution of the observations, take account of more than one of the effects listed as (i)–(iv). Thus Method A (if rising and setting stars were equally represented in the mean) would eliminate effects (ii) and (iii) from the observations as a whole. Method B would similarly take account of effects (ii) and (iii) and might be expected to give smoother results if the determinations of the absorption coefficients were greatly affected by individual errors. Method C might take account of effect (i) but was rejected because it involved an abrupt change at the zenith. Method D would approximately account for one form of effects (iii) and (iv). Methods A and D were applied to the 21 comparisons of primary stars. It was found that the average deviation in the mean magnitudes derived by the two methods was $0^{m}{\cdot}005$, no single deviation exceeding $0^{m}{\cdot}010$. The residuals of observed comparisons relative to values expected from assigned magnitudes however were rather less for Method A than Method D. Further, Method A gave results showing less scatter than did Method B. Accordingly Method A was used to reduce all the results except for nine nights when no absorption coefficient was determined and the grand mean coefficient (B) was used instead.

7. *Reductions and results.*—After preliminary reduction certain measurements were rejected either because of cloud or haziness noted at the time of measurement

or because of irregularities in the extinction curve. Out of about 2500 measurements some 250 were not used for these reasons. Most of the rejected measures were made on seven unsatisfactory nights. All the readings taken on these nights were rejected.

Magnitudes for the seven primary stars were obtained from a least squares solution for the 21 comparisons, an arbitrary zero being adopted for the magnitude scale. The solution aimed at assigning a set of magnitudes to the seven stars which would best represent the 21 observed magnitude differences. Next a magnitude was obtained for each secondary star as the mean of the results of the comparisons with the two primary stars. Each tertiary magnitude was found from the single comparison with a primary star. The internal uncertainty attaching to these results was estimated as follows:

(i) Primary stars s.d. $= \pm 0^{m}{\cdot}002$.

(ii) Secondary stars $= \pm 0^{m}{\cdot}005$.

(iii) Tertiary stars $= \pm 0^{m}{\cdot}008$.

It was desired to link the present observations with the zero of the North Polar sequence. Two methods presented themselves, viz.

(*a*) by comparison with the Harvard Mimeogram magnitudes,

(*b*) by comparison with certain results given by Eggen.

The Harvard Mimeogram results (**4**) were brought to the International Photovisual Scale (IPv) by the equation given by C. Payne-Gaposchkin,

$$\mathrm{IPv}(h) = \mathrm{HPv} + 0{\cdot}10 + 0{\cdot}06C_i. \qquad (1)$$

The colour index used in this equation ($C_i = \mathrm{IPv} - \mathrm{IPg}$) was here computed for each star from the spectrophotometric gradients G given by Gascoigne (**2**) or else by Greenwich (**5**). The definition of G gives

$$\mathrm{IPv} - \mathrm{IPg} = 1{\cdot}086(1/\lambda_{pv} - 1/\lambda_{pg})G.$$

The effective wave-lengths λ_{pg} and λ_{pv} were taken from the work of Seares and Joyner (**6**). It was known that colour index was not strictly proportional to gradient, but using the above computed values of C_i in equation (1) did not introduce any appreciable error as the colour correction was so small.

The photoelectric results (m_{4550}) were also reduced to the wave-length λ_{pv} by using the expression

$$\mathrm{IPv}(s) = m_{4550} + 0{\cdot}25 + 1{\cdot}086(1/\lambda_{pv} - 1/4550)G.$$

Although the gradients employed were determined with band widths of only 2–3 A. they had been shown by Gascoigne to agree well with the gradients measured photoelectrically by J. S. Hall (**7**) using a band width of 400 A. Presumably no error would be made in applying them to the 100 A. band used here.

Fig. 4 (*a*) compares the IPv values derived from both the Mimeogram and the m_{4550} results. The differences $\mathrm{IPv}(h) - \mathrm{IPv}(s)$ were plotted against $\mathrm{IPv}(s)$ for individual stars. Double stars with components differing in brightness by less than 5^{m} have been marked with a cross. The values $\mathrm{IPv}(h) - \mathrm{IPv}(s)$ were also plotted against gradient (Fig. 5). The results showed that whilst there was no systematic colour effect, the two magnitude scales deviated at the bright end.

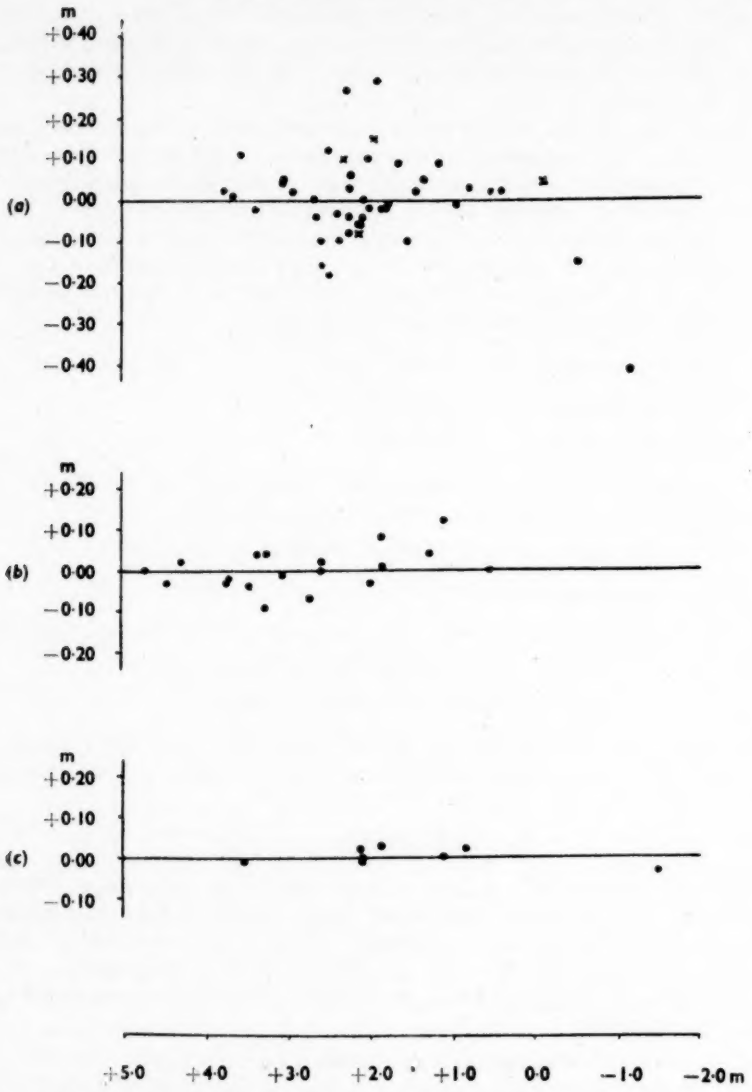

FIG. 4.—*Comparison with Harvard, Stromlo Photographic and Lick Results.*

(*a*) IPv(h)−IPv(s) vs. IPv(s).
(*b*) m_{4850}(pg)−m_{4850}(pe) vs. m_{4850}(pe).
(*c*) m_{4850}(Lick)−m_{4850}(Stromlo) vs. m_{4850}(Stromlo).

Least squares solutions gave the constants in the following equations:—

$$\text{(i)}\quad \mathrm{IPv}(h) = \mathrm{IPv}(s) - 0{\cdot}09 + 0{\cdot}11\mathrm{IPv}(s) - 0{\cdot}025(\mathrm{IPv}(s))^2,$$

$$\text{(ii)}\quad \mathrm{IPv}(h) = \mathrm{IPv}(s) + 0{\cdot}04 - \frac{0{\cdot}126 \pm 0{\cdot}029\,(\text{s.d})}{\text{antilog } 0{\cdot}4\mathrm{IPv}(s)}.$$

The second equation gave a slightly better fit than the first, the s.d. of one residual being (i) $\pm 0^{m}\cdot 0151$ and (ii) $\pm 0^{m}\cdot 0146$. The second equation was derived by assuming that the actual light intensities after correction for colour (L_s and L_h) were related by the expression

$$L_h = aL_s b^{cL_s}.$$

This is of course a purely empirical relation.

As the linearity of the photometer scale had been carefully examined it was unlikely that material scale error existed in the photoelectric results. This view was upheld by a comparison of the m_{4550} results with some unpublished measures generously made available by Professor Woolley. These results were obtained by an improved version of the method described by Woolley and Gottlieb (**8**). They have been determined photographically with a band width of 250 A. Their scale was established with the aid of carefully measured sectors, and colours were obtained. The two scales were compared at $\lambda = 4550$ A. and the difference (photographic–photoelectric) was plotted against the photoelectric results (see Fig. 4 *b*). There was no systematic deviation with magnitude and the mean deviation over a range of 4^{m} was $\pm 0^{m}\cdot 04$.

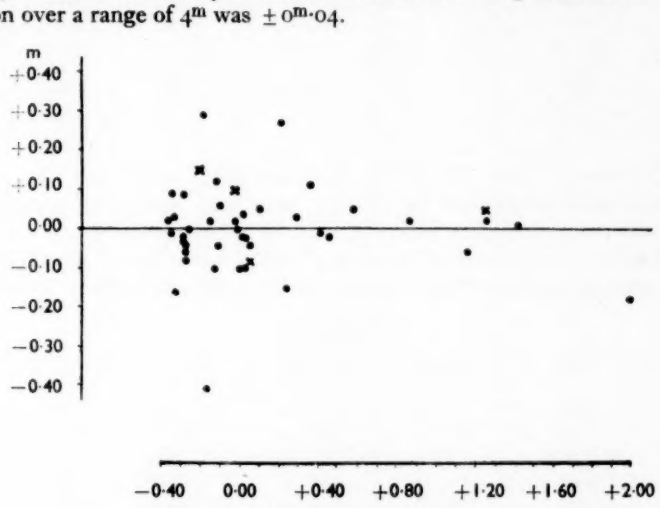

FIG. 5.—IPv(*h*) − IPv(*s*) vs. Gradient.

The m_{4550} scale also agreed with the above-mentioned photoelectric scale given by Eggen. Eggen's results were expressed on a system (Pg_p) which was directly linked with the North Polar Sequence (**9**) so that the zero-points agreed between the sixth and eighth magnitudes.

The results for the eight stars available for comparison (**10**) gave the following relation:—

$$m_{4550} = Pg_p - 0\cdot 16C_p.$$

In this equation C_p is a colour defined by Eggen.

Table II shows values of Pg_p and C_p as well as figures for m_{4550} as computed from Eggen's results and as observed. The deviations between the two sets of results (computed–observed) are plotted in Fig. 4 (*c*). The maximum deviation is $0^{m}\cdot 03$ over a range of 5^{m} in brightness and 1^{m} in colour.

Because of this agreement the zero-point for the m_{4550} catalogue (Table III) has been chosen to agree with the zero-point of the Pg_p scale, i. e. the m_{4550} results, when corrected for colour would be expected to agree with the IPg scale at the mean magnitude of the six stars of the North Polar Sequence (7^m) chosen by Eggen to define the zero of his scale. This means that the listed m_{4550} figures are in general $0^m{\cdot}25$ brighter than magnitudes which could be derived by reducing the Harvard Pv system to $\lambda_{eff}=4550$. The most notable exception to this statement is the magnitude of α C Maj which on the photoelectric scale is $m_{4550}=-1{\cdot}49$ whilst the derived figure is $-1{\cdot}53$. Deviations of over $0^m{\cdot}1$ have been noted between photographic and photoelectric results for the brighter stars of the North Polar Sequence (**9, 11, 12**).

TABLE II

Values of m_{4550} as observed and as computed from Eggen's results

Star	Obs.	Pg_p	C_p	m_{4550}	
				computed	observed
γ Gemi	t	1·88	−0·065	1·89	1·86
α C Maj	s	−1·53	−0·07	−1·52	−1·49
β Leon	s	2·11	+0·08	2·10	2·10
α Cor B	s	2·12	−0·05	2·13	2·11
α Ophi	s	2·11	+0·10	2·09	2·10
α Aqil	s	0·88	+0·165	0·85	0·83
ε Pegs	t	3·74	+1·37	3·52	3·53
α Psc A	p	1·11	+0·015	1·11	1·11

8. *Catalogue.*—Table III gives the magnitudes at $\lambda=4550$ for 63 stars. The magnitudes determined by primary, secondary and tertiary methods are respectively denoted by the letters p, s and t. Double stars, the components of which differ in brightness by less than 5^m, are denoted by (d) as it is considered that the spectral range for these results may be outside the selected band.

TABLE III

Catalogue

Star	α (1950) h m	δ (1950) ° ′	m_{4550}	Obs.
α Andr	00 06	+28 49	1·963	t
β Hydi	00 23	−77 32	3·172	t
α Phoe	00 24	−42 35	3·114	t
β Ceti	00 41	−18 16	2·708	t
α Erid	01 36	−57 29	0·274	p
α Hydi	01 57	−61 49	2·998	t
γ Hydi	03 48	−74 24	4·369	t
β Orio	05 12	−08 15	0·138	t
γ Orio	05 22	+06 18	1·434	s
ζ Orio	05 38	−01 58	1·598	t (d)
κ Orio	05 45	−09 41	1·922	s
β C Maj	06 20	−17 56	1·772	s
α Cari	06 23	−52 40	−0·686	p
γ Gemi	06 35	+16 27	1·857	t
α C Maj	06 43	−16 39	−1·488	s
α Pict	06 48	−61 53	3·326	t*
ε C Maj	06 57	−28 54	1·295	s
δ C Maj	07 06	−26 19	2·305	t
η C Maj	07 22	−29 12	2·347	s
α C Min	07 37	+05 21	0·608	s†
ζ Pupp	08 02	−39 52	2·032	s

TABLE III (*cont.*)

Catalogue

Star	α (1950) h m	δ (1950) ° ′	m_{4550}	Obs.
γ Velr	08 08	−47 12	1·571	t (d)
ε Cari	08 21	−59 21	2·794	t
δ Velr	08 43	−54 32	1·880	t (d)
λ Velr	09 06	−43 14	3·395	t
β Cari	09 13	−69 31	1·596	p
ι Cari	09 16	−59 04	2·318	s
κ Velr	09 21	−54 48	2·290	s
α Hyda	09 25	−08 26	3·002	t
α Leon	10 06	+12 13	1·238	s†
β Leon	11 47	+14 51	2·101	s
α Cruc	12 24	−62 49	0·536	t (d)
γ Cruc	12 28	−56 50	2·642	t
γ Cent	12 39	−48 41	2·038	t (d)
β Cruc	12 45	−59 25	1·035	s
α Virg	13 23	−10 54	0·773	t†
β Cent	14 00	−60 08	0·402	s
θ Cent	14 04	−36 07	2·716	t
α Boot	14 13	+19 26	0·780	t
α Cent	14 36	−60 38	0·114	t (d)
γ Tr Au	15 14	−68 30	2·800	p
α Cor B	15 33	+26 53	2·114	s†
δ Scor	15 57	−22 29	2·202	s
α Scor	16 26	−26 19	2·323	t
α Tr Au	16 43	−68 56	2·903	t
ε Scor	16 47	−34 12	3·032	t
δ Arae	17 27	−60 38	3·454	t
λ Scor	17 30	−37 04	1·380	s
α Ophi	17 33	+12 36	2·096	s
θ Scor	17 34	−42 58	2·081	s
κ Scor	17 39	−39 00	2·196	s
ε Sgtr	18 21	−34 25	1·742	p
σ Sgtr	18 52	−26 22	1·883	s
α Aqil	19 48	+08 44	0·834	s
δ Pavo	20 04	−66 19	3·975	t*
α Pavo	20 22	−56 54	1·718	s
β Pavo	20 40	−66 23	3·451	t
ε Pegs	21 42	+09 39	3·531	t
α Grus	22 05	−47 12	1·585	p
β Grus	22 40	−47 09	3·363	t
β Octn	22 41	−81 39	4·179	t*
α Psc A	22 55	−29 53	1·108	p
α Pegs	23 02	+14 56	2·405	s

* Magnitudes based on three observations only.

† These stars are listed by Gŭssow and Guthnick (**13**) as having slight variation of amplitude of the order of $0^m{\cdot}1$. In the present work, the standard deviations of individual comparisons for α C Min and α Leon were amongst the highest found ($0^m{\cdot}036$ and $0^m{\cdot}041$ respectively). The stars α Cor B and α Virg showed only normal scatter (0·02 s.d. for individual comparisons). As, in general, such comparisons were made on from three to six nights, variations could escape detection.

9. *Acknowledgments.*—The impetus to commence this narrow-band photometry came from Professor Woolley. The outline of the method was developed during talks with him and we are greatly indebted for frequent discussions during the course of the work and his continued interest in the results. Further, the

unpublished results of his collaboration with Mr Gottlieb have been made freely available.

Dr Gascoigne's cooperation in various discussions, in the adjustment of the spectrograph and in making available his results prior to publication has been much appreciated.

Dr Eggen has also helped in this latter respect and without his cooperation Table II could not have been included at this stage.

We are indebted to Mr P. W. A. Bowe for preparing the evaporated film filters.

Commonwealth Observatory,
Mount Stromlo,
Canberra, Australia:
1950 *November* 14.

References

(1) N. Milford, *C.R.*, **230,** 718, 1950.
(2) S. C. B. Gascoigne, *M.N.*, **110,** 15, 1950.
(3) Mary Banning, *J.O.S.A.*, **37,** 686, 1947.
(4) C. Payne-Gaposchkin, *Harv. Obs. Mimeograms Series* III, 1938.
(5) Royal Observatory, Greenwich, *M.N.*, **100,** 189, 1940.
(6) F. H. Seares and Mary C. Joyner, *Ap. J.*, **98,** 302, 1943.
(7) J. S. Hall, *Ap. J.*, **94,** 71, 1941; **95,** 231, 1942.
(8) R. v. d. R. Woolley and K. Gottlieb, *M.N.*, **110,** 206, 1950.
(9) O. J. Eggen, *Ap. J.*, **111,** 65, 1950.
(10) O. J. Eggen, *Ap. J.*, **114,** 141, 1951.
(11) J. Stebbins and A. E. Whitford, *Ap. J.*, **87,** 237, 1938.
(12) W. Hassenstein, *A.N.*, **269,** 185, 1939.
(13) M. Güssow and P. Guthnick, *Kl. Veröff. Berlin-Babels.*, **8,** 39, 1930.

PHOTOELECTRIC OBSERVATIONS OF SOME SPECTROSCOPIC BINARIES

A. R. Hogg, K. Gottlieb, G. V. Simonow and Beryl Hall

(Communicated by the Commonwealth Astronomer)

(Received 1950 December 30)

Summary

Observations of six southern spectroscopic binary stars were made with an electron multiplier photometer. Of the stars examined *a* Cari, θ^2 Cruc and ν Cent were found to have no regular light variation with the spectroscopic period, θ^2 Cruc shows some irregular variation of amplitude $\pm 0^m.02$. 66 Erid and 19 Erid were not fully covered but no variations were detected. σ Scor was found to have a variation similar to that of a dwarf Cepheid. μ Cent (which is not actually a spectroscopic binary but was used as a comparison star) was found to vary in an irregular fashion with a range of $0^m.2$.

Suitable southern spectroscopic binaries were selected from Moore's Fourth Catalogue (**1**) for photoelectric observation in the expectation of discovering shallow eclipses. The programme included the stars set out in Table I which also gives the comparison stars used. The comparison stars were selected to be, as far as possible, of the same spectral class as the variable so as to avoid differential absorption effects. The observations were made almost entirely with an electron multiplier photometer attached to the Farnham 6-inch refractor. This instrument and the technique adopted have been described in a previous paper dealing with the eclipsing variable ζ Phoe (**2**) which had also been included in the present programme. A few observations were made with a multiplier photometer on the Oddie 9-inch refractor (**3**).

TABLE I

Binary and comparison stars

(1900 Positions)

Star	R.A.	Dec.	Mag.	Sp.	Period	Comparison	R.A.	Dec.	Mag.	Sp.
	h m	° ′			d		h m	° ′		
19 Erid	03 29	−21 58	4·32	B8	6·2236	17 Erid	03 26	− 5 25	4·80	B9
66 Erid	05 02	− 4 47	5·19	B9	5·5224	62 Erid	04 51	− 5 20	5·46	B9
a Cari*	09 08	−58 33	3·56	B3	6·744	3663†	09 09	−61 54	4·18	B3
θ^2 Cruc	11 59	−62 36	4·98	B3	3·4380	4573†	11 53	−61 53	5·70	B5
ν Cent	12 36	−41 11	3·53	B2	2·6252	ϕ Cent	13 52	−41 37	4·05	B3
σ Scor	16 15	−25 21	3·08	B1	0·2468	τ Scor	16 30	−28 01	2·91	Bo
μ Cent	13 44	−41 59	3·32	B2p	...	ϕ Cent	13 52	−41 11	3·53	B3

Fig. 1 gives results for some of these stars. No systematic variation is shown in 66 Erid, *cf.* J. Stebbins (**4**), 19 Erid, *a* Cari, θ^2 Cruc or ν Cent, *cf.* R. E. Wilson (**5**). Comparison of the curves for θ^2 Cruc and ν Cent, which were obtained by the same technique, suggests that as the former shows appreciably more scatter, there may be some irregular small-scale variations in the light of either θ^2 Cruc or its comparison star. No definite periodicity could be determined.

* L. Boss, *P.G.C.*, 2473, 1910.

† F. Schlesinger, *Catalogue of Bright Stars*, 1930.

σ Scor.—This system exhibits two types of radial velocity variation, viz. a change with the very short period of $0^d{\cdot}2468$ and a change with a longer and somewhat varying period of about 33^d (Henroteau (**6**)). Strictly speaking the short-period variation dealt with here is most likely not of the binary type and the star is included in Moore's Catalogue because of the long-period variation, which however has not been examined photometrically. Henroteau classifies the star as being of the β C Maj type on account of its spectroscopic changes. Such stars are characterized by a period of a few hours and light variations of very small amplitude have been detected in some members of the class. Stebbins (**4**) has compared the variations of σ Scor with π Scor and concluded that there was some

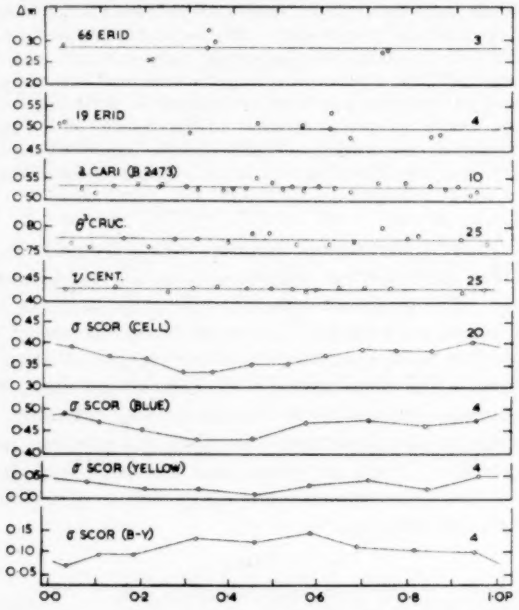

FIG. 1.—*The light curves of some spectroscopic binaries. The ordinates represent the magnitude differences between the binary and the comparison star listed in Table I. The figures on the right show the average number of comparisons meaned to obtain each of the plotted points. The curve marked σ Scor (B–Y) gives the colour change of the star.*

kind of variation with a range of at least $0^m{\cdot}03$ but the observations were insufficient to derive a complete light curve. Three sets of measures have been made in the present case, viz.:—

(*a*) A series on seven nights in 1947 using a 931A multiplier on the 6-inch Farnham refractor without any filter on the cell.

(*b*) A series on two nights in 1950 using a 1P21 multiplier on the 9-inch Oddie refractor in two colours corresponding to a blue filter (Schott F3653, 2 mm.) and a yellow filter (Schott F4937, 2 mm.).

The results of all sets showed a variation which could be represented by a period of $0^d{\cdot}246841$ derived from the epochs of minimum light for the 1947 and 1950 observations, viz.:—

$$\text{J.D.} = 2432\ 284{\cdot}08 \quad \text{and} \quad \text{J.D.} = 2433\ 396{\cdot}10,$$

by assuming that 4505 cycles elapsed in that interval. The spectroscopic period given by Henroteau, viz. $0^d{\cdot}246834$ required 4505·2 cycles. Owing to the considerable lapse of time between the spectroscopic and photometric observations and the very short period it is inadvisable to attempt to identify the two sets of results.

The earlier series is shown in Fig. 1, by the curve marked "cell". The normals are the means of about twenty comparisons, with standard deviations about $0^m{\cdot}006$ per normal. The range is $0^m{\cdot}08$ and the form of the light variation is similar to that shown by other β C Maj stars. The two-colour curves are also shown in Fig. 1 marked "yellow" and "blue" respectively; here the points are means of four comparisons. These confirm the earlier results. The curve marked B–Y shows the colour. Corrections were applied to bring the colour to the zenith. The curve makes the star bluer at maximum light as is the case for Cepheids generally.

μ Cent.—This star exhibits variable line emission (for references see Merrill and Burwell (**7**)). Early in the present century it showed the Balmer series in emission as far as *Hϵ* and also bright lines of ionized iron, but by 1918 all bright hydrogen had disappeared. Gerasimovic (**8**) investigated the photographic density of plates exposed at times when the bright lines were present and absent. He concluded from measures on six plates that the star would be fainter by $0^m{\cdot}1$ or $0^m{\cdot}2$ when the lines were not visible.

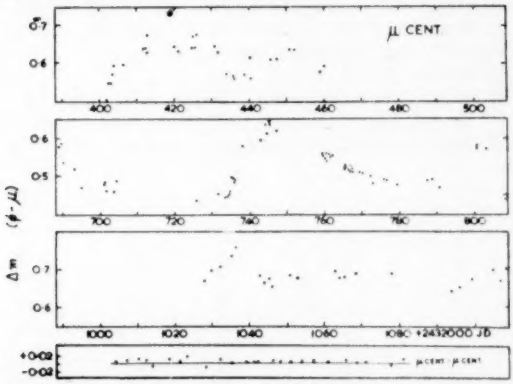

FIG. 2.—*Light variations of μ Cent. The points for the upper curves are the means of about 25 comparisons. The lowest diagram marked μ Cent–μ Cent represents the mutual comparison of successive observations of μ Cent. Thus measures a, b and c of μ Cent have been compared in the ratio $b : \frac{1}{2}(a+c)$. The deviations of this comparison from zero magnitude show the instrumental and atmospheric scatter which, for the night plotted, is represented by a standard deviation of $0^m{\cdot}006$ per comparison. This value is below average.*

In the Spring of 1947 irregularities were noticed in the comparison of ν Cent and μ Cent. In the light of later information these irregularities were attributed to changes in the light from μ Cent. No short period could be discovered, although irregular variations amounting to $0^m{\cdot}05$ were found to occur in the course of a few days or less. Observations were carried out for the 1948 and 1949 seasons with ϕ Cent as a comparison star and again no short-periodic variations of a regular nature could be found. The magnitude difference between ν Cent and ϕ Cent was found to be constant ($0^m{\cdot}428$) and this figure was used to bring all results to a common basis. The observations are shown plotted against the time in Fig. 2,

where the normals are means of about 25 comparisons. There is a slow variation which in the 1948 results seems to have a period of about 60 days but this is not persistent and the general picture is of an irregular variable. The light level for the 1949 season was about $0^m{\cdot}1$ above that for the previous year and the complete range of variation was $0^m{\cdot}2$. Unfortunately the complete period of the observations was not covered by spectrograms. Dr Gascoigne has kindly made available some objective prism spectrograms taken on J.D. 2,432,754; 2,433,012; 2,433,020. These show a bright line superposed on the absorption line at $H\beta$. The emission line is displaced somewhat to the red of the centre of the broad absorption band. There is no difference in the three spectrograms available that might not be attributed to seeing conditions and it is not possible to make any statement about a correlation between the light output and the spectral changes except that the $0^m{\cdot}1$ change of light level between 1948 and 1949 was not associated with any marked changes in the emission lines.

Commonwealth Observatory,
Mount Stromlo,
Canberra, Australia:
1950 *December* 20.

References

(1) J. H. Moore, *L.O.B.*, **18**, 1, 1936.
(2) A. R. Hogg, *M.N.*, **111**, 315, 1951.
(3) A. R. Hogg and P. W. A. Bowe, *M.N.*, **110**, 373, 1950.
(4) J. Stebbins, *Publ. Washburn Obs.*, **15**, 69, 1926.
(5) R. E. Wilson, *L.O.B.*, **8**, 130, 1914.
(6) F. Henroteau, *Publ. Dom. Obs., Ottawa*, **8**, 45, 1923; **8**, 54, 1930.
(7) P. W. Merrill and C. Burwell, *Ap. J.*, **110**, 387, 1949.
(8) P. B. Gerasimovic, *H.B.*, No. 854, 1, 1928.

OCCULTATIONS OF STARS BY THE MOON OBSERVED AT THE NIZAMIAH OBSERVATORY, HYDERABAD, DURING THE YEAR 1950

(Communicated by the Director)

(Received 1951 February 9)

TABLE I

No.	Star	Mag.	Phase	Date 1950	U.T.	Obs.
					h m s	
1	N.Z.C. 2227	5·8	R	Jan. 13	22 47 20·4	M.G.
2	N.Z.C. 35	6·4	D	,, 23	13 48 2·7	M.G.
3	N.Z.C. 756	6·5	D	,, 29	14 6 21·9	M.G.
4	N.Z.C. 771	6·1	D	,, 29	18 15 5·2	M.G.
5	N.Z.C. 773	6·9	D	,, 29	18 35 38·7	M.G.
6	N.Z.C. 1093	6·4	D	,, 31	21 30 55·1	M.G.
7	N.Z.C. 1576	5·3	R	Feb. 4	16 58 4·8	M.G.
8	N.Z.C. 1712	3·8	D	,, 5	23 25 36·4	M.G.
9	N.Z.C. 1712	3·8	R	,, 6	0 31 49·0	M.G.
10	B.D.+23° 560	8·3	D	,, 24	13 35 50·5	M.G.
11	N.Z.C. 562	6·6	D	,, 24	13 39 44·1	M.G.
12	B.D.+23° 562	8·2	D	,, 24	13 53 56·2	M.G.
13	B.D.+23° 567	7·8	D	,, 24	14 10 55·6	M.G.
14	B.D.+23° 564	9·0	D	,, 24	14 18 0·6	M.G.
15	B.D.+24° 578	7·3	D	,, 24	14 34 2·5	M.G.
16	N.Z.C. 1149	4·2	D	,, 28	14 48 6·9	M.G.
17	N.Z.C. 1279	6·4	D	Mar. 1	14 13 39·6	M.G.
18	N.Z.C. 2157	6·1	R	,, 8	23 43 52·9	M.G.
19	N.Z.C. 1712	3·8	D	April 1	18 33 57·0	M.G.
20	N.Z.C. 1181	6·8	D	,, 24	14 57 31·5	M.G.
21	N.Z.C. 1644	4·1	D	,, 28	14 24 52·1	M.G.
22	N.Z.C. 2538	6·8	D	Aug. 22	14 19 34·0	M.G.
23	N.Z.C. 2677	6·8	D	Sept. 19	14 50 6·7	M.G.
24	N.Z.C. 3225	7·1	D	Oct. 20	13 17 18·8	M.G.
25	N.Z.C. 3236	7·1	D	,, 20	17 15 37·8	M.G.
26	N.Z.C. 3240	6·6	D	,, 20	18 19 0·8	M.G.
27	N.Z.C. 146	4·4	D	,, 24	13 9 53·5	M.G.
28	N.Z.C. 3405	7·0	D	Dec. 15	15 46 57·0	M.G.
29	N.Z.C. 3520	6·0	D	,, 16	15 24 14·8	M.G.
30	N.Z.C. 203	6·9	D	,, 18	14 8 55·2	M.G.
31	N.Z.C. 425	7·0	D	,, 20	12 49 32·5	M.G.
32	N.Z.C. 440	4·6	D	,, 20	17 14 11·4	M.G.
33	N.Z.C. 438	6·7	D	,, 20	17 47 50·5	M.G.
34	N.Z.C. 541	4·0	D	,, 21	14 26 20·8	M.G.
35	N.Z.C. 542	5·8	D	,, 21	14 34 52·0	M.G.
36	N.Z.C. 543	6·5	D	,, 21	14 38 25·8	M.G.

The last column indicates the initials of the observer, Mahomed Ghouse.

The instrument used throughout was the 15-inch Grubb refractor. The corrections to the standard clock were determined from observations with the transit instrument. The reductions were carried out by S. Aravamuthan

assisted by V. V. Raghaviah on a Facit calculating machine, after suitably modifying the formulae given in the Supplement to the *Nautical Almanac* for 1938. A correction of $-0^{h}\cdot00076$ was applied to the observed time, to allow for the error of $-1''\cdot5$ in the mean longitude of the Moon.

TABLE II

No.	$\sigma'-\sigma$	$\cos(\rho-\psi)$	$\sin(\rho-\psi)$	No.	$\sigma'-\sigma$	$\cos(\rho-\psi)$	$\sin(\rho-\psi)$
	"				"		
1	+0·8	−0·66	+0·75	19	+1·1	+1·00	−0·03
2	+0·1	+0·47	+0·88	20	+0·6	+0·76	+0·65
3	+0·6	+0·99	+0·12	21	+1·3	+1·00	+0·03
4	−0·2	+0·58	+0·81	22	−1·1	+0·34	−0·94
5	−1·3	+0·16	−0·99	23	−0·2	+0·95	−0·30
6	−2·0	+0·96	−0·28	24	−0·5	+0·96	+0·27
7	+0·7	−0·92	+0·39	25	+0·5	+0·80	−0·59
8	+0·1	+0·97	+0·24	26	0·0	+0·98	−0·18
9	+0·7	−0·76	+0·65	27	−0·2	+1·00	−0·03
10	+1·8	+0·99	−0·15	28	−0·8	+0·96	+0·27
11	+0·3	+0·97	−0·23	29	+0·5	+0·43	+0·90
12	−1·0	+0·62	−0·78	30	−1·8	+0·87	+0·49
13	+0·1	+0·84	−0·54	31	−0·4	+1·00	−0·04
14	−0·2	+0·44	−0·90	32	+0·5	+0·99	−0·16
15	+1·8	+0·99	−0·11	33	−1·0	+0·40	+0·92
16	−1·1	+0·97	−0·25	34	−1·2	+0·89	−0·45
17	−0·9	+0·49	+0·87	35	−0·4	+0·98	+0·21
18	+0·1	−0·79	−0·61	36	−0·1	+1·00	+0·05

The mean places for 1950·0 of the five stars (Nos. 10, 12, 13, 14 and 15) are given in Table III. For star Nos. 10, 12, 14 and 15, proper motions have been applied to the coordinates given in the catalogue in computing the mean place for use in the reduction.

TABLE III

No.	R.A. (1950·0)	Dec. (1950·0)	Remarks
	h m s	° ′ ″	
10	3 46 17·68	+24 14 42·5	A. G. Berlin B1201, $\mu_\alpha+0^s\cdot0017$; $\mu_\delta-0''\cdot040$ (Yale)
12	3 46 27·00	+24 05 48·7	A. G. Berlin B1203, $\mu_\alpha+0^s\cdot0015$: $\mu_\delta-0''\cdot038$ (Yale)
13	3 46 57·46	+24 11 54·0	Boss GC4609
14	3 46 47·04	+24 05 41·0	A. G. Berlin B1208, $\mu_\alpha+0^s\cdot0003$; $\mu_\delta+0''\cdot010$ (Yale)
15	3 47 28·71	+24 20 43·4	A. G. Berlin B1218, $\mu_\alpha+0^s\cdot0015$; $\mu_\delta-0''\cdot012$ (Yale)

Nizamiah Observatory,
Hyderabad,
Deccan, India:
1951 *February* 1.

CONTENTS

Printed in London by Taylor & Francis, Ltd., 1951 November